HEINRICH HEINE
UNIVERSITÄT DÜSSELDORF

Modulation of β-adrenergic receptor structure and function by cardiopathogenic autoantibodies

Inaugural-Dissertation

zur Erlangung des Doktorgrades
der Mathematisch-Naturwissenschaftlichen Fakultät
der Heinrich-Heine-Universität Düsseldorf

vorgelegt von

Beatrice Bornholz
aus Potsdam

Düsseldorf, Dezember 2010

Aus dem Institut für Klinische Chemie und Laboratoriumsdiagnostik
der Heinrich-Heine Universität Düsseldorf

Gedruckt mit der Genehmigung der
Mathematisch-Naturwissenschaftlichen Fakultät der
Heinrich-Heine-Universität Düsseldorf

Referent: Prof. Dr. Friedrich Boege
Koreferent: Uni-Prof. Dr. Peter Westhoff

Tag der mündlichen Prüfung: 12. April 2011

MEINER FAMILIE

Table of Contents

„Corpora non agunt nisi fixata“

Paul Ehrlich

(Stoffe wirken nur, wenn sie gebunden werden)

Summary

At least two human diseases are known to be caused by autoantibodies that bind to hormone receptors and alter their function. One is Grave's disease a pathologically enhanced growth and endocrine function of the thyroid gland caused by autoantibodies that stimulate the receptor of the thyroidea stimulating hormone. The other is *myastenia gravis,* an intermittent weakness of skeletal muscles caused by autoantibodies blocking the nicotinic acetyl choline receptor of the neuromuscular endplate. Over the last two decades, several new diseases and target receptors have been added to this list. One is dilated cardiomyopathy, a progressive dilatation and dysfunction of the human heart of largely unknown origin. This disease is now thought to be caused by autoantibodies against β_1-adrenergic receptors, which are the transducers of the stimulatory effect of adrenaline and noradrenaline on the heart rate and contractile force. In the blood of patients with dilated cardiomyopathy IgG antibodies that bind to β_1-adrenergic receptors and alter receptor function are frequently found. Their removal by immunoadsorption improves heart function. Experimental immunisation of rodents with the respective β_1-adrenergic receptor epitopes induces comparable autoantibodies and symptoms and these can be conferred via serum transfer to other healthy animals. Thus, β_1-adrenergic receptor autoantibodies could be a target for the therapy of the hitherto incurable disease. However, it is unknown how pathogenic autoantibodies interact with the β_1-adrenergic receptor and trigger changes in receptor structure and function leading to the disease. Such knowledge is required to design, indicate and monitor autoantibody-directed therapy.

To elucidate the impact of autoantibodies on receptor function, I expressed various biofluorescent constructs of the human β_1-adrenergic receptor in a human cell line. This allowed me to titrate IgGs binding to the native receptor on the cell surface, to measure activation-related changes in receptor conformation via intramolecular fluorescence energy transfer (FRET), to monitor dynamics of receptor internalisation and recycling via total internal reflection fluorescence (TIRF), and to determine receptor-mediated changes in cellular cAMP levels. These parameters were used to

compare autoantibodies with true receptor ligands and to compare *bona fide* pathogenic auto-antibodies removed from patients in the course of successful IgG adsorption therapy with autoantibodies purified analogously from the blood of matched healthy volunteers.

The investigation shows that: IgG capable of binding to the native human β_1-adrenergic receptor on the cell surface were present in all patients with dilated cardiomyopathy and all healthy volunteers. However increased levels of such IgG discriminated patients from volunteers above the 80^{th} percentile. All receptor-specific IgG triggered conformational receptor activation or inactivation; some also inhibited agonist-induced receptor internalisation. cAMP-responses to isoproterenol were potentiated by IgG inducing conformational receptor activation and attenuated by IgG inducing conformational receptor inactivation or inhibiting receptor internalisation. Receptor activation and inhibition of receptor internalisation were more pronounced and frequent by patient IgG. Clinical response to immunoadsorption was best correlated to receptor internalisation inhibition.

For the first time this study provides direct evidence that IgG autoantibodies against β_1-adrenergic receptors act as allosteric agonists or antagonists. Furthermore, it shows that they can activate or inactivate β_1-adrenergic receptors. Also for the first time it is shown that these autoantibodies can inhibit receptor internalisation. These properties are independently related to left ventricular dysfunction and act additive or counteractive to endogenous cAMP regulation. Given this heterogeneity, clinical screening seems best based on receptor-specific IgG levels alone, whereas IgG impact on receptor function could determine therapeutic options.

Zusammenfassung

Autoimmunantikörper die an Hormonrezeptoren binden und deren Funktion modifizieren, sind bewiesenermaßen Auslöser für mindestens zwei Krankheiten. Eine davon ist die so genannte Basedowsche Krankheit. Sie ist durch eine pathogene Vergrößerung der Schilddrüse, einhergehend mit einer erhöhten endokrinen Funktion charakterisiert. Ursache dieser Krankheit sind Antikörper, die stimulierend auf den Thyroid Hormon Rezeptor wirken. Die andere bekannte Krankheit ist *myastenia gravis*, eine periodisch auftretende Muskelschwäche ausgelöst durch Autoantikörper, die den Nikotin Acetyl Rezeptor der motorischen Endplatte blockieren. In den letzten 20 Jahren wurden Hinweise auf viele weitere Autoimmunkrankheiten und beteiligte Rezeptoren gefunden. Eine davon ist die dilatative Kardiomyopathie (DCM), die sich in einer fortschreitenden Vergrößerung und Dysfunktion des Herzens manifestiert und deren Ursprung unbekannt ist. Bisherige Theorien gehen davon aus, dass diese Krankheit durch Autoantikörper gegen β_1-adrenerge Rezeptoren ausgelöst wird, die als Signalüberträger von Adrenalin und Noradrenalin stimulierend auf die Herzrate und Kontraktionskraft des Herzens wirken. Im Blut von Patienten mit DCM konnten Autoimmunantikörper gegen den β_1-adrenergen Rezeptor (β_1-AR) gefunden werden, die vermutlich die Rezeptorfunktion beeinflussen. Durch Immunadsorption bei der DCM Patienten die Autoantikörper entzogen werden, kann eine Verbesserung der Herzleitung erzielt werden. Immunisierungsexperimente mit Epitopen des β_1-AR in Nagetieren zeigen, dass vergleichbare Autoimmunantikörper und vergleichbare Symptome erzeugt werden können, welche via Serumtransfer auch auf gesunde Tiere übertragbar sind. Somit sind Autoantikörper gegen den β_1-AR ein viel versprechendes Ziel für neue Therapieansätze dieser bisher unheilbaren Krankheit. Dennoch ist unklar, wie die vermutlich pathogenen Autoantikörper mit dem β_1-AR interagieren, dessen Struktur verändern und letztlich DCM verursachen. Basiswissen über diese Zusammenhänge ist jedoch Vorraussetzung für eine frühzeitige Diagnose sowie für Entwicklung und Monitoring einer gegen die Antikörper gerichteten Therapie. Um zu klären welchen Einfluss Autoantikörper auf die Rezeptorfunktion haben, wurden verschiedene biofluoreszente Konstrukte des β_1-adrenergen Rezeptors in menschlichen Zellen exprimiert. Das ermöglichte es, die IgG bindenden

Autoantikörper zu titrieren und Konformationsveränderungen des Rezeptors mittels intramolekularem Förster-Resonanz-Energie-Transfer (FRET) zu messen. Außerdem wurden mit diesem Modell die Dynamik der Rezeptorinternalisierung und das Recycling mittels Totaler-Interner-Reflektionsmikroskopie (TIRF) und die rezeptorvermittelte Veränderungen der zellulären cAMP Konzentrationen untersucht. Diese Methoden wurden genutzt um den Effekt von Autoantikörpern aus DCM Patienten mit natürlichen Rezeptor Liganden, als auch gereinigten Antikörpern von gesunden Probanden zu vergleichen. IgG-Antikörper, die in der Lage sind an den β-AR zu binden, finden sich sowohl in der Gruppe der DCM Patienten als auch in allen analysierten Proben der Kontrollgruppe gesunder Probanden. Eine Differenzierung zwischen beiden Gruppen mit 80% Effizienz ist allein aufgrund verschieden hoher rezeptorspezifischer IgG-Konzentrationen möglich. Alle rezeptorbindenden IgGs bewirken eine konformationsabhängige Aktivierung oder Inaktivierung des β_1-AR. Für einige IgGs konnte eine Hemmung der Agonisten vermittelten Rezeptorinternalisierung beobachtet werden. Die cAMP-Antwort auf Isoproterenol wurde durch IgGs, die aktive Rezeptorkonformationen induzieren potenziert und Antikörper die die inaktive Rezeptorkonformationen induzieren oder die Internalisierung hemmen reduzierten die cAMP Antwort nach Gabe von Isoproterenol. Rezeptoraktivierung und die Hemmung der Rezeptorinternalisierung kamen bei IgGs aus Patienten ausgeprägter und häufiger vor. Die beste Korrelation zwischen den klinischen Daten der Patienten nach Immunadsorption und den getesteten Parametern ergab sich für die Daten der Internalisierungshemmung. Diese Arbeit erbringt den ersten Hinweis, dass gegen den β_1-AR gerichtete IgG Autoantikörper, als allosterische Agonisten oder Antangonisten agieren. Es konnte gezeigt werden, dass sie den Rezeptor entweder aktivieren oder auch inhibieren, und, dass diese Autoantikörper die Rezeptorinternalisierung hemmen. Dieses Eigenschaften stehen unabhängig von einander in Bezug zur linksventrikulären Herz Dysfunktion und wirken verstärkend oder hemmend auf die endogene cAMP Regulation. Die unterschiedlichen beobachteten Effekte zeigen, dass eine valide klinische Diskriminierung zwischen Patient und Proband nur basierend auf den Unterschieden in der IgG-Konzentration am effektivsten möglich ist. Darüber hinaus könnten spezifische Effekte der IgGs auf die β_1-AR Funktion dazu beitragen therapeutische Ansätze zu individualisieren.

1. Introduction

Dilated cardiomyopathy (DCM) is a heart muscle disease characterised by dilatation of the left ventricle as well as a decreased systolic function. Its etiology is still unknown. However, immunological abnormalities such as the presence of a high concentration of autoantibodies in DCM patient's blood have been reported. Autoantibodies are part of the adaptive immune system and cause several autoimmune diseases, most notably Grave's disease and *myasthenia gravis*. DCM seems to be an autoimmune disease directing the antibody defence against the heart and there preferentially against the β_1-adrenergic receptor (β_1-AR). This work investigates the molecular effects triggered by pathogenic autoantibodies derived from patients suffering from DCM on β_1-ARs. Accordingly, I will introduce the clinical pattern of DCM, move on to clarify the term immune diseases in general and then introduce the main target of DCM, the β_1-AR in detail.

1.1 Dilated Cardiomyopathy

DCM is the most frequent cause of heart failure in young adults. In DCM a portion of the myocardium is dilated (Richardson et al. 1996). Mostly left but also right ventricular systolic pump function of the heart is impaired, leading to progressive cardiac enlargement and hypertrophy, a process called remodelling (Schenke-Layland et al. 2009). DCM has a poor prognosis and often leads to heart failure and premature death. Currently there is no cure for DCM. Pharmaceutical treatment is similar to that in other heart failure diseases and can only alleviate the symptoms. With an annual incidence of up to 100 patients and a prevalence of 400 patients per million (Lefkowitz et al. 2005) DCM is one major cause of heart transplantations in the world which remain limited by scarcity of suitable organs (Elliott 2000). However, the etiologies of DCM remain largely unknown. In 1995, the WHO divided DCM according to pathophysiology into four groups: 1. idiopathic (of unknown cause), 2. alcoholic/ toxic, 3. familial/ genetic and 4. viral/ autoimmune {Richardson,

1996 #360; Jahns, 2008 #548}. Idiopathic DCM represents the biggest group of about 60-70% out of total DCM cases (Jahns et al. 2006). The high percentage of idiopathic DCM cases may be related to the difficulty in diagnosing viral myocarditis (a heart muscle inflammation caused by virus infection), as there are no definitive diagnostic criteria for myocarditis and the clinical presentation based on echocardiography is very similar between all DCM patients (Elliott 2000).

1.1.1 Autoimmune pathogenesis of DCM

Patients with DCM have been examined in several studies and various immunological characteristics associated with autoimmunity and infections were found. Already in 1968, it has been reported by Orinius that heart disease occurs in humans years after a coxsackie virus infection (Orinius 1968). Twenty years later, coxsackie B virus-specific RNA was found in myocardial biopsies from patients with myocarditis and DCM (Bowles et al. 1986). There is increasing evidence, that these and other viral infections of the heart trigger DCM by various inflammatory and autoimmune mechanisms including the presence of viral genomes in the myocardium, an increased immune activity with elevated cytokine levels and the induction of autoantibodies against heart antigens (i.e. mitochondrial proteins, muscarinic receptors or β-adrenergic receptors) (Levine et al. 1990; Magnusson et al. 1994; Mann 2002; Yudowski et al. 2009).

Of these, the hypothesis that DCM is an autoimmune disease caused by humoral autoimmunity against β_1-ARs is the only one that fulfils all the criteria for autoimmune diseases postulated in 1957 by Witebsky namely that an autoimmune reaction has been identified in the form of autoantibodies, the corresponding antigen is known and an analogous immune response causes a similar disease in experimental animals (Witebsky et al. 1957).

1.1.2 Humoral autoimmune reactions against cardiac receptors

The hypothesis that DCM is a disease caused by autoantibodies against hormone receptors crucial in the regulation of cardiac function has been shaped according to the pathogenesis of Chagas heart disease, a slowly evolving inflammatory cardiomyopathy caused by the infection with the protozoan *Trypanosoma cruzi* (Cunha-Neto et al. 2006). About 30% of Chagas patients develop antibodies against the ribosomal P2-β-protein of this parasite (Lopez Bergami et al. 2005). There is evidence that those antibodies are able to cross-react with the human β_1-AR present on cardiomyocytes (Labovsky et al. 2007). First evidence that such autoantibodies are also present in patients suffering from DCM was published 20 years ago (Limas et al. 1989). Later it was shown that these antibodies reduced the number of receptors on the cell surface, and radioligand binding experiments revealed an inhibition of ligand binding to the receptor by preincubation with patient serum (Limas et al. 1990; Magnusson et al. 1990; Magnusson et al. 1994). Numerous clinical studies show that in DCM patients, prevalence (Jahns et al. 1999) and cAMP stimulatory potency (Nikolaev et al. 2007) of β_1-AR autoantibodies are correlated to more reduced cardiac function (Jahns et al. 1999), increased mortality (Stork et al. 2006), more severe ventricular arrhythmia (Chiale et al. 2001), and higher incidence of sudden cardiac death (Iwata et al. 2001).

Molecular homologies between myocyte surface proteins and microbial proteins have been proposed as one possible mechanism for the induction of cross-reacting autoantibodies directed against cardiac membrane receptors. The presence of sequence homologies between the pathogen and endogenous proteins is called ‘molecular mimicry’ (Rose et al. 2000; Olson et al. 2001; Rose 2001). This mechanism has been referred to as the ‘bystander effect’ (Fairweather 2004), in contrast to direct tissue damage by the immune system due to the exposure of self-antigens by microorganisms during an active infection. Molecular mimicry clearly seems the pathogenic mechanism in Chagas heart disease. However, in DCM it is difficult to determine, whether pathogens mimic self-antigens, release sequestered self-antigens, or both.

A causal link between humoral autoimmunity and the clinical symptoms of DCM was provided by the work of Felix and coworkers, who demonstrated significant improvements of the clinical condition upon exchanging the patients IgG with pooled IgG from healthy donors. In numerous clinical studies it was shown that in patients with heart failure due to DCM IgG-directed adsorption significantly improved cardiac function and reduced myocardial inflammation of the patients (Dörffel et al. 1997; Felix et al. 2000; Müller et al. 2000; Staudt et al. 2002). While these studies clearly showed that the clinical symptoms of DCM are caused by IgG autoantibodies, they did not allow a conclusion as to which specific antibodies and targets are involved in the autoimmune pathogenesis.

A number of animal experiments suggest that interactions of autoantibodies and the second extracellular loop of the human β_1-AR are causative in DCM. Immunisation of rodents induces left ventricular dilation and dysfunction (Jahns et al. 2004; Buvall et al. 2006) among other effects compatible with chronic cardiac dysfunction (Matsui et al. 1999; Fukuda et al. 2004; Jane-wit et al. 2007). These effects are reversible upon removal of the antibodies (Matsui et al. 2006), transferable via serum transfusions (Jahns et al. 2004; Matsui et al. 2006; Jane-wit et al. 2007; Liu et al. 2008) and at least partially abrogated by β_1-AR antagonists (Matsui et al. 2000).

On the basis of these findings it is currently postulated that autoimmunity against extracellular loop domains of β_1-ARs is a cause or cofactor of chronic left ventricular dysfunction (Freedman et al. 2004) and a potential therapy target (Felix et al. 2002; Wallukat et al. 2002; Ronspeck et al. 2003; Matsui et al. 2006; Dragun et al. 2009). However, biomarkers mandating and monitoring such therapy should be based on precise knowledge of how the autoantibodies affect receptor activity (Dragun et al. 2009). Until now it is unknown how presumably pathogenic autoantibodies interact with the β_1-AR and trigger changes in receptor structure and function leading to the disease. Such knowledge is required to design, indicate and monitor autoantibody-directed therapy.

1.2 The cardiac β_1-adrenergic receptor

1.2.1 Classes and functions of β-adrenergic receptors

The β-ARs are a class of receptors named after adrenaline (epinephrine), and are stimulated by catecholamines (sympathomimetic "fight-or-flight" hormones released by the adrenal glands in response to stress that bind to the AR). They are further categorized into three types; β_1-ARs, which cause lipolysis and cardiostimulation and β_2-ARs, which elicit bronchodilatation and vasodilatation. Knowledge of the β_3-AR is small so far. Investigations show that it may be regulator of metabolic functions and thereby assists in myocardial relaxation. β_3-AR seems to adjust the production of nitric oxide as well (Biolo et al. 2006). There are genetic indications that another β-AR subtype (β_4) might exist but it has so far not been demonstrated as a protein or ligand binding capacity (Granneman 2001).

β_1 and β_2 receptors exhibit differences in their affinities for receptor agonists and selective antagonists whereby they can be distinguished pharmacologically (see Fig 1.1). Even though the two receptors are stimulated by isoproterenol (full agonist) the β_1-AR subtype possesses a higher binding affinity for epinephrine (10- to 30-fold) (Biolo et al. 2006). Additionally the β_1-AR is the dominant subtype in the non-failing heart, representing 70-80% of all β-ARs (Bristow et al. 1986).

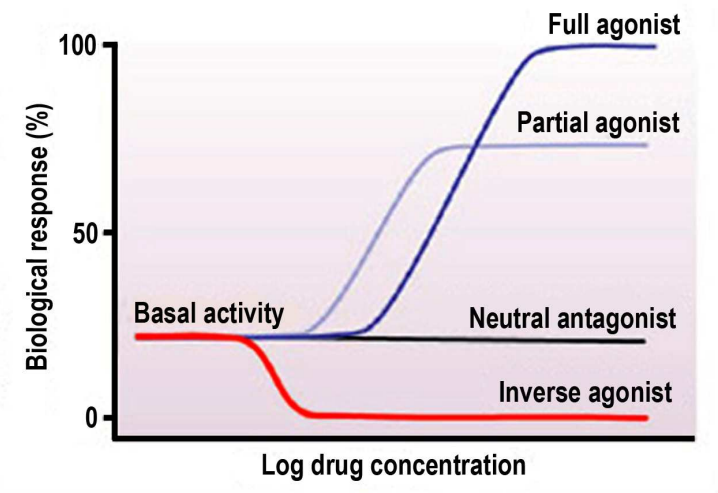

Figure 1.1: Biological response of agonist and antagonist binding to the β-AR.
Many G-protein coupled receptors (GPCRs) exhibit basal, agonist-independent activity. Inverse agonists inhibit this activity, and neutral antagonists have no effect. Agonists and partial agonists stimulate biological responses above the basal activity. Efficacy is not directly related to affinity; for example, a partial agonist can have a higher affinity for a GPCR than a full agonist. Figure adapted from (Rosenbaum et al. 2009).

β-ARs are transmembrane proteins which transduct signals into myocardial cells by coupling and activation of intermediary guanine nucleotide binding proteins (G-protein). These proteins can act excitatory (Gs) or inhibitory (Gi). They are the limiting factor for the cardiac response to an adrenergic stimulus. After norepinephrine binds to an AR, instantly a signalling-cascade is constituted in order achieve a response inside the cell (see section 1.3). Therby kinase-dependent pathways transmit the signal, governing the chronotropic or inotropic cardiac response (Kobilka 2007).

1.2.2 Ligand binding and conformational activation of β-ARs

β-ARs belong to the G-protein coupled receptor (GPCR's) superfamily (Kobilka et al. 1998; Collins 2000). GPCRs show certain similarities concerning their molecular structure. They all possess seven transmembrane spanning domains (Fig. 1.2). The hydrophobic membrane crossing domains are α-helices with a length of 20 to 24 amino acids (Dohlman et al. 1987). The receptor features three loops (ECI – ECIII) and an N-terminus extracellularly located. The C-terminus and three loops reside intracellularly (ICI – ICIII). The C-terminus and the inner loop CIII exhibit several phosphorylation sites whereas the extracellular N-terminal region includes several N-glycosylation sites. The ligand binding domains are shaped by the membrane crossing sections while intracellular sections of the IC-III loop and the C-terminus bind to the G-protein (Fig 1.2).

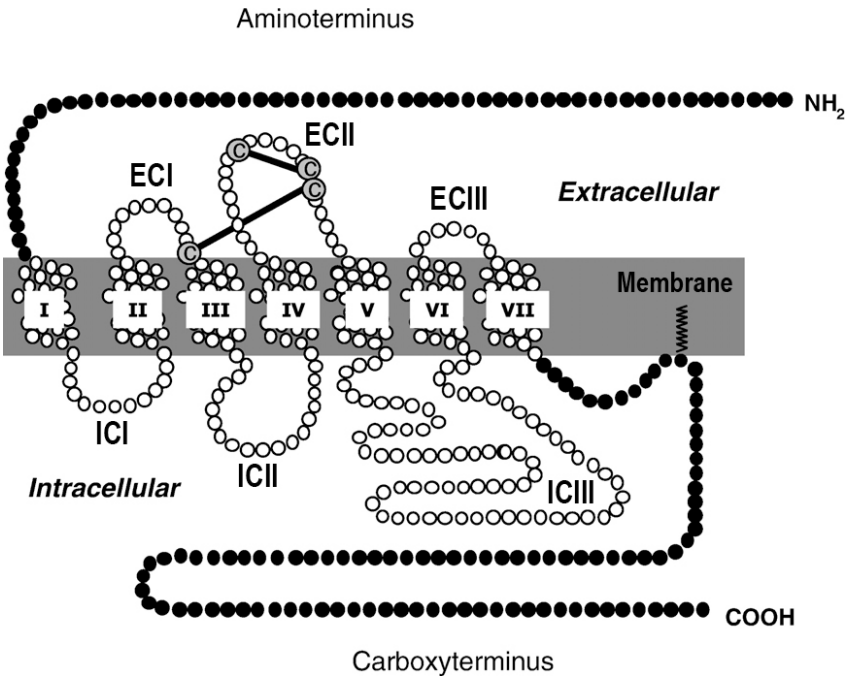

Figure 1.2: Schematic representation of the β_1-AR structure.

Seen are seven transmembrane spanning domains with three extracellular loop and three intracellular loops. Adapted from (Jahns et al. 2006) and modified.

Ligand binding requires correct folding the binding-pocket. Data indicate that one or both extracellular loops (ECI/II) are crucial for the formation of β_1-AR binding-pocket. The 1st and the 2nd extracellular β_1-AR loop also seem to represent the target for the binding of autoantibodies. Therefore it seems likely that autoantibodies directed against these loops are able to influence ligand binding, can change receptor conformation, and have an impact on receptor activity (Jahns et al. 2000).

Activation of β_1-AR by true agonists involves a series of conformational changes that enable coupling to G-proteins (Kobilka et al. 1998; Kobilka et al. 2007). Activation of the β_1-subtype also encompasses receptor dimerisation (Hebert et al. 1996; Mercier et al. 2002), but it is not clear, whether this plays a role in G-protein coupling (Kobilka et al. 2007). Agonists promote receptor conformations fully active in G-protein coupling, whereas antagonists block the ligand binding site without altering basal receptor activity. In contrast, inverse agonists promote receptor conformations, which are incapable of G-protein coupling (Milligan et al. 1997; Kenakin 2003) but may have a potential to stimulate other signalling pathways (Luttrell et al. 2002; Azzi et al.

2003; Lefkowitz et al. 2005). Unliganded β-ARs seem to show some basal activity, possibly due to spontaneous oscillations between active and inactive conformations (Chidiac et al. 1994; Hopkinson et al. 2000) and this may explain constitutive receptor activities in overexpression systems (Engelhardt et al. 2001).

Activation associated changes in receptor conformation encompass a spatial rearrangement of intracellular receptor domains that can be monitored by intramolecular fluorescence energy transfer (Granier et al. 2007). This has been used to measure the millisecond activation switch of G-protein coupled receptors in the living cell by incorporating fluorescence proteins into the C-terminal domain and the adjacent intracellular loop of the receptor (Hoffmann et al. 2005). Such Förster resonance energy transfer (FRET) sensors have been successfully employed to uncover differences in catecholamine responses in genetic variants of the human β_1-AR (Rochais et al. 2007). A similar strategy was used in this study to determine IgG-effects on receptor conformation.

1.2.3 β-adrenergic signal transduction

Hormones and neurotransmitters interact with β-ARs and thereby trigger a multicomponent signal transduction system. Ligand binding triggers a conformational change enabling the receptor to interact with heterotrimeric G-proteins consisting of an α-, β- and γ-subunit. This leads the α-subunit to exchange a bound guanosine 5'-diphosphate molecule (GDP) against a guanosine 5'-triphosphate molecule (GTP) and to dissociate from the βγ-subunits. The GTP-bound form of the α-subunit is the effector-modulating moiety. The stimulating α-subunit activates adenylate cyclase (AC), the major intracellular signalling protein which activates the cyclic adenosine 3'-5'-monophosphate (cAMP) production (Fig.1.3). The second messenger cAMP activates protein kinase A (PKA), a kinase that regulates the activity of several cellular proteins either directly i.e. the L-type Ca^{2+} channel or indirectly influencing transcription (Rosenbaum et al. 2009). Specific phosphodiesterase proteins (PDEs) can downregulate cAMP levels. Recent evidence suggests that there exists an alternative signalling pathway involving an active receptor conformation different from the one involved in adenylate cyclase stimulation (Azzi et al. 2003) that leads to

activation of the mitogen-activated protein (MAP)-kinase pathway through β-arrestins (Lefkowitz et al. 2005).Repeated occupation of the receptor by an agonist re-induces the binding of the regulatory unit to the receptor and restarts the process. cAMP activates protein kinases which in turn phosphorylate the receptor (see Fig 1.3).

If the stimulus is constantly intense the receptor has to be turned off after its activation and the transduction of the signal. This is realised by a process called desensitisation (chapter 1.2.4 and see Fig 1.3.

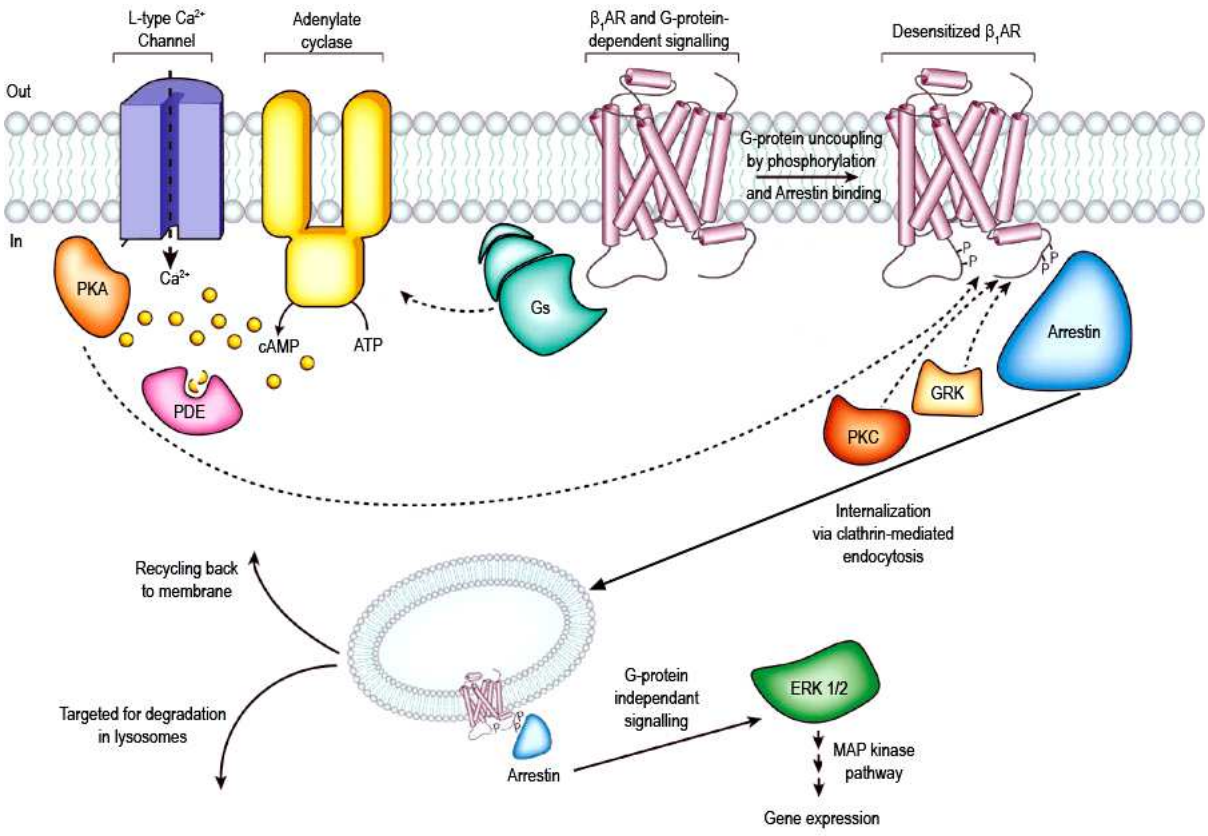

Fig. 1.3: β_1-AR activates G-protein which regulates adenylate cyclase.
Adenylate cyclase generates cyclic AMP (cAMP), which activates protein kinase A (PKA), a kinase that regulates the activity of several cellular proteins including the L-type Ca^{2+} channel. cAMP second messenger levels are downregulated by specific phosphodiesterase proteins (PDEs). Phosphorylation by a G-protein-coupled receptor kinase (GRK) or protein kinase C (PKC) and subsequent coupling to arrestin, a signalling and regulatory protein, promotes the activation of extracellular signal-regulated kinases (ERK) or prevents the activation of G proteins and promotes the internalisation of the receptor through clathrin-coated pits. Modified after (Rosenbaum et al. 2009).

1.2.4 Desensitisation

Desensitisation (Fig. 1.3) describes the process of a decline in physiological response to a specific signal over time, irrespective of a constant stimulus of steady intensity. Agonist induced desensitisation is assisted by three key processes which are described in the following.

• The receptor gets less competent to activate the G-protein due to an efficient (seconds to minutes) uncoupling mechanism. Receptor phosphorylation by i.e. G-protein coupled receptor kinase (GRK) and protein kinase C (PKC) seem to be the main elucidator for this event (Fig. 1.3).

• Another way of desensitisation is enabled by receptor sequestration which means an agonist-promoted rapid internalisation process of receptors to a compartment (vesicle) inside the cell occurs which is arrestin dependent (1.3). It is suggested that these receptors can be recycled. That implies internalised receptors return to the cell surface in a functional constitution after removal of the agonist. An alternative hypothesis acts on the assumption that the receptor is targeted for degradation in lysosomes (Campbell et al. 1991). Former work using total internal reflection fluorescence microscopy of biofluorescent receptors has demonstrated that there exist multiple pathways of internalisation and recycling (Yudowski et al. 2006; Yudowski et al. 2007; Yudowski et al. 2009). A similar approach was used in this work to quantify receptor cycling.

• Persistent presence of agonists leads to a downregulation of the receptor, whereby total number of ARs is influenced resulting in a decreased ligand binding capacity of the cell. (Campbell et al. 1991).

1.2.5 Impact of autoantibodies on receptor function

DCM autoantibodies were shown to be members of the well-known class of immunoglobulin G (IgG) that are produced by plasma-B cells, normally as a consequence of an infection and thereby activation of the humoral immune response (Staudt et al. 2004). IgG antibodies consist of two heavy and two light chains forming a ‘Y’ and having a molecular mass of 150 Kilo Dalton (kd). Antigen interaction resides

at the short ends of the antibody, with two identical antigen binding sites (Fab) those contain two heavy polypeptide chains and two light chains linked by disulphide bridges. These binding sites are highly variable (Fig. 1.4). All human antibody molecules share almost the same amino acid sequence, but heavy and light chains both contain variable regions (VL/VH) in which the sequence differs extensively in different antibodies and this confers to the antigen binding specificity.

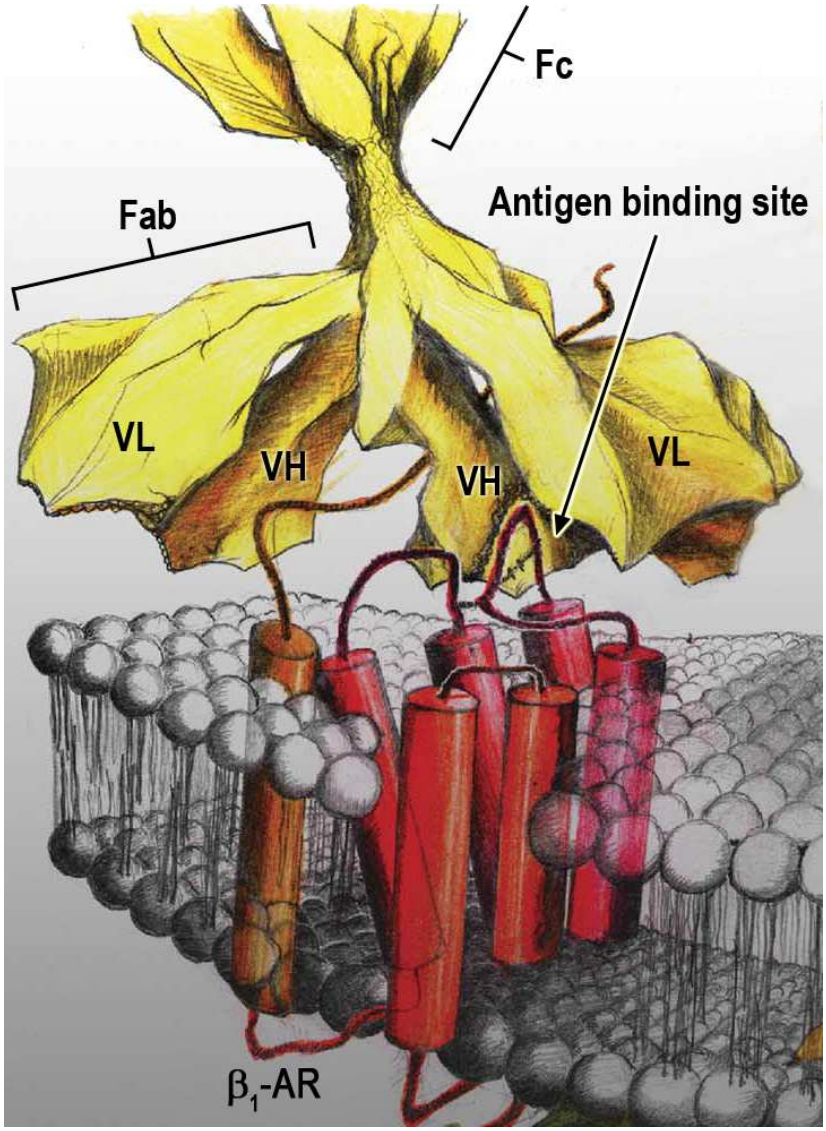

Figure 1.4: Immunoglobulin G (IgG) binding to the β_1-AR.

IgG binds with its antigen binding sites to the β_1 -adrenegic receptor at its 2nd ectracellular loop (ECL2). The N-terminus seems to bee involved in the binding as well. The IgG antibody consists of 2 Fab (antigen binding) fragments and a constant (Fc) part. The Fab Fragments consists of Light (VL) and Heavy (VH) strains. The antigen binding sits in front of the Fab arms.

There is a host of partially contradictive data on how autoantibodies found in sera of patients with DCM modulate β_1-AR function. DCM patient autoantibodies seem to combine stimulating and attenuating effects on the β_1-AR. Some autoantibodies

decrease the response of adenylate cyclase to isoproterenol {Limas, 1990 #104; Rosenbaum, 1994 #101; Jahns, 2000 #33}, suggesting a cardiodepressant activity. Others enhance basal and agonist stimulated adenylate cyclase activity (Magnusson et al. 1994; Jahns et al. 1999; Jahns et al. 2000; Nikolaev et al. 2007) and induce positive chronotropic and inotropic responses in isolated cardiomyocytes (Magnusson et al. 1994; Christ et al. 2001; Staudt et al. 2001; Wallukat et al. 2001; Christ et al. 2006), suggesting a cardiostimulatory activity and a sensitising of the heart for catecholamines.

In a subgroup of patients, enhancement of basal and attenuation of agonist-stimulated adenylate cyclase activity could be observed in the very same serum samples (Jahns et al. 2000), suggesting that these autoantibodies could decrease the amplitude of β-adrenergic cardiac regulation. Furthermore, positive chronotropism (acceleration of heart rate) induced by autoantibodies in isolated cardiomyocytes seemed not always stringently linked to an increase in cellular cAMP levels and subsequent desensitisation of the receptor in the same manner as stimulation by β-adrenergic agonists (Magnusson et al. 1994; Magnusson et al. 1996).

A similar discrepancy was reported for the effects of β_1-adrenergic agonists and receptor autoantibodies on the amplitude of L-type Ca^{2+} transients in isolated cardiomyocytes, suggesting that the autoantibodies activate the receptor in a manner different from true agonistic ligands (Christ et al. 2006). Another finding revealed that β_1-AR autoantibodies are potent stimulators of the ERK1/2 pathway (Tutor et al. 2007). As putative allosteric modulators, which have the ability to bind topographically distinct from the actual binding site and either have a positive or negative effect on the receptor, autoantibodies could induce an elongation or reduction of an already existing signal induced by agonist or antagonist. Autoantibodies could also attenuate the signal or influence the signal transduction. It is the objective of this work to elucidate the autoantibody impact on receptor conformation in order to provide a molecular mechanism that may explain these seemingly inconsistent observations and hypotheses.

1.3 Aim of the study

As outlined in Fig. 1.5, it is known that autoantibodies against the first and the second extracellular loop of the β_1-adrenergic receptor are frequently found in heart insufficiency of various etiologies. Their prevalence is associated with Chagas disease, dilated cardiomyopathy, or ischaemic heart disease, but not with cardiomyopathies of other etiology. Their therapeutic removal leads to long-termed hemodynamic improvements. A similar chain of evidence has been provided by immunisation experiments of rodents. Thus, it seems quite clear that these autoantibodies cause the disease. However, it is unclear, how the antibodies affect receptor function on the molecular level, and how such effects are related to cardiopathogenesis and disease progression. This work wants to close this gap of knowledge (see Fig. 1.5) by elucidating the molecular mechanism by which autoantibodies alter receptor conformation and activity. The aim is to investigate, how these molecular effects could interfere with normal receptor regulation by catecholamines to result in the disease phenotype, and, furthermore, to find out, which of these molecular effects allow a discrimination of cardiopathogenic autoantibodies isolated from patients with dilated cardiomyopathy from presumably apathogenic autoantibodies found in healthy subjects of similar age and sex. This study thus aims to provide an analytical basis to indicate and monitor therapeutic concepts of blockade or removal of pathogenic autoantibodies.

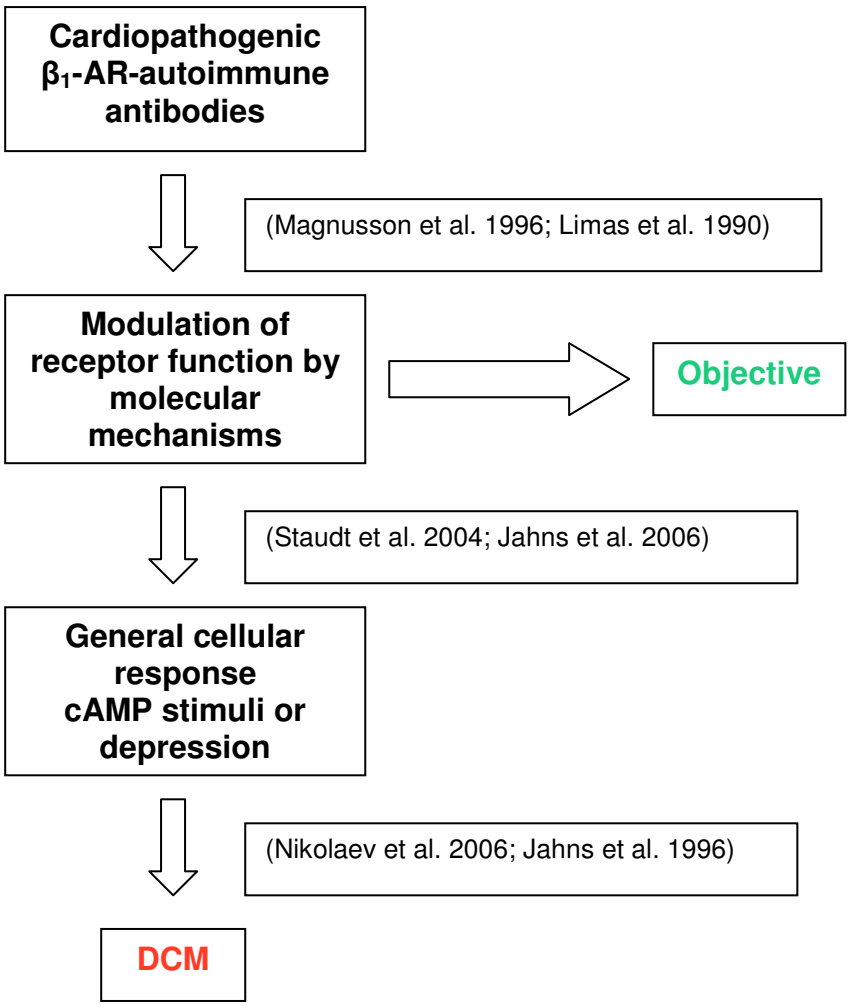

Figure 1.5: Schematic flow-chart to classify the thesis's aim.

Cardiopathogenic autoantibodies were found in the early 90th and rodent studies revealed that the autoantibody could be experimentally generated, could induce DCM symptoms, and this was even transferable to healthy individuals. General cellular response and the controversy between stimulating and depressing effects of IgG were revealed in the beginning of the century. However, the molecular modulation of the β_1-adrenergic receptor function is still not clear and which is why this work was initiated.

2. Material

2.1 Vectors and cDNAs

2.1.1 Expression vectors

Vectors for expression of β_1-AR in human cells (see 3.1.1), were based on the bicistronic expression vector pMC-2PS-delta HindIII-P (see appendix 8.1.B) (Mielke et al. 2000), in which the puromycin resistance gene (pyromycin-N-acetyltransferase, pac) constitutes the second cistron, followed by the simian virus 40 (SV40) polyadenylation signal. In front, pac is linked by an IRES element (Internal Ribosomal Entry Site) to a multiple cloning site (MCS), for the insertion of the gene of interest. A cytomegalovirus promotor (CMV) fused to the myeloproliferative sarcomvirus (MPSV) LTR enhancer repeat ensures a high transcription level of the bicistronic message in various mammalian cells and the transcriptional linkage ensures a fixed simultaneous expression of pac and a gene of interest. To enable the constitutive expression of YFP-tagged proteins, the plasmids pMC-YFP-P-N (see appendix 8.1.C) and pMC-YFP-P (Christensen et al. 2002; Linka et al. 2007) were used in which cloning of the gene of interest into the MCS enables N-terminal or C-terminal fusion to the a yellow fluorescent protein (YFP).

2.1.2 cDNA

The cDNAs of human β_1-AR was kindly gifted from Prof. Dr. T. Frielle, described in (Frielle et al. 1989).

2.1.3 DNA oligonucleotides

All nucleotides used for PCR amplification, oligohybridisation and DNA sequencing were purchased in HPLC grade from IBA (Göttingen, Germany). Primers were listed in tble 2.1.

Table 2.1: Primers with MluI and ApaI restriction sites for β_1-AR used in this work.

Construct	Primer	Sequence
pMC-β_1-AR-YFP-P-N	1) 5`-N-MluI-β_1-AR	5´-GGG CGG ACG CGT ATG GGC GCG GGG GTG CTC GTC CTG-3´
	2) 3´-N-β_1-AR-ApaI	5´-GGG CGG GCC CCT ACA CCT TGG ATT CCG AGG CG-3´
pMC-β_1-AR-YFP-P	3) 5`-C-MluI-β_1-AR	5´-GGG CGG ACG CGT GCC ACC ATG C GGC GCG GGG GTG CTC GTC CTG-3´
	4) 3´-C-β_1-AR-ApaI	5´-GGG CGG GCC CCC CAC CTT GGA TTC CGA GGC GAA G-3´

2.2 Microbiology

2.2.1 Escherichia coli strains

DH5α — Genotype: supE44 ΔlacU169 (Φ80lacZΔM15) hsdR17 recA1 endA1 gyrA96 thi-1 relA1 (Hanahan 1983)

SURE (Stop Unwanted Rearrangement Events) — Genotype: e14-(McrA-) Δ(mcrCB-hsdSMR-mrr)171 endA1 supE44 thi-1 gyrA96 relA1 lac recB recJ sbcC umuC:Tn5 (Kanr) uvrC [F´proAB lacIqZΔM15 Tn10 (Tetr)], Stratagene, (La Jolla, USA)

2.2.2 Bacterial growth media

LB-medium (1 l) — 10 g Trypton, 5 g yeast extract, 10 g NaCl, adjusted to pH 7.5 (by NaOH)

LB-agar — 10 g agar in 1000 ml LB medium (see above)

TB-medium (1 l) 12 g Trypton, 24 g yeast extract, 4 ml Glycerol, dissolved in 900 ml H_2O and autoclaved. 100 ml of sterile phosphate-buffer (0.17 M KH_2PO_4, 0.72 M K_2HPO_4) were added after autoclaving

SOB-medium (1 l) 20 g Trypton, 5 g yeast extract, 0.5 g NaCl, 0.184 g KCl were dissolved in 1 l H_2O, adjusted to pH 7.0 (NaOH) and autoclaved. Before use, 5 ml of 2 M $MgCl_2$ and 20 ml of 1 M $MgSO_4$ were added.

For selection 50 µg/ml ampicillin was added to the media.

2.3 Cell culture

2.3.1 Cell line

HEK 293 Human primary embryonal kidney cell (Graham et al. 1977) #DSM ACC 305, (DSMZ, Braunschweig, Germany)

2.3.2 Supplements and Antibiotics

If not otherwise specified, listed products were purchased from Gibco/Invitrogen, Carlsbad, USA.

Dulbecco's Modified Eagle Medium (DMEM) high glucose
CO_2 Independent Medium (without L-glutamine)
PBS (Ca^{2+}, Mg^{2+} free),
Foetal Bovine Serum (FCS)
Penicillin (10.000 U/ml) and Streptomycin (100 µg/ml) solution
EDTA solution (0.65 µM)
GlutaMAX-I Supplement, 200 mM

Puromycin	(Sigma, St. Louis, USA)
Hygromycin	(Sigma, St. Louis, USA)
DMSO	(Sigma, St. Louis, USA)

2.3.3 Media

Growth medium	DMEM high glucose, 10% FCS, 100 U/ml penicillin, 100 µg/ml streptomycin
Selection medium I	DMEM high glucose, 10% FCS, 100 U/ml penicillin, 100 µg/ml streptomycin, 0.4 µg/ml puromycin
Selection medium II	DMEM high glucose, 10% FCS, 100 U/ml penicillin, 100 µg/ml streptomycin, 100 µg/ml hygromycin
CO_2-independent medium	CO_2-independent medium, 20% FCS, 100 U/ml penicillin, 100 µg/ml streptomycin, 1% GlutaMAX-I

2.4 Buffers and Stock Solutions

6x Agarose loading buffer	15% Ficoll type 400, 40 mM Tris-HCl (pH 8.5), 40 mM glacial acetic acid, 2 mM EDTA, 0.25% bromphenol blue
5x Laemmli buffer	156.25 mM Tris-HCl (pH 6.8), 25% glycerine, 5% SDS, 0.2% bromphenol blue
20x NuPAGE MOPS SDS Running Buffer	supplied by Invitrogen, Carlsbad, USA
10x (Phosphate-Buffered Saline)	1.4 M NaCl, 27 mM KCl, 100 mM Na_2HPO_4 $2H_2O$, 18 mM KH_2PO_4
PBST	1x PBS, 0.05% Tween20
50x TAE buffer	2 M Tris-HCl (pH 8.5), 2 M acetic acid, 0.1 M EDTA
TE buffer	10 mM Tris-HCl (pH 8.0), 0.1 mM EDTA
10x TGS buffer	2.5 M Tris, 1.92 M glycin, 0.1% SDS
10x TBS (Tris-buffered saline)	24.2 g Tris Base, 80g NaCl, pH 7.6 with conc. HCl, filling up to 1 l ddH_2O
TBST	10x TBS, 0.1% Tween20

HBSS (Hanks Balanced Salt Solution)	5.4 mM KCl, 0.3 mM Na_2HPO_4, 0.4 mM KH_2PO_4, 4.2 mM $NaHCO_3$, 1.3 mM $CaCl_2$, 0.5 mM $MgCl_2$, 0.6 mM $MgSO_4$, 137 mM NaCl

2.5 Enzymes

GC-Rich PCR System	Roche, Mannheim, Germany
Expand High Fidelity PCR system	Roche
DNase I free RNase	Roche, Basel, Switzerland
Quick Ligation Kit	NEB, Ipswich, USA
Restriction Enzymes:	
1) Apa I, Mlu I	Amersham, Little Chalfont, USA
2) Bam H1, Pst I	Fermentas, St Leon-Roth, Germany
3) EcoRI, HindIII, NotI, PspOMI, SpeI, XmnI, SmaI, ClaI	NEB, Ipswich, USA
RNase A	Qiagen, Hilden, Germany

2.6 Chemicals

Tween20 (Polysorbate 20)	Sigma, St. Louis, USA
Polyacrylamid Rotiphorese Gel 30	Roth, Karlsruhe, Germany
TEMED	Roth
APS (Amoniumperoxidsulfat)	Roth
Ethidium bromide solution (1%) (EtBr)	Roth
Digitonin High purity	Calbiochem, Darmstadt, Germany
Ultima Gold™	Perkin Elma, Wiesbaden, Germany
IBMX	Sigma
AEBSF hydrochlorid (Pefablock)	Applichem, Darmstadt, Germany
Aprotinin	Applichem
Leupeptin hemisulfat	Applichem

Phenylmethansulfonylfluorid (PMSF)	Applichem
Dithiothreitol (DTT)	Applichem

2.6.1 Agonistic or antagonistic ligands of β-ARs

Table 2.2 β-AR agonistic or antagonistic ligands used in this work.

Name	Specific for	Class	Source
(-)-isoproterenol	$\beta_1+\beta_2$	agonist	Sigma, St. Louis, USA
CGP 20712A	β_1	antagonist	Sigma
Alprenolol	β_1	selective antagonist	Sigma
Bisoprolol	β_1	selective antagonist	Sigma
Propanolol	$\beta_1+\beta_2$	antagonist	Sigma
Metoprolol	β_1	invers antagonist	Sigma
ICI 118551	β_2	antagonist	Sigma
[^{3}H]-(-)-CGP12,177	β_1	antagonist	Amersham, Buckinghamshire, UK

2.7 Antibodies and Peptides

2.7.1 Primary antibodies

Table 2.3 Primary antibodies used in this dissertation.

Antibody	Antigen	Origin	WB/IP	Source
JL-8	GFP	Mouse monoclonal	1:4000 (WB)	#632381, Clontech, Mountain View, USA
Anti-GFP (7.1, 13.1)	GFP	2 Mouse-monoclonals	1:50 (IP)	#1814460, Roche Living Colors A.v, Basel, Switzerland
β-1-AR (V19)	β_1-AR	rabbit polyclonal	1:200 (WB)	#sc-568, Santa Cruz Biotechnology Inc., Heidelberg, Germany
Goat Anti-ADRB1 Antibody	β_1-AR	goat	1:1500 (WB+IP)	# EB07133, Everest Biotech, Germany
Anti-phospho-p42/p44 MAP kinase	Erk1/2	mouse monoclonal	1:2000 (WB)	# 9106, Cell Signaling Technology Inc., USA
p44/42 MAPK (Erk1/2)	p-Erk1/2	rabbit polyclonal	1:1000 (WB)	# 9102, Cell Signaling Technology Inc.

2.7.2 Secondary antibodies

Table 2.4 Secondary antibodies used in this dissertation.

Name	Origin	Dilution	Source
ECL Mouse IgG, HRP-Linked Whole Ab	sheep	1:40000	Amersham, Little Chalfont, UK
ECL Rabbit IgG, HRP-Linked Whole Ab	donkey	1:10000	Amersham
Cy3™ Conjugated goat anti human IgG	goat	1:3200	Jackson Immune Research Europe Ltd, Suffolk, UK
Cy3™ Conjugated rabbit anti sheep	rabbit	1:4000	Jackson Immune Research

2.7.3 Other (Blocking) Proteins

Rabbit-IgG	Sigma, St. Louis, USA
Goat-serum (GS)	Sigma
Bovin serum albumin (BSA)	Sigma

2.7.4 Peptide homologs to the β_1-AR

Table 2.5 Peptides used in this work.

Name	Sequence	Source
Pep1	VWGRWEYGSFFCEL (first extracellular loop)	nanoTools, Freiburg, Germany
Pep2	LMHWWRAESDEARRCYNDPKCCD (second extracellular loop)	nanoTools
Pep3	DSDSSLDEPCRPGFASESKV (C-terminus)	nanoTools

2.7.5 IgG samples from DCM patients and healthy volunteers

IgG-fractions were retrieved from IgG immunoadsorption of ten patients and ten healthy volunteers. Samples were very kindly gifted from Prof. Felix, Prof. Staudt and Dr. Herda from Universitätsklinikum Greifswald Innere Medizin B. Pooled IgGs from healthy blood donors used for immunosubstitution therapy named Sandoglobulin® and Privigen® (CSL Plasma, Marburg, Germany) were also kindly gifted from the group in Greifswald.

2.8 Consumed items

Immobilon-P (PVDF) Transfer Membrane	Millipore, Bedford, USA
NuPAGE Novex 4-12% Bis-Tris Gel	Invitrogen, Carlsbad, USA
Gel cassette Novex, 1 mm	Invitrogen
1 Kb plus DNA Ladder	Invitrogen
Peq Gold Protein marker II	PeQlab, Erlangen, Germany
PeqGold Protein marker IV (prestain)	PeQlab
Dynabeads 100.04D ProteinG-anti IgG	Invitrogen
Protease inhibitor cocktail P2714 (Composition: AEBSF, Aprotinin, Bestatin,E-64, EDTA und Leupeptin)	Sigma, St. Louis, USA

2.9 Kits

QIAquick Gel Extraction Kit	Qiagen, Hilden, Germany
QIAGEN Plasmid Maxi Kit	Qiagen
DNeasy Mini Kit	Qiagen
Effectene Transfection Reagent	Qiagen
BCA Protein Assay Reagent	Pierce, Rockford, USA
ECL Plus Western Blotting Reagents	Amersham, Little Chalfont, UK
ECL Direct Labeling and Detection System	Amersham
cAMP Direct Biotrak™ EIA (non-acetylation protocol)	GE Healthcare, Freiburg, Germany

2.10 Instruments

Horizontal Gel Electrophoresis Apparatus Horizon 11.14	Whatman/ Biometra, Göttingen, Germany
Vertical polyacrylamid gel electrophoresis system Novex Mini-Cell Electrophoresis	Invitrogen, Carlsbad, USA
Semi-dry blot chamber multiphor II novablot	Amersham, Little Chalfont, UK
PCR Cycler Mastercycler	Eppendorf, Hamburg, Germany
Photometer Biophotometer	Eppendorf
PH meter Calimatic 766	Knick, Berlin, Germany
Special accuracy weighing machine AE-166	Mettler Toledo, Giessen, Germany
Ultrasound Homogeniser Sonopuls	Bandelin, Berlin, Germany
Dounce homogeniser	Wheaton Inc., Millville, USA
Incubator shaker SM-30	Edmund Bühler, Tübingen, Germany
Incubator function line B12	Heraeus, Hanau, Germany
Clean bench Hera Safe	Heraeus

Thermomixer Comfort	Eppendorf
Incubator Hera Cell	Heraeus
Rotor for reaction tubes	Labor-Brand, Gießen, Germany
Luminscent image analyser LAS-4000	Fujifilm, Tokyo, Japan
Epifluorescent Inverse Microscope Axiovert 100	Carl Zeiss, Jena, Germany
Delta TC3 Culture Dish System	Bioptechs Inc., Butler, USA
Digital Camera Spot-RT SE Monochrom	Diagnostic Instruments, Sterling Heights, USA
Confocal Laser Scanning Microscope (LSM 510 Meta with a 63X /1.3 DIC oil immersion objective)	Carl Zeiss
Tirf-Microscope IX-81, fast CCD camera, 60X (NA 1.49) oil immersion objective	Olympus Deutschland GmbH, Hamburg, Germany
Centrifuge Centrikon H-401	Heraeus
Betacounter LS 1801	Beckman Instruments, Fullerton, USA
Heto Speed Vac Concentrator	Heto-Holten, Allered, Denmark
Speed vac pump	KnF-Neuberger Laboport, Freiburg, Germany
Centrifuge Rotixa / P	Hettich, Tuttlingen, Germany
Centrifuge 5417R	Eppendorf
Cell Counter Countess™	Invitrogen
Freezing box Cryo 1°C Freezing Container	Nalge Nunc, Rochester, USA
Water-bath WBT-22	P-D Industriegesellschaft mbH Medingen, Dresden, Germany
Autoclave V 150	Systec, Wettenberg, Germany
Magnet Rack Dynal MPC-M	Invitrogen

2.11 Computer software and statistic analysing programs

ImageJ 1.4.2Q	National Institute of Health, Bethesda, USA
GraphPad PRISM 4.0a	GraphPad Software Inc., USA
Meta Series 6.3 Software	Molecular Devices, Downingtown, USA
Zeiss Laser Scanning Mikroskop 510 Meta Software Version 3.2, Service Pack 2	Zeiss, Oberkochen, Germany
Multi Gauge	Fujifilm, Tokyo, Japan

3. Methods

3.1 Cloning

3.1.1 Plasmid construction

The wild type sequence of the human β_1-AR retrieved from the pcDNA3-β_1 template (2.1.2) was inserted in front of the IRES sequence in pMC2PSΔHindIII (Mielke et al. 2000) by linker PCR (using primer pair 1 and 2 in 2.1.3), thereby generating pMC-β_1-AR (Fig. 3.1, Wild type). To construct β-adrenergic-YFP fusion proteins, generation of the vector pMC-β_1-AR-YFP-N (see appendix 8.1C) by subcloning the cDNA of β_1-AR into pMC-YFP-P-N (see 2.1.1) was performed. YFP of pMC-YFP-P-N was extended in frame at the 5'end with the sequence encoding the β_1-AR, generating pMC- β-AR-YFP-P (Fig. 3.1 image 2).

For kinetic studies, constructs of β_1-AR containing internal YFP were prepared by insertion of the coding sequence for YFP into the third intracellular loop by removal of the coding sequence between Pro292 and Gly304 (β1) (Figure 4.1). In a following step this YFP was exchanged by a CFP and insertion of CFP into the third intracellular loop of the receptor achieved constitution of a FRET -donor/acceptor pair (3.1 image 4) reporting the activation associated conformational receptor switch and this was accomplished by overlap extension PCR (Horton et al. 1989). All inserted fragments were verified by sequencing.

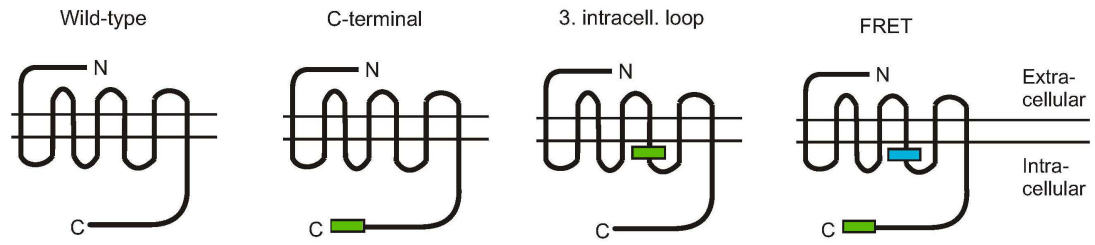

Figure 3.1: β_1-AR constructs.

The first image shows the wild type construct encoding for the β_1-AR. The other three images show constructs where the human β_1-AR was fused to YFP at the C-terminal end or to the 3rd intracellular loop or both, respectively.

3.1.2 Overlap extension PCR

PCR used to generate the basic fusion construct of β_1-AR by bicistronic plasmid construction (Fig. 8.1). To recombine two proteins, fragments of their genes are generated in separate PCRs using primers (see 2.1.3) designed to create products which contain complementary sequences at their ends. These PCR products overlap partially and extension of the matching sequence produces a molecule in which the original sequences are 'spliced' together (Horton et al. 1989).

PCR conditions:

Denaturation	3' 95°C

Addition of polymerase

Denaturation	30" 94°C	25 cycles
Anealing	30" 56°C	
Elongation	2' 72°C	
Final elongation	8' 72°C	

3.1.3 Standard PCR

To generate the construct metioned in Figure 3.1 PCR was performed using the expand high fidelity PCR Kit (Roche). To reduce non-specific amplificons and increase the target yield, Hot Start PCR was used under the following conditions:

Denaturation	2’ 96°C	

Addition of polymerase

Denaturation	30” 94°C	25 cycles
Anealing	30” 55°C	
Elongation *	1-3’ 72°C	
Final elongation	12’ 72°C	

*) Depending on the length of the expected PCR product

3.1.4 Purification of PCR products

PCR products were purified from primers and nucleotides before restriction digestion using the Qiaquick PCR purification Kit (Qiagen) according to the manufacturer’s protocol. The purified fragments were finally dissolved in 30 µl 10 mM Tris pH 8.0 buffer.

3.1.5 Gel electrophoresis and recovery of DNA from agarose gels

DNA fragments can be separated in an electric field according to their size by agarose gel electrophoresis. The used concentration of the agarose was dependent on the size of the DNA fragments. Agarose was melted by boiling in 1x TAE buffer. After cooling to 60°C, EtBr was added to a final concentration of 1 µg/ml and the solution was poured into a horizontal casting tray and allowed to solidify. For electrophoresis, the gel was placed in a gel chamber and was covered with 1x TAE buffer. Samples mixed with 6x DNA loading buffer were loaded onto the gel and separated. Electrophoresis was performed at 90-120 V for 45 min. After the run, the

separated DNA bands were visualized using a transilluminator at 280 nm and size was analysed using DNA size marker.

3.1.6 Restriction digestion

3.1.6.1 Analytical restriction digestion

Analytical restriction digestion was used to check for the correct orientation and length of the inserted DNA fragment into the plasmid vector. 1-2 µg of plasmid DNA was digested with 5 units of restriction enzyme (2.5) using the buffer recommended by the manufacturer. Digests were incubated for 1 h at 37°C. The DNA fragments were analysed by agarose gel electrophoresis.

3.1.6.2 Preparative restriction digestion

The preparative restriction digestion was used to isolate specific DNA fragments. 2-4 µg of plasmid DNA was digested with 5-10 units of restriction enzyme in the appropriate buffer for 1 h at 37°C. DNA was separated by agarose gel electrophoresis. The DNA bands were cut from the gel as visualized at a transilluminator (280 nm). DNA was extracted from the gel using a Qiagen gel extraction kit according to manufacturer's instruction.

3.1.6.3 Partial restriction digestion

Plasmid DNA (4-5 µg) was digested with a single cutting enzyme (5-10 units) at 37°C. After 1 h appropriate dilutions (2, 0.57, 0.163, 0.046 units) of the multi cutting enzyme were added to the final volume of 35 µl. The partial digestion was carried out at 37°C for 15 min and analysed with agarose gel electrophoresis and DNA of interest was excised and purified as described (3.1.5).

3.1.7 Ligation

To insert restriction fragments into vectors, the Quick Ligation kit (NEB) was used according to manufacturer's instructions. Ligation was performed in a final volume of 10 µl for 10 min at RT and then transferred to 4°C before transformation (see 3.1.8.2).

3.1.8 Transformation and isolation of plasmid DNA

3.1.8.1 Generation of competent *E. coli* cells

E.coli cells were grown in 1 L SOB medium at 18°C and harvested by centrifugation (4000 x g, 20 min, 4°C), at a OD_{600} of 0.5-0.8. The cells were gently resuspended in 40 ml ice-cold TB buffer (10 mM Pipes, 55 mM $MnCl_2$, 15 mM $CaCl_2$, 250 mM KCl), incubated for 20 min on ice and again sedimented (4000 x g, 20 min, 4°C). Cells were resuspended in 20 ml ice-cold TB buffer and DMSO was added gently to a final concentration of 7%. After 10 min incubation on ice, aliquots (0.2 ml) were frozen in liquid nitrogen and stored at -80°C.

3.1.8.2 Transformation of *E. coli*

An aliquot of competent cells (0.2 ml) was mixed with 2 µl ligation reaction mixture, incubated on ice for 30 min, heat shocked at 42°C for 30 sec and immediately transferred to on ice. LB-media (0.5 ml, 37°C) was added to the cells, mixed and incubated for 1 h at 37°C under vigorous shaking (250 rpm). Thereafter, transformed cells were transferred to LB-agar plates containing 50 µg/ml ampicillin.

3.1.8.3 Plasmid preparation at a small scale (Minipreps)

Single colonies from the selection plate were picked and inoculated in 2.5 ml TB medium containing 50 µg/ml ampicillin and incubated overnight at 37°C under shaking (250 rpm). After approximately 14 hours, 2 ml of the culture were pelleted (6800 x g, 2 min, 4°C). The cell pellet was mixed with 400 µl lysis solution (0.2 N NaOH, 1% SDS), immediately neutralised with 300 µl 7.5 M NH_4oAC, kept for 10 min on ice to precipitate genomic DNA and proteins before lysates were cleared by centrifugation (14000 x g, 10 min, 4°C). Plasmid DNA was precipitated from the supernatant with 500 µl 2-propanol and pelleted (14000 x g, 30 min, 4°C). The DNA pellet was washed with 70% EtOH, dried and resuspended in 50 µl TE (10 mM Tris-HCl pH 8.0, 1 mM EDTA) supplemented with 50 µg/ml RNaseA. The plasmids sequence was finally confirmed by restriction digestions and sequencing.

3.1.8.4 Plasmid preparation at a large scale (Maxipreps)

A single colony from a selection plate was picked and inoculated in a primary culture of 3 ml selective TB medium (containing 50 µg/ml ampicillin) and incubated for approximately 8 h at 37°C under shaking (250 rpm). Afterwards the starter culture was diluted into 250 ml selective TB medium and grown overnight under the conditions mentioned above. Bacterial cells were harvested by centrifugation (6000 x g, 15 min, 4°C) and the purification of plasmid DNA was performed with Plasmid Maxi Kit Qiagen according to the manufacturer's protocol. DNA concentration was determined spectrophotometrically at 260 nm.

3.1.8.5 Sequencing of plasmids

Sequencing of the constructs was performed by the BMFZ (Biologisch-Medizinisches Forschungszentrum) of the Heinrich-Heine-University Düsseldorf (Germany). Obtained sequences were compared to expected ones using Ape Software.

3.2 Cell culture

3.2.1 Maintenance of mammalian cells

HEK-293 cells were maintained as subconfluent monolayer cultures in growth medium (see 2.3.3) at 37°C in a humidified atmosphere containing 5% CO_2. For passage, cell layers were washed once with PBS, detached by a short treatment with EDTA (0.625 µM in PBS) and reseeded upon dilution with culture medium (1:6 every 2 days).

3.2.2 Freezing and thawing of cells

For freezing cells were detached, resuspended and centrifuged (300 x g) for 3 min. The cell pellet was resuspended in 1 ml FCS containing 10% DMSO and transferred to cryo-tubes (1.8 ml) and transferred to 2-propanol freezing boxes. Tubes were transferred to liquid nitrogen for long term storage after 24 h at -80°C.

For thawing procedures, cryo tubes were thawed in a water bath (37°C). Cells were immediately transferred into Falcon tubes with 5 ml culture medium (37°C) and centrifuged (300 x g) for 3 min, medium containing DMSO was replaced and cells were seeded to a new culture flask.

3.2.3 Transfection and selection of HEK293 cells

Confluent cells ($1x10^6$) were diluted (1:5) 24 hours before transfection. Cells were transfected with 1 µg DNA using Effectene Transfection Reagent (Qiagen) according to the manufacturer's instructions. For cotransfection studies, a total of 2 µg DNA was used. Transient expression could be estimated by microscopy after 12-24 hours with a transfection efficiency varying between 20-90% depending on the construct used. 24 h after transfection, media containing Effectene reagent were replaced by fresh media and incubated overnight at 37°C. Thereafter cells were appropriately diluted into tissue culture dishes and stable cell clones were selected with selection medium (see 2.3.3). Stable expressing clones were expanded and maintained in selection medium.

3.3 Protein analysis

3.3.1 Preparation of whole cell lysates

HEK293 cells ($3x10^6$) were pelleted washed and resuspended in 100 µl PBS. Cell lysis was performed by adding 100 µl of 2x lysis buffer (250 mM Tris-HCl, pH 6.8, 2% glycerol, 4% SDS, 20 mM DTT, 1.4 M urea, 20 mM EDTA, 2 mM PMSF, 5 mM pefa block, 0.04% bromphenol blue) and homogenising by ultrasound (15 s at 20% power). Subsequently, samples were boiled (98°C, 5 min) and warm aliquots equivalent to $3x10^5$ cells were loaded onto SDS-polyacrylamide gels.

3.3.2 Preparation of βAR-solubilisates

Cells were solubilised with 0.5% digitonin, (Calbiochem, Darmstadt, Germany) and incubated for 10 min followed by homogenisation with a Dounce plunger (4° C, 5 min) in 25 mM TRIS, pH 7.5, containing 150 mM NaCl and a standard protease inhibitor cocktail (Sigma, Munich, Germany). β-ARs were separated from the membrane after sedimentation of debris (10000 x g, 10 min.) and solubilisates (supernatants) were split into aliquots and stored at -80°C.
Protein content was determined by the Pierrce BCA protein assay according to manufacturer's protocol.

3.3.3 Polyacrylamide gel electrophoresis

Electrophoresis was performed in 1x TGS buffer (chapter 2.4) or for NuPAGE gels in 1x MOPS SDS running buffer (chapter 2.4) at voltage of 50-160V.

3.3.4 Immunoblotting

3.3.4.1 Western Blot

After separation, proteins were electrophoretically transferred from the gel to a PVDF membrane by the semi-dry method. Briefly, five 3MM paper filters soaked in K-buffer (40 mM 6-aminohexan acid pH 7.6) were stacked on the cathode side of the gel, while the PVDF membrane soaked in MeOH, one 3 MM paper filter soaked in A2-buffer (25 mM Tris-HCl pH 10.4, 20% MeOH), and two paper filters soaked in A1-buffer (300 mM Tris-HCl pH 10.4, 20% MeOH) were stacked on the anode side of the gel. Subsequently, the stack was placed between two graphite plates and the protein transfer was carried out at 0.8 mA/cm^2 for 1-2 h (depending on the size of the protein of interest). After transfer, the PVDF membrane was incubated in PBS containing 0.05% Tween 20 and 5% milk powder overnight at 4°C. After blocking, the membrane was briefly washed with PBS containing, 0.05% Tween 20 and incubated for 1 h with the primary antibody diluted in PBS containing, 0.05% Tween 20 and 1%

BSA and washed three times (3x 10 min). The membrane was then incubated for 1 h with the secondary peroxidase conjugated antibody diluted in PBS containing, 0.05% Tween 20 and 1% BSA. The membrane was again washed and the protein bands were visualised by chemiluminescence using the ECL Plus system (Amersham) and a luminscent image analyser (LAS-4000 see 2.10). Band intensities were analysed by the analysing program Multi Gauge (see 2.11).

3.3.4.2 Immunoprecipitation

β_1-AR-solubilisates (3.3.2) were subjected to immunoprecipitation with human IgG immobilised on Dynabeads 100.04D according to manufacture's instructions. Subsequent steps followed published procedures (Jahns et al. 1996; Linka et al. 2007). Solubilisates or immunoprecipitates were analysed with SDS-polyacrylamide (12%) gel electrophoresis and GFP-directed immunoblotting (3.3.4.1).

3.4.1 Immunocytochemistry

3.3.4.1 Fixation of cells

Cells were grown on microscop coverslips, washed in PBS and either incubated with human autoimmunoantibodies (0.67 µg/ml in PBS for 20 min at 37°C) or FCS free medium. Cells were washed, prefixed for 5 min in a two-well system, where the slide was placed in one well and the other well contained 37% formaldehyde. This vapour formaldehyde prefixation ensured that cellular structures survived the following procedures. To guarantee complete fixation of the cells, the slides were also incubated with ice cold 100% acetone for 5 min on ice. All subsequent steps were carried out at room temperature and in a humidified atmosphere. After washing with PBS, cells were blocked for 1 h in blocking buffer (PBS containing 5% goat serum). After washing once with wash buffer (PBS with 0.5% goat serum) the bound antibody was counterstained by incubation (1 h) with Cy3™-conjugated goat anti-human-IgG secondary antibody. Coverslips were then washed three times for 10 min in PBS, overnight at 4°C and again three times for 1 h at room temperature. Slides were finally mounted in antifade solution (PBS containing 1.5% N-propyl-galate and 60% glycerol), and inspected by confocal microscopy.

3.4 Microscopy

3.4.1 Fluorescence microscopy

Epifluorescent images were acquired using an inverted microscope equipped with a cooled charge coupled device camera. For observation of living cells, cells were grown and inspected in CO_2-independent medium (see 2.3.3) using live-cell chambers to keep the cells at 37˚C.

3.4.2 Confocal microscopy

Confocal imaging of living cells and fixed specimen was performed at 37°C using a Zeiss LSM 510 inverted confocal laser scanning microscope equipped with a 63x/1.4 NA oil-immersion objective. Cells were grown in CO_2-independent medium and Zeiss incubator XL facilitated 37 °C during live imaging microscopy.

3.4.3 Förster (Fluorescence) Resonance Energy Transfer (FRET)

FRET, also known as fluorescence resonance energy transfer, is a technique describing energy transfer between two fluorophores (see Figure 3.2). A donor fluorophore transfers energy to an acceptor fluorophore if it is in proximity less than 10 nm through nonradiative dipole–dipole coupling (see Figure 3.2). This mechanism is termed "Förster resonance energy transfer" named after the scientist Theodor Förster (Stryer 1978). The Förster Effect can be used for different types of methods that all take advantage of the fact that energy can be transfered using two flourophores in very close proximity (Fig. 3.2). FRET measurements, Acceptor Photobleaching (3.4.4) and Fluorescence lifetime imaging (3.4.5) are methods using this effect and used in this work.
Cells grown on glass slides were maintained in serum free media (DMEM) at 37°C under an LSM 510 Meta inverted confocal microscope. To monitor conformational changes of the receptors by changes in intramolecular FRET-efficiency, the donor

CFP was excited at 458 nm and fluorescent emission was recorded using the Meta detector. CFP and YFP emission spectra were separated by emission fingerprinting and corrected for bleaching during image acquisition.

FRET-efficiency was expressed as the ratio of emission intensity

$$\frac{(I_{YFP})}{(I_{CFP})}.$$

This method is capable of reporting the activation associated intramolecular switch of receptor conformation by a drop in the ratio of FRET-acceptor and -donor fluorescence emission (I_{YFP}/I_{CFP}). Maximal decreases (Δ_{max}) of I_{YFP}/I_{CFP} upon stimulation.

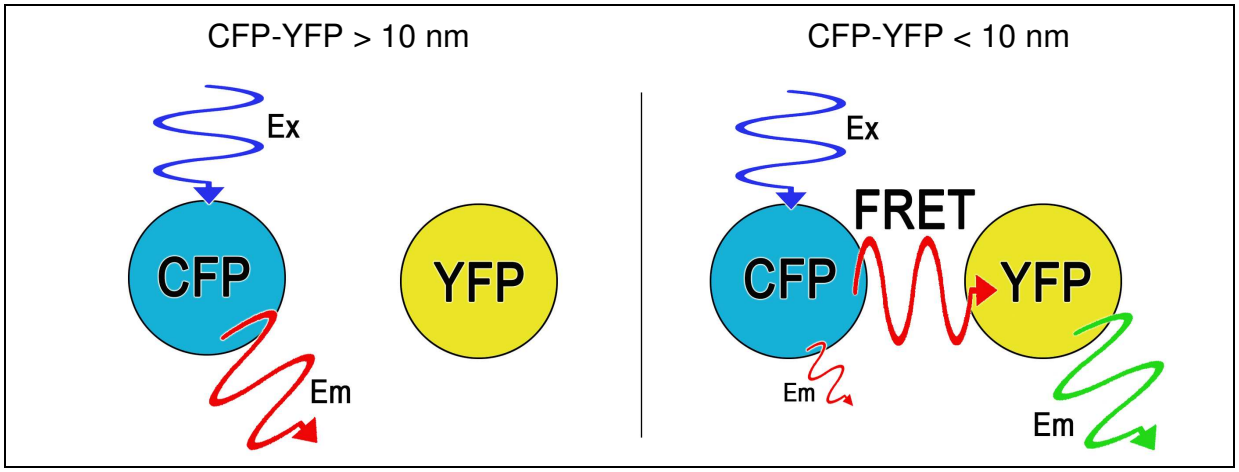

Figure 3.2: The principle of FRET

If one of two fluorophores gets excited it emits light. If the same fluorophore gets excites while being in close proximity to another fluorophore it emits less light and due to an energy transfer instead the other fluorophore is emitting light.

3.4.4 Acceptor- Photobleaching

The principle of this method is to bleach the acceptor fluorophor of a FRET construct and measure the fluorescence intensity over time. For Fluorescence Photobleaching experiments, a single optical section was acquired. Photobleaching decays were measured by irradiating a section usually from the size of one cell with the laser and recording the fluorescence intensity for each laser shot. Curves were recorded for a

range of laser pulses. The imaging scans were acquired with a laser power attenuated to 4% of the bleach intensity. Images were taken at 2 s intervals before and after bleaching of a choosen area with nominal laser power of 100 iterations. For quantitative analysis, fluorescence intensities of the bleached region in YFP and CFP channel were measured at each time point. Data were corrected for extracellular background intensity and for the overall loss in total intensity as a result of the bleach pulse itself and the imaging scans. Unless stated otherwise, photobleaching experiments were analysed by calculating the relative intensity of the bleached area.

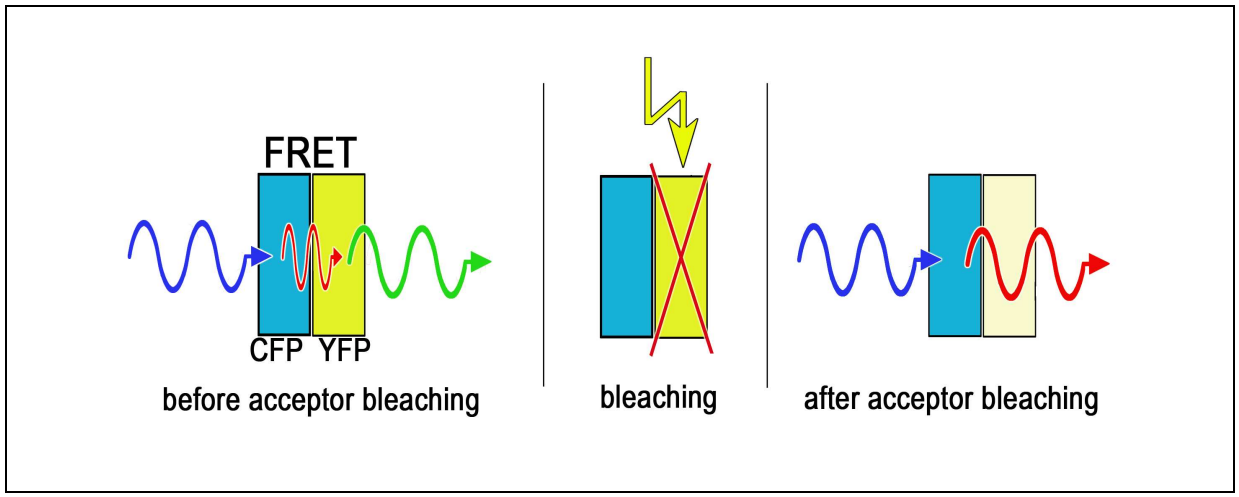

Figure 3.3: Principle of fluorescent photobleaching.
Fluorescence photobleaching is a method to measure the appearance of FRET. If one fluorophore gets excited and fluorophores emmite light FRET occurs. If then the acceptor fluorophore is bleached away the emmited energy of the donor fluorophore will be stronger.

3.4.5 Fluorescence Lifetime Imaging Microscopy (FLIM)

Principle of FLIM is to measure the lifetime of the fluorophore remaining in different energy states after being excited.
Cells grown on coverslips were maintained in serum free medium (DMEM) at 37℃ under a DCS-120 Confocal Scanning FLIM system (Becker & Hickl GmbH) mounted on an IX-71 inverted microscope equipped with a 60X (NA 1.2) water immersion objective (2.10) and placed inside a cage incubator (Okolab, Naples, Italy). The FRET donor CFP was excited using a 405 nm diode laser (Becker & Hickl GmbH)

with a pulse repetition rate of 50 MHz. Fluorescence signals in the CFP channel (BP 460–500 nm) and the YFP channel (BP 520-550 nm) were detected using H7422P-40 photomultipliers (Hamamatsu, Herrsching) connected to two TCSPC-150 modules (Becker & Hickl GmbH). Fluorescence lifetime imaging (FLIM) of living cells was done by continuous fast scanning. To describe fluorescence lifetime, TCSPC data were fitted by a double exponential decay function using SPC Image software (version 2.9.1, Becker & Hickl GmbH). Mean lifetime τ_m was calculated from multi exponential decay of each pixel in a lifetime image according to:

$$\tau_m = \sum_{i=1}^{N} a_i \tau_i / \sum_{i=1}^{N} a_i$$

with the intensity coefficient a_i given as relative amplitude.

3.4.6 Total Internal Reflection Microscopy (TIRF)

Receptor cycling was determined by TIRF of cells cultured under an IX-81 inverted microscope equipped with a fast CCD camera and a 60X (NA 1.49) oil immersion objective (Olympus Deutschland GmbH). The illumination angle was adjusted to create an evanescent wave exciting YFP-fluorescence in a 200 nm cytosolic slice above but not including the basal cell membrane. Following addition of (–)-isoproterenol and/or receptor autoantibodies, the density of biofluorescent receptosomes in this cell slice was measured over a time period of 1000 s and averaged (using ImageJ, see 2.11).

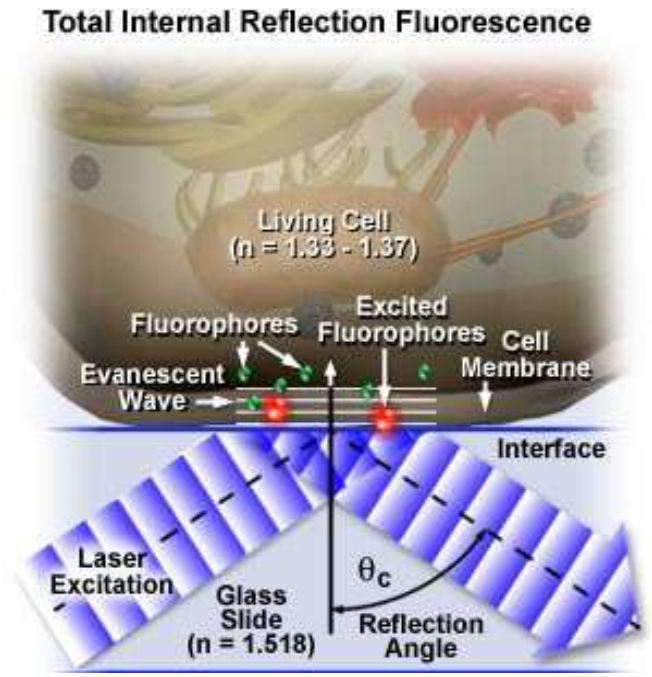

Figure 3.4: TIRF principle.
The laser excites energy onto a glass slide and an evanescent wave is generated at the interface of two media that have different refracting indices. This wave declines exponentially and in consequence only excites fluorophores at a distance of approximately 200nm insight the cell. Therefore this technique allows to visualise events exclusively at or just beneath the cell membrane of living cells. Picture adapted from www.olympusmicro.com.

3.5. Signal transduction analysis

3.5.1 Ligand-binding assay

Receptor expression and number in intact cells was measured using the β_1AR antagonist [^{3}H]-(–)-CGP12,177 (2.6.1). Stable transfected HEK293 cells (3.2.3) were seeded into 96 well plates coated with poly-L-Lysin and grown at 37°C for 24 h. Cells at a density of 0.5-1x10^4 were incubated with [^{3}H]-(–)-CGP12,177 (5–1200x10^{-12} mol/L) in a final volume of 0.2 ml of HBSS buffer supplemented with HEPES (pH 7.4). Affinity of isoproterenol was determined under the same conditions by displacement of [^{3}H]-(–)-CGP12,177 (5.67 pM) by unlabeled isoproterenol (10^{-9}-10^{-3} mol/L). Binding at 37°C was terminated after 45 min followed by threefold medium exchange. Cells were lysed by incubation for 30 min with 1 ml NaOH (0.5 M) at RT on a shaker. Afterwards 800 µl lysate from each well was taken and together with 4 ml szintillation-solution (LumaLSCR) properly mixed and analysed with a counter (LS 1801). Non-specific binding was determined as < 2.5% of total binding. Maximum specific binding (B_{max}) and the dissociation constant (K_D) were determined using non-linear regression and assuming a K_D-value of [^{3}H]-(–)-CGP12,177 for β_1-ARs of 2 × 10^{-10} mol/L (Lemoine et al. 1992).

3.5.2 Ligand competition assay

For competition binding studies with the β_1-selective adrenergic antagonist CGP20,712A (Lemoine et al. 1991) and the β_2-selective adrenergic antagonist ICI118,551 (Lemoine et al. 1985), cells were homogenised in 2.5×10^{-2} mol/L TRIS, pH 7.5, containing a standard protease inhibitor cocktail (Sigma, Munich, Germany). Homogenates were sedimented (40,000 x g for 20 min at 4°C), resuspended in 7.5×10^{-2} mol/L TRIS, pH 7.4, 1.2×10^{-3} mol/L $MgCl_2$, 2×10^{-3} mol/L EDTA, and 5-20 µg of protein were incubated with 5×10^{-11} mol/L [125I]-(–)-cyanopindolol (Amersham Biosciences, Freiburg, Germany), 500 µM Gpp(NH)p (Sigma, Munich, Germany), and various concentrations of displacing ligand. Non-specific binding was determined in the presence of 10^{-5} mol/L isoproterenol as < 15% of total binding. Binding reactions were carried out for 90 min at 25°C and terminated by rapid filtration through Whatman GF/C glass fiber filters presoaked in PBS containing 0.3% polyethyleneimine using a Brandel cell harvester. Data were analysed with Prism.

3.5.3 cAMP-Assay

To generate lysates facilitating cAMP measurements, HEK293 cells were cultured in 6-well plates (Greiner Bio-one, The Netherlands) at a density of $3x10^5$ cells/well and hold for 24 h in serum free medium. Cells were washed with PBS and incubated for 20 min with samples of interest. Cellular processes were stopped by aspirating the medium, scraping the cells from the plate; centrifuging (800 rpm) for 5 min and adding 1 ml ice cold 98% Ethanol to the cell pellet. The Following steps followed published procedures by (Hoonakker et al. 2010).

Cells were then sonificated for 10 s at 50% power, centrifuged (2000 x g for 15 min) and the supernatant was dried in a Speed Vac at 60°C. Dried supernatant was then dissolved in assay buffer (Amersham) and frozen by –80°C. Assay was performed after manufactures instructions for the non acetylating cAMP assay from Amersham.

3.6 IgG-sample preparation

3.6.1 IgG samples from DCM patients and healthy volunteers

IgG-fractions were retrieved from unselective IgG immune adsorption of ten patients (table 3.1) suffering from DCM refractory to conventional therapy (Dorffel et al. 2004, Felix, 2002 #75). Patients were admitted to therapy with New York Heart Association (NYHA) states III - IV, left ventricular ejection fractions (LVEF) of 19-31% and left ventricular enddiastolic diameters (LVED) of 52-84 mm under stable medication. Each IgG sample represents the absorber eluent of an individual patient and treatment cycle. Control IgG was extracted by the same protocol from blood samples of a matched group of ten healthy volunteers (table 3.1). As further controls served pooled IgGs from healthy blood donors used for immunosubstitution therapy Sandoglobulin® and Privigen® (2.7.5). IgG concentrations were determined by procedures accredited for clinical diagnosis. For specificity control, IgGs were preabsorbed with a 1000-fold molar excess of peptides (nanoTools, Freiburg, Germany) homologous to the first or the second extracellular loop of the human β_1-AR (2.7.4).

Table 3.1: Clinical characterisation of DCM patients and healthy volunteers (controls).

	Controls (n=10)	DCM Patients (n=10)
Age (y)	37,5 ± 3,8	52,7 ± 2,5
Sex (m/f)	9/1	9/1
LVEF (%)	61,9 ± 1,4	27,3 ± 1,5
LVEDD (mm)	48,7 ± 1,3	71,3 ± 3,2
NYHA	N/A	2,6 ± 0,2
Medication		
ACE-I (%)	0	100
ARB (%)	0	10
β-blocker (%)	0	100

Diuretics (%)	0	90
Myocardial biopsy		
Inflammation present (%)*	N/A	80
Viral RNA present (%)	N/A	30

* Inflammation was considered to be present if immunohistochemistry of myocardial biopsies revealed focal or diffuse mononuclear infiltrates with >14 leucocytes per mm^3 (CD3+ T-lymphocytes and /or CD68+ macrophages) in addition to enhanced expression of HLA class II molecules.

- ACE-I, Angiotensin converting enzyme inhibitors; ARB, angiotensinogen receptor blocker; β-blockers, β-adrenergic receptor blocking agents; diuretics as pharmacological treatments available.
- NYHA - The New York Heart Association provides a simple way of classifying the extent of heart failure for example in patients with DCM. It places patients in one of four categories based on how much they are limited during physical activity; the limitations/symptoms are in regards to normal breathing and varying degrees in shortness of breath and angina pain (is a type of chest pain that occurs before myocardial infarction).

3.7 Statistics

Quantitative results are represented as mean values ± standard error of the mean of measurements carried out in duplicate or triplicate on independent cell clones expressing the same construct. Data sets were compared by an unpaired U-test and the zero hypotheses were rejected on a probability level of <0.05 (i.e. $P<0.05$ was considered significant).

4. Results

The primary aim of this study was the investigation of autoantibodies effecting the β_1-adrenergic receptor (β_1-AR) function. I tried to figure out what is the molecular mechanism behind the autoanitbody induced alteration of receptor conformation and activity.

To investigate this I established an experimental model of fluorescently labelled β_1-ARs in human embryonic kidney cells and characterised this model by microscopy and immunoblotting techniques. To figure out receptor binding capacity the receptor quantity was determined. Therefore ligand binding and affinity assays were performed. The conformational switch was investigated by FRET analysis and second messenger measurements enable to investigate signal transduction and therefore activity of the receptor.

After characterising the cell constructs, autoantibodies retrieved from immunoadsorption of patients with dilated cardiomyopathy (DCM) were specified in terms of concentration and alteration of the β_1-AR using similar techniques. I thus will first introduce the results gained in experiments used for characterisation of the constructs, then show how autoantibodies derived from patients were ranged in therapy analytics and further will describe the results of the investigation of β_1-AR modulation induced by autoantibodies. Finally statistical analyses of the retrieved results are shown.

4.1 Characterisation of the experimental model

4.1.1 Stable expression of biofluorescent human β_1-adrenergic receptors in HEK 293 cells

Human β_1-ARs bearing in-frame the sequence of CFP in the third intracellular loop and/or the sequence of YFP appended to the C-terminus were expressed in HEK 293 cells. For each construct (Fig. 4.1A), several cell clones supporting constitutive expression of biofluorescent receptors in the cell membrane were isolated and

characterised. In GFP-directed immunoblotting (Fig. 4.1B), the recombinant receptors exhibited the expected electrophoretic mobility (given theaddition of one or two GFP-like moieties) and a double-banded pattern known to reflect physiological heterogeneity in glycosylation (Dohlman et al. 1987; Boege et al. 1988; Jahns et al. 1996). Receptor associated fluorescence was exclusively located in the outer cell membrane. Double-labelled constructs exhibited a complete overlap in the patterns of the two labels (Fig. 4.1C, top), and brief exposure to isoproterenol induced internalisation of the receptors into vesicles (Fig. 4.1C, bottom). Time frame (10 min) and extent (30%) of receptor internalisation were as reported by others (McLean et al. 2000; Xiang et al. 2002; Burgi et al. 2003). These control experiments ascertained that the heterologous receptors were of the proper size, appropriately folded and inserted into the cell membrane, and responsive to agonists.

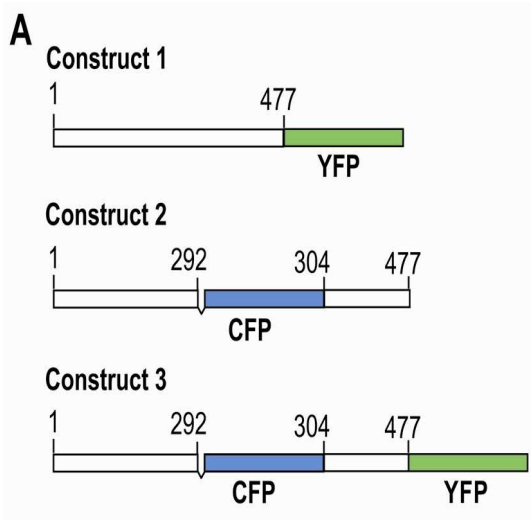

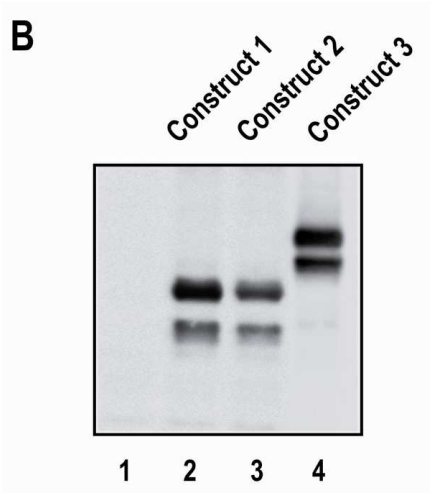

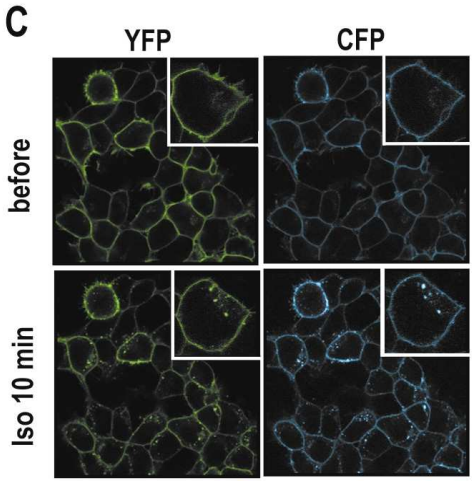

Figure 4.1: Constructs of the β_1-AR targeted with CFP and YFP.

(A) Human β_1-AR was fused to YFP at the C-terminal end (constructs 1 and 3). Alternatively (construct 2) or in addition (construct 3), CFP was inserted into the third intracellular loop replacing residues 293-303. **(B)** GFP-directed immunoblotting of untransfected cells (lane 1) or cells expressing constructs 1 (lane 2), 2 (lane 3), or 3 (lane 4). **(C)** Cells expressing construct 3 were subjected to confocal imaging in mid plane of yellow (left) and blue fluorescence (right) before (top) and 10 min after (bottom) exposure to 10^{-5} mol/l isoproterenol.

4.1.2 Ligand binding characteristics of the hererologously expressed β_1-AR

It is important to know the quantity of receptors on the cell surface to figure out the amount of ligand one has to use. Binding of the β-adrenergic agonist isoproterenol to cells transfected with β_1-AR bearing the FRET sensor (construct 3) was assessed by competition with [^{3}H]-(-)-CGP12,177 (Fig. 4.2). To avoid depletion of radioligand by extensive binding to overexpressed receptors a high concentration of radioligand (> 5×10^{-9} mol/l) was used in a high volume of buffer (200µl) resulting in a simple logarithmic curve (Fig. 4.2). The dissociation constant (K_D) values for isoproterenol were estimated by non-linear regression of data as 90.5 ± 4.9 pM, assuming a K_D-value of [^{3}H]-(-)-CGP12,177 for β_1-ARs of c.a. 200 pM (Lemoine et al. 1992). Similar experiments were done with cells transfected with construct 1 and 2 (Table 4.1).

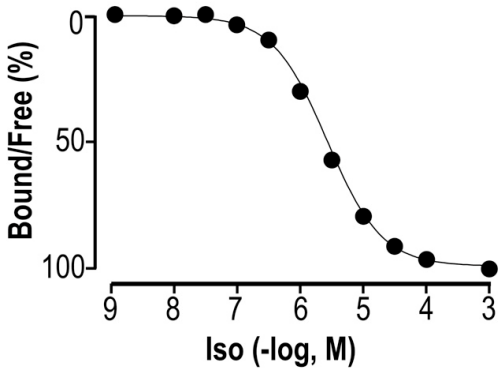

Figure 4.2: Agonist binding to β_1-AR bearing the FRET sensor.

Displacement of [^{3}H]-(-)-CGP12,177 binding by unlabelled isoproterenol in intact cells expressing construct 3 was measured and plotted.

The β_1-subtype of the three receptor constructs was confirmed by binding competition of the unlabeled β_1-selective adrenergic antagonist CGP20,712A (Lemoine et al. 1991) and the unlabeled β_2-selective adrenergic antagonist ICI 118,551 (Lemoine et al. 1985) against the β-subtype unselective radiolabeled β-adrenergic antagonist [^{125}J]-Cyanopindolol. The K_D-value of [^{125}J]-Cyanopindolol was directly determined by the equilibrium binding isotherm as 122 ± 24 pM and was not significantly different in cells transfected with any of the three constructs and untransfected cells (data not shown).

The ligand binding data summarised in Table 4.1 show that the C-terminally YFP-fused receptors were 1000-fold more abundant than endogenous binding sites, and receptors bearing in addition or instead an internal CFP moiety in the third intracellular loop were 600-fold more abundant. All heterologous receptors exhibited β_1-AR ligand binding characteristics, whereas endogenous binding sites accounting for less than 0.2% of B_{max} in the transfected cell lines exhibited β_2-AR binding characteristics (Lemoine et al. 1992). In summary it was thus ascertained that the receptor constructs were fully functional with respect to ligand binding and of the appropriate receptor subtype.

Table 4.1: Ligand binding characteristics of biofluorescent human β_1-ARs stably expressed in HEK 293 cell clones (mean ± SEM, n =3).

	[^{3}H]-(-)-CGP12,177 B_{max} 10^6 sites×cell^{-1}	[^{3}H]-(-)-CGP12,177 K_D pM	CGP20,712A K_i nM	ICI118,551 K_i $^+$ nM	ISO K_i $^+$ nM
untransf.	0.010 ± 0.002	512.0 ± 22	687.1 ± 1.5	0.21 ± 0.14	125 ± 5.8
Construct 1*	8.0 ± 0.66	189.0 ± 64	8.6 ± 1.1	144.0 ± 1.1	111.4 ± 1.3
Construct 2*	4.8 ± 0.89	243.0 ± 38	7.9 ± 2.8	186.0 ± 2.8	133.0 ± 6.1
Construct 3*	4.4 ± 0.52	198.0 ± 42	8.8 ± 2.1	175.0 ± 8.2	129.0 ± 9.2†

*) Numbering of constructs see Figure 4.1A.

†) Maximum specific binding (B_{max}) and dissociation constant (K_D) of isoproterenol (ISO) were also determined in intact cells by displacement of [^{3}H]-(-)-CGP12,177 as 3.42 ± 0.38 × 10^6 sites per cell and 100 nM, respectively.

$^{+)}$ Dissociation constant (Ki) is an applicable measure of bond-tightness between a receptor and a corresponding receptor inhibitor.

4.1.3 Stimulation of intracellular cAMP via the β_1-AR constructs

Exposure of cells expressing construct 1 or 3 to the full agonist isoproterenol induced increases in intracellular cAMP up to 20-fold, whereas 10-fold increases were induced by the phosphodiesterase inhibitor IBMX. cAMP levels were marginally (<1.5-fold) altered by the inverse agonist CGP20,712A and cAMP response to isoproterenol showed a stringent dose dependence. The lowest concentration of isoproterenol detectable as a > 2-fold increase in intracellular cAMP was 5 nM (Fig. 4.3B), attesting to a high sensitivity of the cells for β_1-AR stimulation. In untransfected HEK 293 cells, cAMP was not significantly stimulated by CGP20,712A or IBMX alone, and marginally (< 2-fold) increased by isoproterenol (Fig. 4.3A). These control experiments ascertained that the heterologous receptors were effectively coupled to cAMP signal transduction, and had a predominantly effect on intracellular cAMP levels despite the known restrictions imposed by the incorporation of fluorescence proteins (McLean et al. 2000). It could therefore safely be assumed that in the transfected cells cAMP responses were highly specific for stimulation through the heterologously expressed β_1-AR. The comparatively high stimulatory effect of the phophodiesterase inhibitor by IBMX alone was assigned to spontaneous oscillations between active and inactive conformations (Chidiac et al. 1994; Hopkinson et al. 2000) also seen in other overexpression systems (Engelhardt et al. 2001). Such conformational idling of the receptors in our model was considered favourable because it might allow detecting IgG interactions with transient conformational states of the receptor.

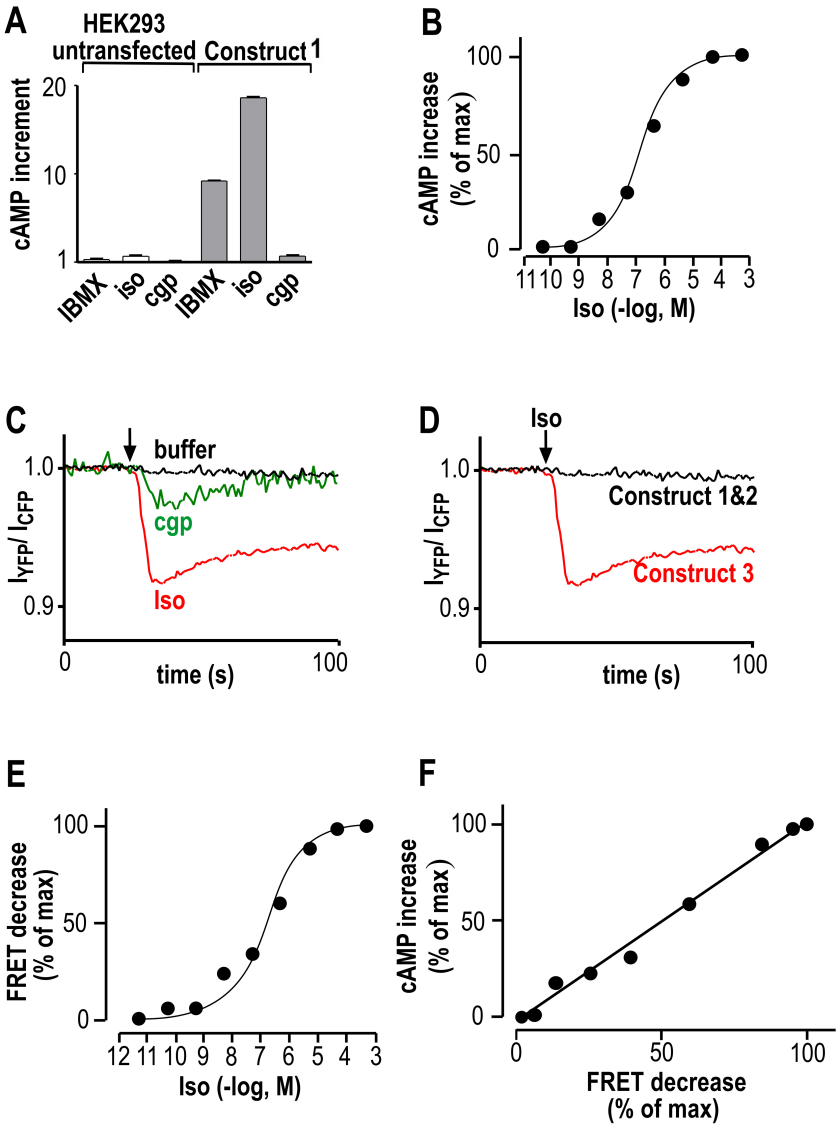

Figure 4.3: Ligand binding, cAMP-stimulation and FRET.

(A) cAMP stimulation (10 min, 37 °C) of cells not transfected (white bars) or expressing construct 1 (grey bars) with 1 mM IBMX, 10^{-5} mol/l isoproterenol (iso), or 10^{-5} mol/l CGP20,712A (cgp, green). cAMP values were normalised to total protein and fold increments were calculated by the ratio of stimulated and unstimulated cells. **(B)** Dose-response of cAMP stimulation by isoproterenol measured in cells expressing construct 1. **(C)** Typical recording of FRET ratios (I_{YFP}/I_{CFP}) recorded over time in cells stably expressing construct 3 and exposed (arrow) to 10^{-5} mol/l isoproterenol (Iso, red), 10^{-5} mol/l CGP20,712A (cgp, green), or buffer alone (black). Ratios were averaged from time lapsed fluorescent images of approximately 40 cells and corrected for bleaching and signal offset due to reagent addition. **(D)** Comparison of FRET responses to 10^{-5} mol/l isoproterenol (arrow) between cells expressing construct 3 (red) and cells coexpressing the constructs 1 and 2 (black). Ratios were averaged from time lapsed fluorescent images of approximately 40 cells and corrected for bleaching and signal offset due to reagent addition. **(E)** Maximal decreases in FRET-efficiency derived from recordings in cells expressing construct 3 (done as in G) in response to isoproterenol (5×10^{-12} - 5×10^{-4} mol/l). Mean values of three independent experiments are normalised to the maximal effect at ligand saturation (5×10^{-4} mol/l). **(F)** Linear correlation (r^2 = 0.92) of cAMP- and FRET responses to isoproterenol (5×10^{-11} - 5×10^{-4} mol/l).

4.1.4 Measurement of activation associated conformation changes of the human β_1-AR via FRET.

Blue (CFP) and yellow (YFP) fluorescent protein moieties constituting a Förster fluorescence energy transfer (FRET) -donor/-acceptor pair were fused in frame at positions of the human β_1-AR expected to be close enough to each other in the resting state to support FRET and to move sufficiently apart upon conformational activation to induce a measurable decrease in FRET efficiency (Hoffmann et al. 2005; Granier et al. 2007; Rochais et al. 2007). In figure 4.3 I could show that exposure of such CFP/YFP-labelled receptors (construct 3 in Fig. 4.1A) to isoproterenol (10^{-5} mol/l) indeed triggered a rapid (response time < 1 sec) drop in YFP/CFP emission ratio (I_{YFP}/I_{CFP}) corresponding to a Δ_{max} value of 0.09 (Fig. 4.3C). A similar response was not inducible by the antagonist CGP20,712A or buffer alone. Agonist-induced changes in FRET efficiency were quantitatively correlated to isoproterenol dose and cAMP stimulation (Fig. 4.3E and F, respectively).

Several control experiments were done to assure that the decrease in the donor/acceptor emission ratio did indeed reflect a decrease in FRET efficiency due to an increase in the distance between the two labelled receptor domains caused by activation associated conformational changes.
Firstly, it was ascertained that decreases in FRET efficiency were due to intramolecular conformation changes and not due to receptor-receptor interactions. It has been shown that activation of human β_1-ARs can involve receptor homo-dimerisation (Lavoie et al. 2002; Mercier et al. 2002). To exclude that this rather than intramolecular conformation changes caused the observed decrease in donor/acceptor fluorescence emission ratio, the two fluorophores were placed in separate receptor molecules coexpressed in the same cell. In other words cells coexpressing the constructs 1 and 2 were compared to cells expressing the construct 3 (constructs see Fig. 4.1A). In the cells coexpressing FRET donor and acceptor in separate receptor molecules, exposure to isoproterenol (10^{-5} mol/l) did not trigger a similar drop in YFP/CFP emission ratio as in the cells expressing the double-labelled FRET sensor receptor (Fig. 4.3D). Thus, the decrease in FRET efficiency could be

assigned solely to intramolecular conformation changes, and a contribution of receptor-receptor interactions to the signal could be excluded.

Secondly, it was ascertained by acceptor photobleaching that the receptor bearing the FRET sensor did indeed support intramolecular FRET between CFP and YFP when not stimulated. FRET occurs when two fluorophores come into very close proximity (<10 nm). Bleaching out the acceptor protein (YFP, green) eliminates the possibility of FRET, and thus should enhance the fluorescence intensity of the donor fluorophore (CFP, blue). As shown in Fig. 4.4 A and B, this was indeed the case with the β_1-AR FRET construct supporting the notion that it contained a functional active FRET pair and supported intramolecular occurring FRET.

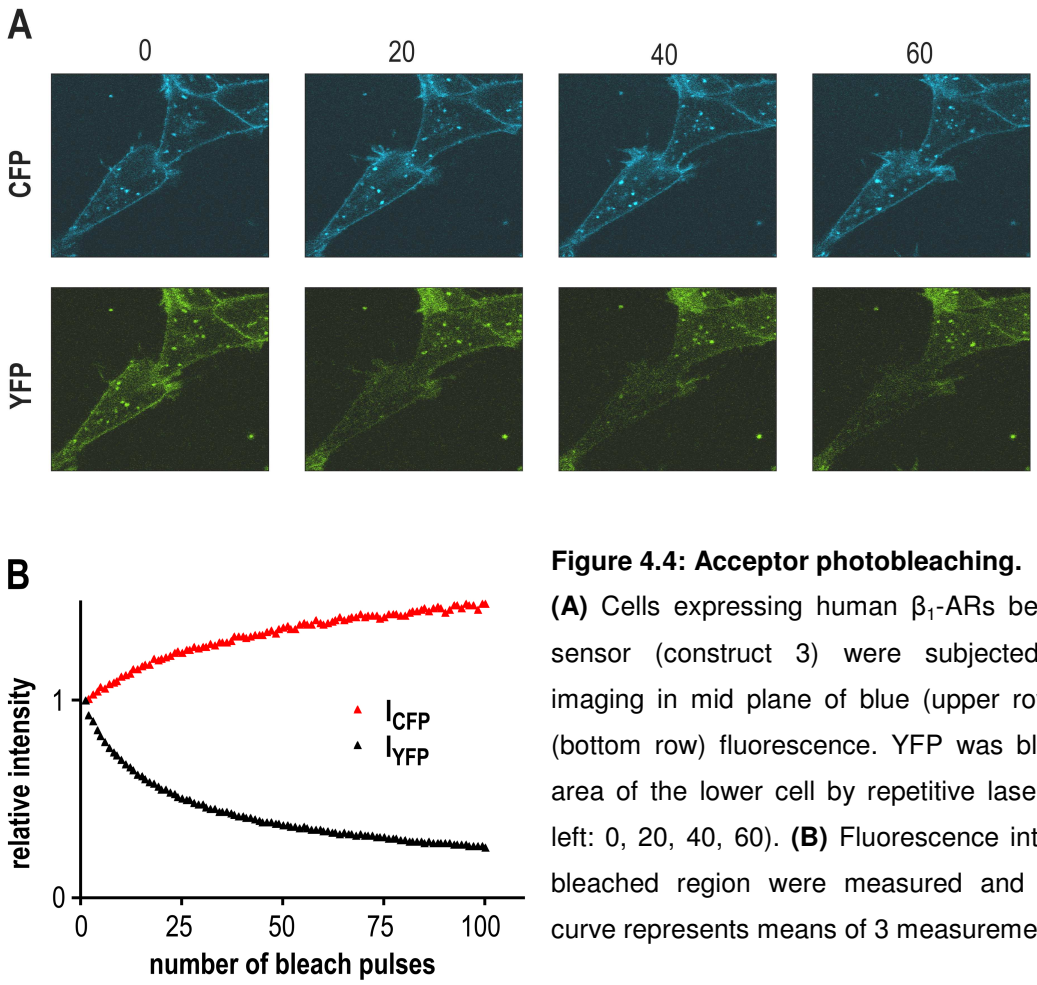

Figure 4.4: Acceptor photobleaching.
(A) Cells expressing human β_1-ARs bearing a FRET sensor (construct 3) were subjected to confocal imaging in mid plane of blue (upper row) and yellow (bottom row) fluorescence. YFP was bleached in the area of the lower cell by repetitive laser pulses (from left: 0, 20, 40, 60). **(B)** Fluorescence intensities in the bleached region were measured and plotted. Each curve represents means of 3 measurements.

Thirdly, it was ascertained that decreases in YFP/CFP emission ratio were due to a decrease in FRET efficiency. Determinations based on fluorescence emission intensity are possibly compromised by channel bleed-through and bleaching (Biskup et al. 2007). To exclude such artefacts, the lifetime of donor fluorescence (CFP), which is decreased by FRET but not by other mechanisms altering I_{YFP}/I_{CFP}, was determined. CFP expressed alone, or as a fusion with the third intracellular loop of the human β_1-AR (construct 2 in Fig. 4.1A), or together with, but not fused to the potential acceptor fluorophor YFP had a mean fluorescence lifetime (τ_m) between 2.80 and 2.89 ns (Table 4.2, rows 1-3). Significantly lower τ_m values (2.28 ± 0.07 ns) were measured when CFP and YFP were expressed as a fusion protein supporting constitutive intramolecular FRET (Table 4.2, row 3). Similarly decreased τ_m values (2.32 ± 0.04 ns) were observed in cells expressing β_1-ARs bearing the CFP/YFP-FRET sensor (construct 3 in Fig. 4.1A) (Table 4.2, row 5), whereas CFP-fused receptors lacking a C-terminal YFP (construct 2 in Fig. 4.5A) exhibited normal τ_m values (2.81 ± 0.03 ns) (Table 4.2, row 4). Thus, the τ_m decrease in construct 3 (the dual labelled receptor construct) indicates constitutive FRET between the C-terminal YFP and the CFP in the third intracellular receptor domain. Fluorescence lifetime images of a representative cell cluster expressing the dual labelled receptor construct are shown in Figure 4.5A. τ_m values of CFP ranging from 1.5 to 3.0 ns are encoded orange to blue. Without stimulation (Fig. 4.5A, top), CFP fluorescence of the receptors was exclusively localised in the outer cell membrane and exhibited τ_m values of 2.32 ± 0.04 ns (encoded green in Fig. 4.5A, top; quantification in Table 4.2, row 5) indicative of FRET. Upon exposure to 10^{-5} mol/l µM isoproterenol (Fig. 4.5A, middle and bottom), lifetime of receptor-associated CFP fluorescence in the membrane shifted towards longer τ_m values (encoded blue). However, this shift was inapparent in quantitative assessments of the entire field of vision (Table 4.2, rows 6 and 7).

Subcellular analysis (Fig. 4.5B and Table 4.2, rows 8-10) revealed a significant increase in τ_m in the outer exhibited a shortening of CFP fluorescence lifetime (τ_m= 2.11 ± 0.18 ns), possibly reflecting a more dense conformation due to partial denaturation of the internalised receptors suggested to play a role in uncoupling of ligand and receptor (Lohse 1993; Gagnon et al. 1998), or a change in the basic

properties of the fluorophor (due to pH alterations inside the vesicles). In receptors localised in the outer cell membrane, the drop in I_{YFP}/I_{CFP} triggered by 10^{-5} mol/l isoproterenol (Fig. 4.3C and D) corresponds to increases in fluorescence lifetime of the donor fluorophor, and, therefore, represents a decrease in FRET efficiency in the cell membrane, which shifted from 2.37 ± 0.04 ns to 2.51 ± 0.03 ns upon exposure to the agonist isoproterenol. This indicates a decrease in FRET efficiency in this receptor subpopulation, in contrast to receptors sequestered into intracellular vesicles (green and orange spots within the circle in Fig. 4.5B, right).

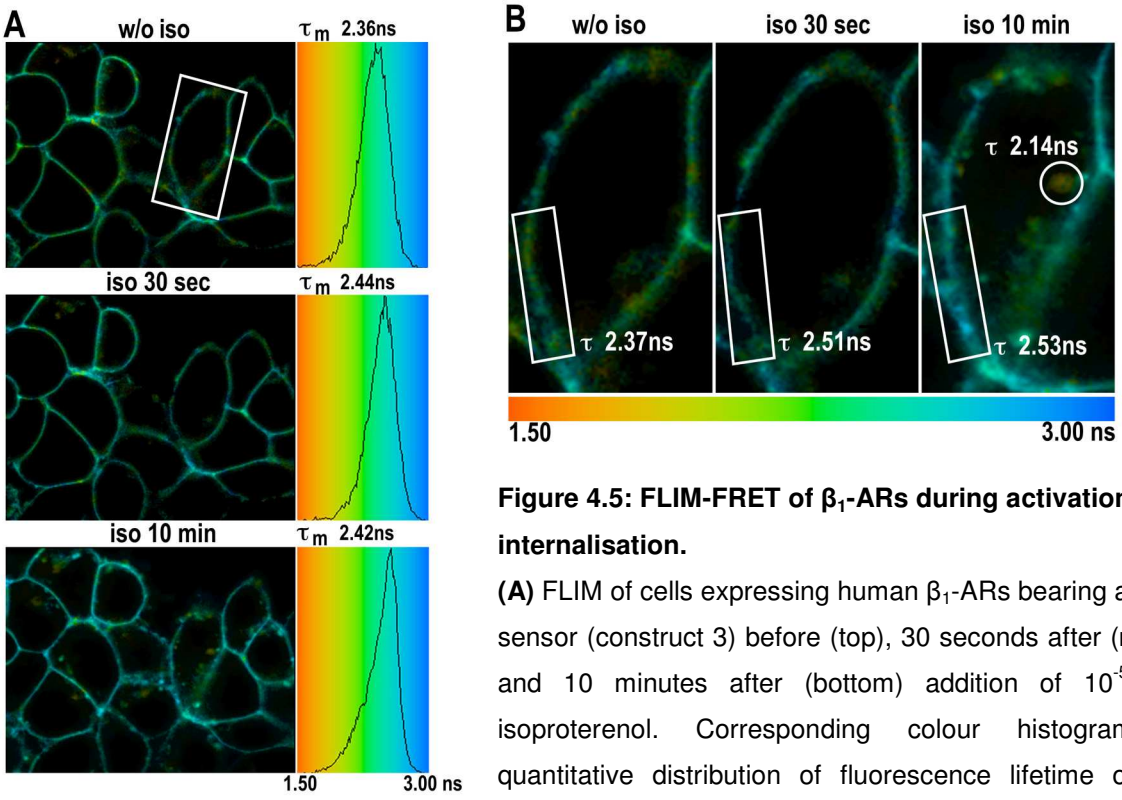

Figure 4.5: FLIM-FRET of β_1-ARs during activation and internalisation.

(A) FLIM of cells expressing human β_1-ARs bearing a FRET sensor (construct 3) before (top), 30 seconds after (middle) and 10 minutes after (bottom) addition of 10^{-5} mol/l isoproterenol. Corresponding colour histograms of quantitative distribution of fluorescence lifetime of CFP measured across the entire field of vision are shown on the right. The white rectangle indicates the area of subcellular analysis in B. **(B)** FLIM of a single cell expressing the construct 3. Quantitative values of fluorescence lifetime (τ_m) of CFP were averaged in a membrane section (boxes) or an intracellular vesicle containing internalised receptors (circle). A corresponding colour histogram of quantitative distribution of fluorescence lifetime of CFP measured across the entire field of vision is shown at the bottom.

In conclusion, the drop in YFP/CFP emission ratio of the receptor construct 3 can be used as a quantitative measure for intramolecular conformational changes of the receptor caused by an increase in distance between the two labelled receptor domains. τ_m values of activated receptors are still smaller than those of CFP alone (see Table 4.2) suggesting a decrease in FRET efficiency, consistent with a minor repositioning of the labelled receptor domains. A similar conclusion was previously drawn from experiments with purified β_2-AR bearing a different FRET pair incorporated at similar positions (Granier et al. 2007). These control experiments ascertain that the dual labelled receptors were capable of reporting the activation-associated conformational switch by a decrease in FRET efficiency (measurable by I_{YFP}/I_{CFP} and τ_m), thus allowing sensitive detection and quantitation of conformational changes related to the activation of human β_1-ARs.

Table 4.2: Measurements of fluorescence lifetime of CFP

Constructs and Conditions*	mean lifetime τ_m [ns]†
CFP only	2.89 ± 0.03
CFP and YFP (not fused)	2.80 ± 0.04
CFP-YFP (fused, constitutive FRET)	2.28 ± 0.07
β_1-AR-CFP (construct 2 in Fig. 4.1A)	2.81 ± 0.03
β_1-AR-CFP-YFP (construct 3 in Fig. 4.1A)	
Unstimulated, whole field of vision	2.32 ± 0.04
1 sec ISO (10 µM), whole field of vision	2.39 ± 0.04
10 min ISO (10 µM), whole field of vision	2.34 ± 0.05
Unstimulated, focus on cell membrane	2.37 ± 0.04
1 sec ISO (10 µM), focus on cell membrane	2.48 ± 0.02
10 min ISO (10 µM), focus on cell membrane	2.51 ± 0.03
10 min ISO (10 µM), focus on internal vesicle	2.11 ± 0.18

*) Constructs were stably expressed in HEK 293 cells.

†) Mean ± SEM of five measurements at 37°C with independent cell samples.

4.2 Prevalence and titer of autoantibodies

4.2.1 Selection of patients and controls

In this study *bona fide* cardiopathogenic and -apathogenic IgG samples were used. Pathogenic IgG samples were derived from immunoadsorption therapy of DCM patients. They were considered pathogenic, because in all DCM patients removal of the IgG by immunoadsorption with subsequent IgG substitution led to a significant and stable increase in left ventricular ejection fractions (LVEF) over an observation period of 12 months following the initial therapy course. In most cases this was accompanied by a decrease in left ventricular end-diastolic diameters (LVEDD) (Fig. 4.6). Thus heart function significantly and durably improved upon IgG removal.

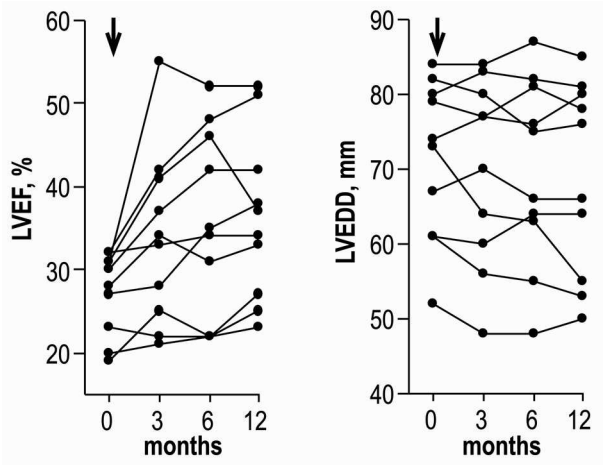

Figure 4.6: Improvement of LVEF and LVEDD in patients suffering from DCM.
Patients showed hemodynamic improvement following immunoadsorption and IgG substitution. Left ventricular ejection fractions (LVEF, left) and end-diastolic diameters (LVEDD, right) before (month 0) and after (months 3, 6, 12) unselective IgG adsorption (↓) were determined as published (Felix et al. 2002; Dorffel et al. 2004).

Apathogenic IgG were purified by analogous immunoadsorption from the blood of matched healthy volunteers that did not suffer from left ventricular dysfunction, and did not develop such a heart condition during 12 subsequent months. Table 4.3 gives a comparative summary of key data characterising patients and controls used in this study.

Table 4.3: Clinical characterisation of DCM patients and healthy volunteers (controls).

	Controls (n=10)	DCM Patients (n=10)
Age (y)	37.5 ± 3.8	52.7 ± 2.5
Sex (m/f)	9/1	9/1
LVEF (%)	61.9 ± 1.4	27.3 ± 1.5
LVEDD (mm)	48.7 ± 1.3	71.3 ± 3.2
NYHA	N/A	2.6 ± 0.2
Medication		
ACE-I (%)	0	100
ARB (%)	0	10
β-blocker (%)	0	100
Diuretics (%)	0	90
Myocardial biopsy		
Inflammation present (%)*	N/A	80
viral RNA present (%)	N/A	30

*) Inflammation was considered to be present if immunohistochemistry of myocardial biopsies revealed focal or diffuse mononuclear infiltrates with >14 leucocytes per mm^3 (CD3+ T-lymphocytes and /or CD68+ macrophages) in addition to enhanced expression of HLA class II molecules.

4.2.2 Comparative quantification of autoantibody levels

Human β_1-AR autoantibodies are known to bind conformational epitopes and poorly crossreact with receptor peptides or denatured receptors (Jahns et al. 1999). Therefore, assays to identify and quantify autoantibody binding to the human β_1-AR were developed. One was immunoprecipitation (IP) of YFP-fused β_1-ARs (construct 1 in Fig. 4.1A) solubilised with digitonin, which were detected by GFP-directed immunoblotting and quantified by densitometry of the blots. Fig. 4.7 shows a representative result of antibodies tested by IP.

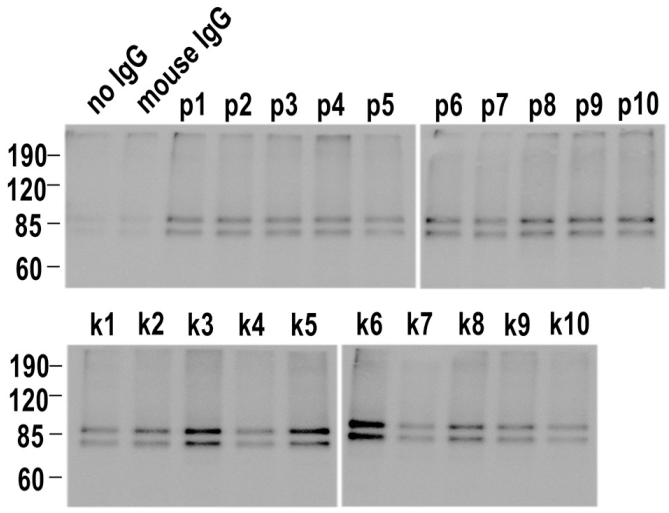

Figure 4.7: Immunoprecitation of YFP fused β_1-AR.

Solubilisates of cells expressing the construct 1 were subjected to immunoprecipitation using magnetic beads saturated with autoimmune-IgG from DCM patients (p1 – p10) or healthy volunteers (k1 – k10). Mouse IgG or noncoated beads (no IgG) served as a negative control. Bound material was subjected to GFP-directed immunoblotting. Marker labelling from 60-190 is indicated in kd.

The other assay was titration of autoantibody binding to native receptor epitopes presented on the surface of living cells. For this, cells expressing YFP-fused β_1-ARs (construct 1 in Fig. 4.1A) were incubated with serial dilutions of autoantibodies normalised to 0.67 mg/l of IgG, and the highest dilution was determined that still exhibits receptor-specific immunostaining upon washing, cell fixation and counterstaining with IgG specific secondary antibodies. Receptor specificity of the autoantibodies was controlled by parallel staining of untransfected cells, staining of transfected cells with secondary antibody alone (Fig. 4.8B, rightmost set of images) and staining of transfected cells with autoantibodies preadsorbed with a peptide homolog of the first or the second extracellular loop of the β_1-AR (Fig. 4.8C middle and right.). With the exception of preabsorption by the peptide homolog of the first extracellular receptor loop, all these controls gave negative results. This shows that the autoantibodies specifically interacted with the second extracellular loop of the native receptor on the surface of living HEK 293 cells and that no other protein or epitope exposed on the surface of the native cells was targeted. Receptor-specific IgG levels in the samples under investigation determined by colocalisation with YFP-fused β_1-ARs on the cell surface (i.e., the maximal dilution of the normalised samples at which colocalisation with biofluorescent β_1-ARs was still detectable) exhibited a poor correlation with corresponding quantitative results of receptor immunoprecipitation and a slightly better correlation with IgG-mediated changes in receptor conformation as quantified by Δ_{max} of I_{YFP}/I_{CFP} (Fig. 4.8E, left and right,

respectively). This discrepancy was assumed to indicate (i) that the native receptor epitope targeted by the autoimmune antibodies is inadequately presented by the solubilised receptor, and (ii) that conformational changes induced by the IgG are not delimited by IgG concentration within the observed range.

Taken together, these data show that β_1-AR-specific autoantibodies were found in all DCM patients, but also in all healthy volunteers and IgG preparations used for substitution following immunoadsorption. However, β_1-AR-specific IgG levels were significantly higher in DCM patients (Fig. 4.8D).

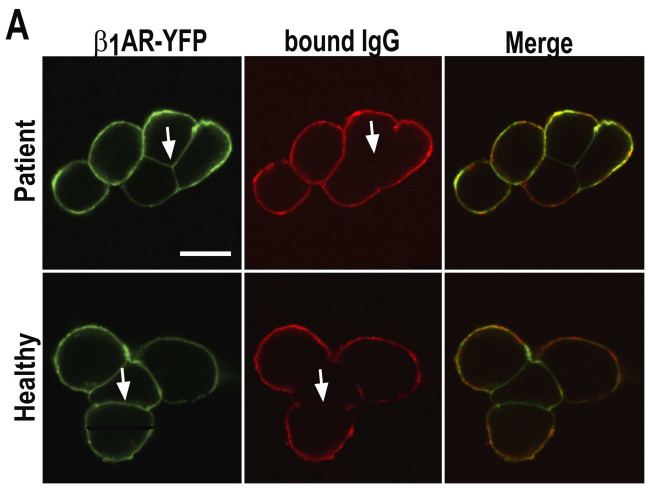

Figure 4.8: Quantification of IgG binding to native human β_1-ARs on the surface of human cells.

(A) Colocalisation (right) of receptor-biofluorescence (left) and IgG-specific immunofluorescence (middle) on the surface of native HEK 293 cells. Arrows indicate cell-cell contacts not reached by IgG diffusion. Specificity controls see Fig. 4.8B. The size bar in the top left panel represents 30 µm and applies to all panels.

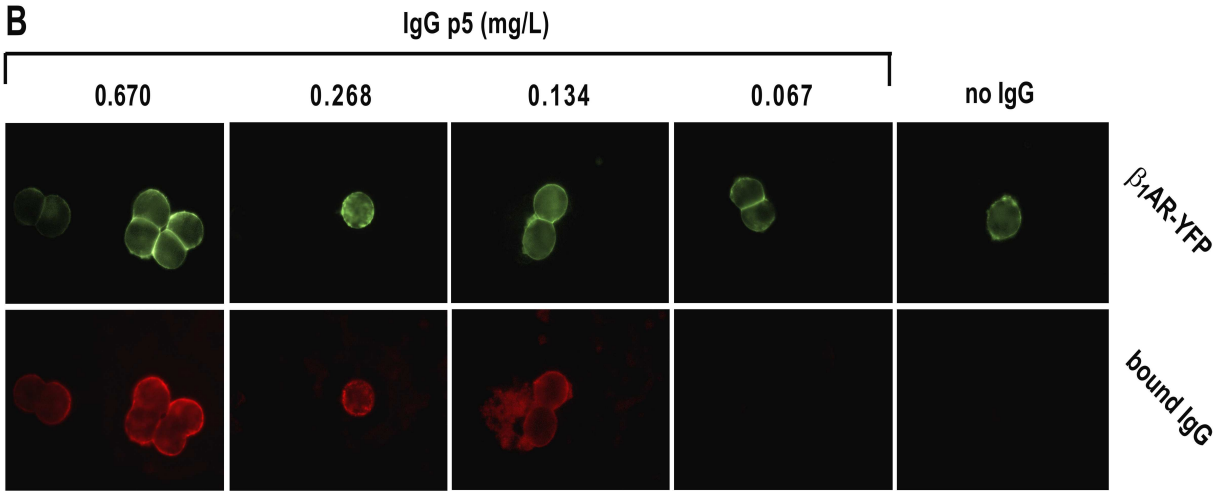

(B) Receptor biofluorescence (top) and IgG-specific immunofluorescence (bottom) on the surface of native HEK 293 cells expressing construct 1 and incubated with decreasing concentrations of (or without) autoimmune IgG (p5).

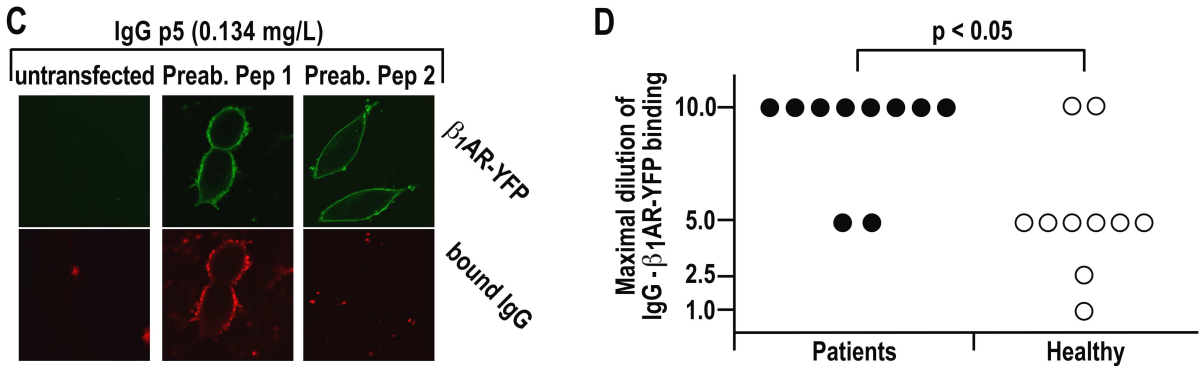

(C) Specificity controls of receptor-IgG binding encompassing staining of untransfected cells (left) and IgG preabsorption with a 1000-fold molar excess of a peptide homolog of the first (middle) or the second (right) extracellular loop of the human β_1-AR. **(D)** Levels of β_1-AR-specific IgG defined by the highest dilution of IgG (normalised to 0.67 mg/l) at which colocalisation with β_1-AR-YFP as shown in A was still detectable. Circles represent means of triplicate determinations of individual IgGs from DCM patients (left) or healthy volunteers (right) done on different days with different cell preparations. SEM were less than one dilution step.

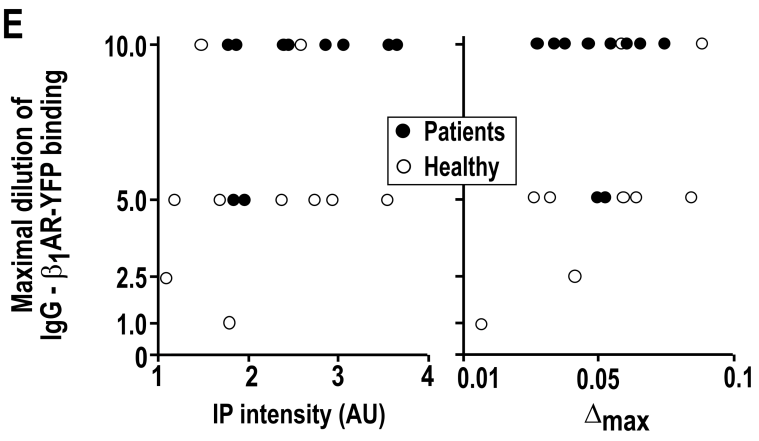

(E) Quantification of receptor specific IgG levels via binding to native YFP-fused β_1-ARs on the cell surface. Samples were normalised to 0.67 mg/l of IgG and subjected to serial dilutions. The quantitative capacity of IgG-receptor binding was determined by the maximal dilution at which IgG-colocalisation with β_1-AR-YFP was still detectable. These values are compared with the quantification of the immunoblotting signals shown in Figure 4.7 (left) or with maximal IgG induced decreases in FRET efficiency (Δ_{max} of I_{YFP}/I_{CFP}) quantified as demonstrated in Figure 4.9A. Linear correlations had a goodness of $r^2 = 0.139$ and 0.151, respectively.

4.3 Impact of autoantibodies on β_1-AR conformation and activity

4.3.1 β_1-AR-specific IgGs trigger conformational changes via allosteric interactions with the second but not the first extracellular receptor loop

Cells expressing the β_1-AR construct with the FRET sensor, capable of reporting conformational changes of the receptor triggered by agonistic ligands were used to investigate whether receptor specific IgG are also capable of triggering conformational changes in the receptor (Fig. 4.9 A). All β_1-AR-specific IgG characterised as in Fig. 4.8 appeared to alter receptor conformation in as much as they induced a decrease in I_{YFP}/I_{CFP} of the FRET sensor. These decreases were quantitatively weaker but otherwise similar to isoproterenol. The effects could be blocked by preincubation with a peptide homolog of the second, but not of the first extracellular loop of the β_1-AR (Fig. 4.9B). Maximal decreases in I_{YFP}/I_{CFP} (Δ_{max}) triggered by patient or control IgG had similar ranges and medians (Fig. 4.9C) and were poorly correlated to β_1-AR-specific IgG levels (Fig. 4.8E). The effects of individual IgG on receptor conformation were not additive to each other or to the effect of isoproterenol, and submaximal IgG effects did not preclude subsequent, maximal effects by isoproterenol (Fig. 4.9D). Thus, all autoantibodies apparently acted through an allosteric mechanism, involving the same IgG-binding site (encompassing the second but not the first extracellular β_1-AR-loop) and triggering the same or a similar conformational switch as isoproterenol.

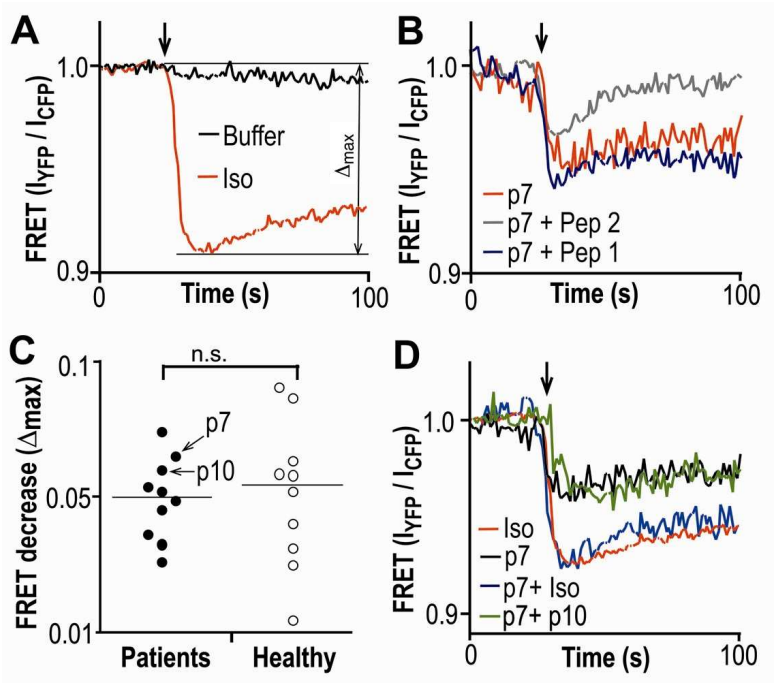

Figure 4.9: IgG impact on receptor conformation measured by a drop in intramolecular FRET efficiency. **(A)** FRET response to 10^{-5} mol/l isoproterenol (red) or buffer (black). Characteristics of the FRET sensor see Fig. 4.2 and 4.3 and Tables 1 and 2. **(B)** FRET response to patient IgG (0.134 mg/l) without (red) or with preadsorption (1000-fold molar excess, 10 min, 37 °C) with peptide homologs of the first (Pep 1, blue) or second (Pep 2, grey) extracellular loop of the human β_1AR. **(C)** Comparison of FRET responses (quantitation of Δ_{max} demonstrated in A) to individual IgG (0.134 mg/l) from DCM patients (left) or healthy volunteers (right) by the U-test (bracket). P7 and p10 identify corresponding IgG samples in B and D. Lines show medians. **(D)** FRET responses to simultaneous incubation with two individual patient IgGs (green) or first patient IgG and then isoproterenol (blue), as compared to each agent alone (black (p7) and red (Isoproterenol)).

4.3.2 Autoantibody-triggered switching of receptor conformation is not stringently coupled to cAMP stimulation

Most β_1-AR-specific IgG from patients and healthy volunteers increased intracellular cAMP to some extent. However, patient IgG had a significantly higher cAMP-stimulatory potency (Fig. 4.10A). This conforms to previous findings (Jahns et al. 1999) but is astonishing because IgG impact on receptor conformation was not significantly different between patients and healthy volunteers (Fig. 4.9C). To address this discrepancy, a correlative matrix of cAMP stimulation and corresponding changes in receptor conformation (FRET decrease) was created, additionally using dose response curves of isoproterenol (Fig. 4.1E and J) to determine the 99% confidential interval of receptor activation via distortion of the ligand binding pocket by an agonist (Fig. 4.10B, dotted lines). Eight out of 10 patient IgG (Fig. 4.10B,

closed circles) exhibited values within or above the isoproterenol confidential interval, suggesting that they behaved as allosteric agonists by inducing receptor conformations coupled to cAMP stimulation as good as, or superior to, isoproterenol. In contrast, half of the IgG from healthy volunteers (Fig. 4.10B, open circles) and both donor IgG pools (Fig. 4.10B, open squares) were below the isoproterenol confidential interval, suggesting that they induced receptor conformations not or only inefficiently coupled to cAMP. Given that IgG from volunteers or donor pools also failed to induce MAP kinase signalling (Fig. 4.11), one can conclude that they behave like β_1-adrenergic partial agonists or antagonists.

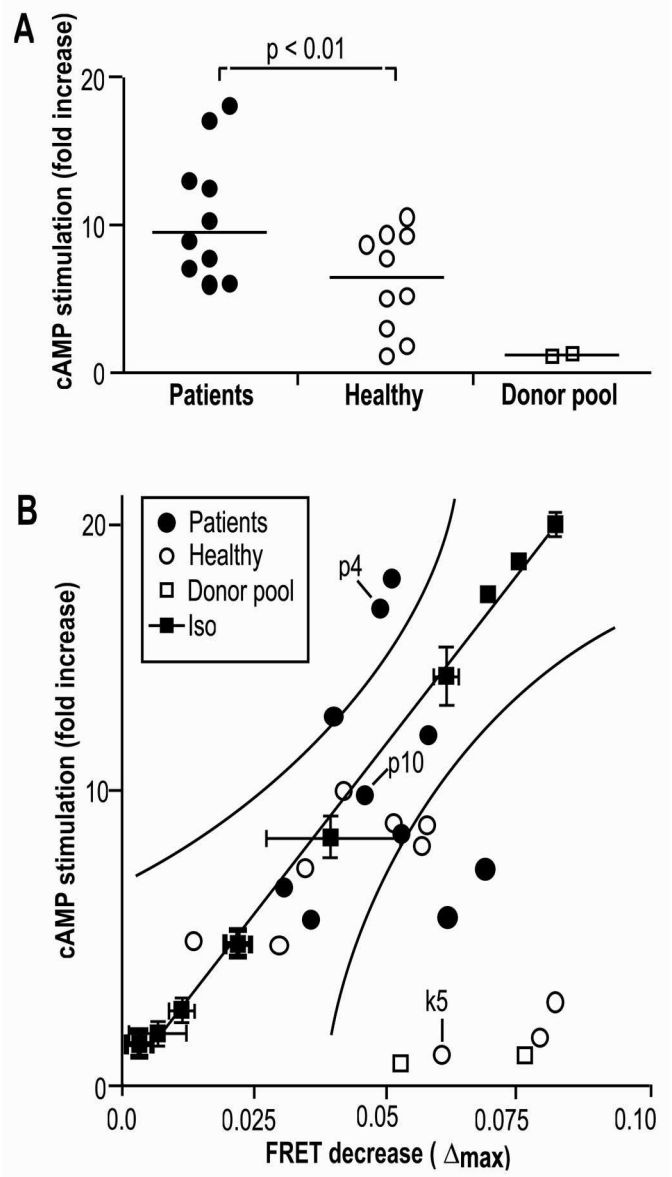

Figure 4.10: β_1-adrenergic cAMP stimulation by IgG and corresponding changes in β_1-AR conformation.

(A) Fold increments of cAMP over basal levels in HEK 293 cells (expressing 10^7 copies of YFP-fused human β_1-ARs/cell (construct 1, Fig. 4.1)) in response to IgG (0.134 mg/l, 20 min, 37 °C) from DCM patients (left), matched healthy volunteers (middle) or pooled blood donors (right). Lines show medians. Symbols represent the mean of 6 measurements on different days with different cell preparations. SEM was less than 10%. Bracket: comparison of groups by the U-test. **(B)** Correlation of cAMP- and FRET responses to IgG from DCM patients (●), healthy volunteers (○) and pooled blood donors (□) (mean, n=3, SEM < 10 %), compared to corresponding responses to isoproterenol (5×10^{-11} - 5×10^{-4} mol/l, for each concentration mean ± SEM, n = 3) (■). Solid and dashed lines: linear regression and 99% confidential interval of isoproterenol data. p4, p10 and k5 indicate IgG selected for the experiments shown in Figure 4.13.

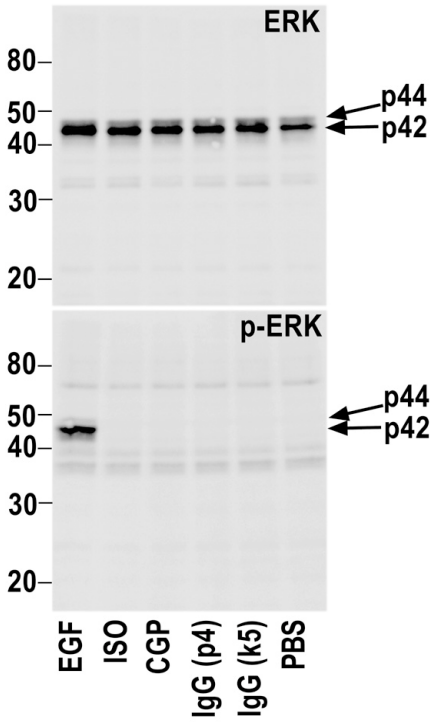

Figure 4.11: Investigation of MAP-kinase signalling by ERK1/2 phosphorylation.

Cells expressing the construct 1 were incubated (10 min, 37 °C) with 1 ng/ml of epidermal growth factor (EGF), 10^{-5} mol/l isoproterenol (ISO), 10^{-6} mol/l CGP20,712A (CGP), or 0.27 mg/l of autoimmune IgG (patient p4 and healthy k5) or kept without addition (PBS). SDS lysis and Western blotting followed and blots were than probed with antibodies specific for total ERK 1 and 2 (top) or specific for ERK 1 and 2 phosphorylated at Thr202/Tyr204 (bottom). Marker (20-80) indicats a ladder in kd. ERK1/2 signed out by a double band at 42/44 kd.

The investigation of MAP-kinase signalling showed that neither Isoproterenol nor autoantibodies from healthy individuals or from DCM patients induced phosphorylation of ERK.

4.3.3 Inhibition of agonist triggered β_1-AR internalisation by autoantibodies.

In the steady state of isoproterenol saturation 20-30 % of the biofluorescent β_1-ARs were located in cytosolic endosomes (Fig. 4.12, top, right), indicative of homologous desensitisation encompassing receptor endocytosis (Gagnon et al. 1998) and subsequent recycling to the cell surface (Yudowski et al. 2009). A similar phenomenon was not observed upon exposure to cAMP-stimulatory autoantibodies (Fig. 4.12, bottom, left). Moreover, preincubation with autoantibodies decreased the amount of receptor internalisation inducible by subsequent exposure to isoproterenol (Fig. 4.12, bottom, right), despite the overruling effect of isoproterenol on receptor conformation in the presence of the autoantibodies (Fig. 4.9D). This suggests that the autoantibodies inhibit receptor internalisation.

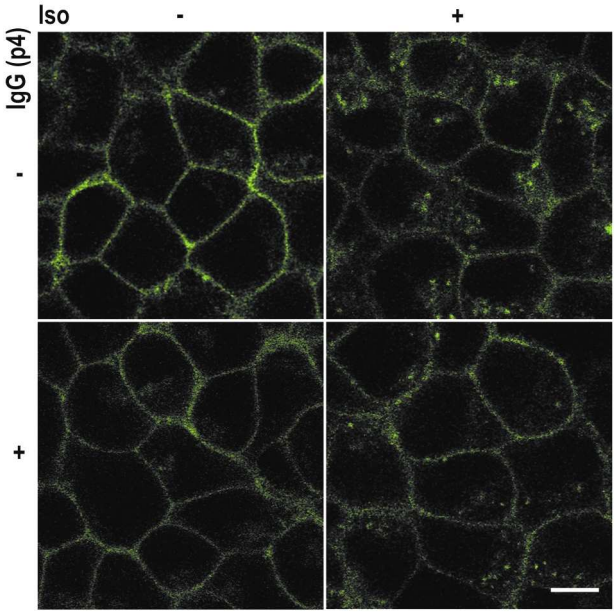

Figure 4.12: IgG inhibition of agonist -induced receptor internalisation.
This figure shows confocal images of cells expressing YFP-fused human β_1-ARs before (top, left) or after (top, right) exposure to isoproterenol (Iso) or after IgG (p4) preincubation (bottom, left) and subsequent Iso exposure (bottom, right). The size bar in the bottom right panel represents 30 µm and applies to all panels.

This phenomenon was quantified using total internal reflection microscopy (TIRF) (Yudowski et al. 2009) monitoring the appearance of receptosomes in a 200 nm cytosolic section immediately above the basal membrane. One to two min after isoproterenol exposure, biofluorescent receptosomes started to appear in the observed cell slice and their density increased steadily over 15 min. Preincubation with autoantibodies significantly delayed onset and rate of agonist-induced receptosome trafficking (Fig. 4.12). Going by the mean rate of receptosome appearance in the monitored slice of a given cell during the first 1000s of agonist exposure, receptor internalisation was significantly more often reduced by patient IgG than by IgG from healthy volunteers or blood donors (Fig. 4.13B). The inhibitory effect was abolished by preadsorption with a peptide homolog of the second but not the first extracellular loop of human β_1-ARs (Fig. 4.13C). Given that β_1-ARs seemed the only proteins targeted by the antibodies on the cell surface (Fig. 4.8A, B and C) this observation suggests that inhibition of receptor internalisation and conformational

activation of the receptor by IgG are mediated through interactions with the same epitope. However, the efficacies of individual IgG samples to trigger the two effects were not correlated (Fig. 4.13D) suggesting that they are independent properties.

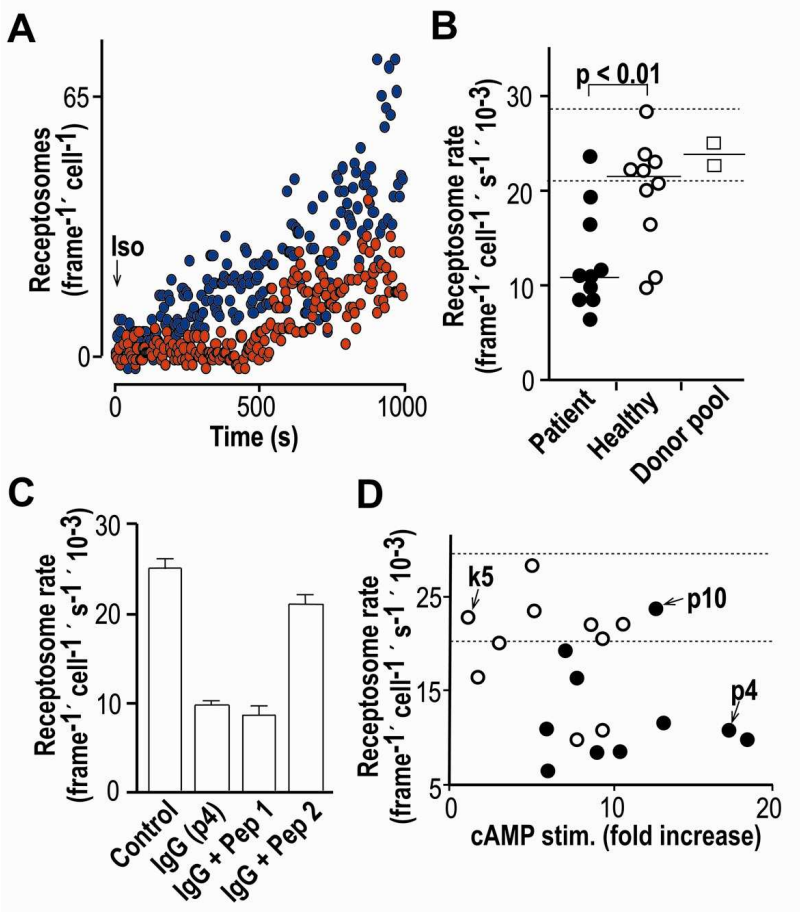

Figure 4.13: Agonist induced-receptor cycling quantified by TIRF.

(A) Number of internalised biofluorescent receptors (receptosomes) quantified by TIRF following Iso exposure (10^{-5} mol/l) without (blue) or with (red) IgG (p4) preincubation (as in 4.12). **(B)** Impact of preincubation with IgG of DCM patients (left), healthy volunteers (middle) or pooled blood donors (right) on mean receptosome frequency averaged over 1000 s of Iso exposure. Bracket: comparison of groups by the U-test. Dashed lines: 98% confidential interval of receptosome rate without IgG preincubation (n=5). **(C)** Decrease of agonist-induced receptosome frequency (mean ± SEM, as in B) in response to IgG preincubation (0.27 mg/l of p4) with and without preabsorption (1000-fold molar excess, 10 min, 37 °C) with peptide homologs of the first or second extracellular receptor loop (Pep 1 and 2, respectively). **(D)** Comparison of IgG capacities to stimulate cAMP and to decrease receptor internalisation. k5, p4 and p10 indicate selected IgG used in A and C. Dashed lines are as in B.

4.3.4 Modulation of β_1-adrenergic catecholamine response by autoantibodies

Inhibition of receptor internalisation and recycling by autoantibodies could modulate cellular cAMP responses to prolonged agonist exposure, which might be more significant than direct allosteric receptor activation or inactivation. It could be shown (Fig. 4.14) that patient IgGs capable of conformational receptor activation but not inhibition of receptor internalisation (p10 in Fig. 4.13D) potentiated cellular cAMP responses to isoproterenol. Whereas β_1-AR-stimulatory IgGs that in addition strongly inhibited receptor internalisation (p4 in Fig. 4.13D) had the opposite effect. They decreased and delayed cellular cAMP responses to isoproterenol. Interestingly, a similar decrease and delay was observed with IgG from a healthy volunteer that neither inhibited receptor internalisation nor activated the receptor (k5 in Fig. 4.13D) but promoted an inactive β_1-AR-conformation (k5 in Fig. 4.10B). Thus, IgG autoantibodies can activate or inactivate β_1-AR or inhibit their internalisation. These properties are independent of each other and act additive or counteractive to endogenous cAMP regulation.

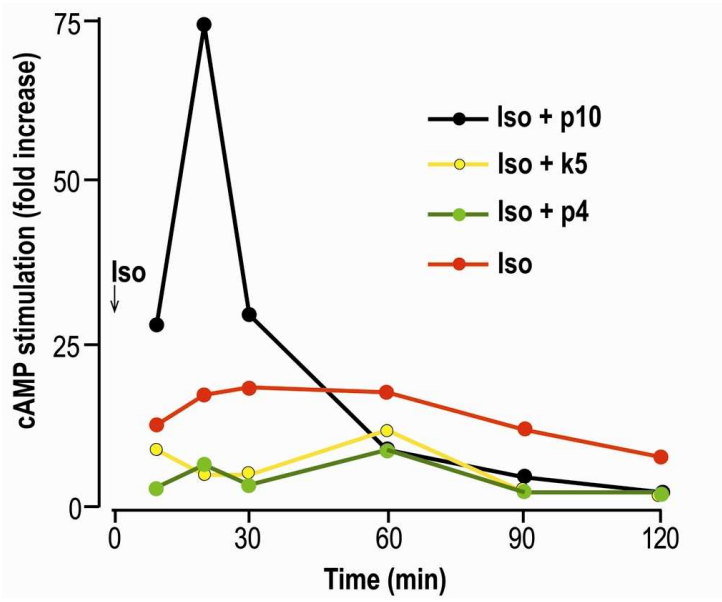

Figure 4.14: cAMP effects of autoantibodies are additive or attenuating.
Fold increment of cAMP over basal level (mean, n=3, SEM < 10%) following Isoproterenol exposure without and with IgG preincubation k5, p4 and p10 indicate selected IgG used in 4.13A, B, D.

4.4 Pathognomonic features of β_1-AR autoantibodies

4.4.1 Features associated with disease activity

Receiver operator curve (ROC) analyses were performed (Fig. 4.15) to identify those properties of β_1-AR-specific IgG that most clearly discriminate DCM patients from healthy volunteers, and thus can be assumed pathognomonic.

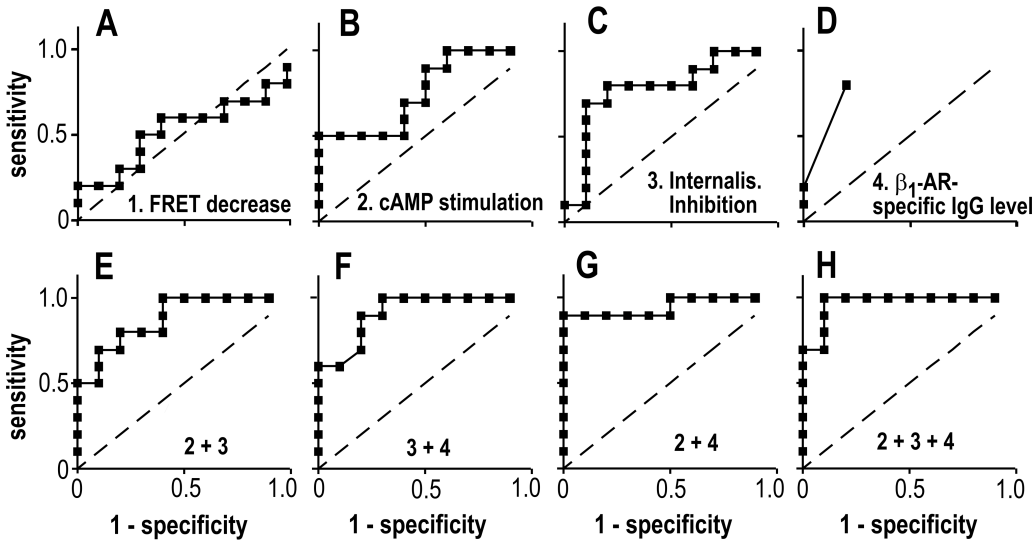

Figure 4.15: ROC analysis of discriminative properties of anti β_1-AR IgG.

IgG from all patients and healthy volunteers (ten each) are included. The following parameters are subjected to ROC analyses:

(A) FRET decrease (Δmax of I_{YFP}/I_{CFP}) in response to 0.134 mg/l of IgG (Fig. 4.9C). **(B)** Fold stimulation of cAMP by 0.27 mg/l IgG (Fig. 4.10A). **(C)** Inhibition of receptor internalisation (receptosome rate in response to 10^{-5} mol/l isoproterenol after IgG preincubation, see Fig. 4.13B). **(D)** β_1-AR-specific IgG level (limiting dilution of IgG-β_1-AR-YFP binding, see Fig. 4.8B). **(E)** cAMP-stimulation $\times$ internalisation inhibition (receptosome rate^{-1}). **(F)** Level of anti β_1-AR IgG $\times$ internalisation inhibition (receptosome rate^{-1}). **(G)** β_1-AR specific IgG level $\times$ cAMP-stimulation. **(H)** β_1-AR specific IgG level $\times$ cAMP-stimulation $\times$ internalisation inhibition (receptosome rate^{-1}). Areas under the ROC curves and 90% confidential intervals derived are plotted in Figure 4.15J.

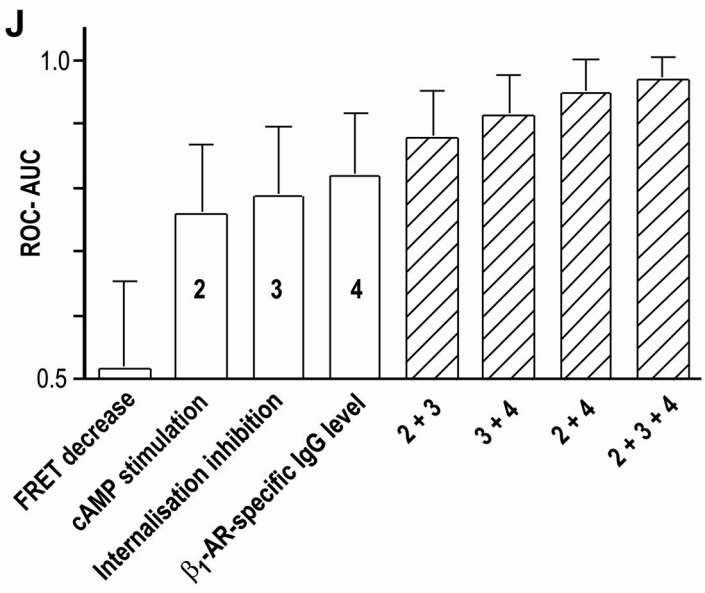

(J) Datasets of patients and healthy volunteers shown in Figure 4.8B, 4.9C, 4.10A and 4.13B or compound values combining these parameters by multiplication were subjected to ROC analysis (details see Fig. 4.15A-H). Columns and error bars represent areas under the ROC curves ± 90% confidential intervals.

Going by the area under the ROC curves (Fig. 4.15J) the level of β_1-AR-specific IgG was the most powerful single parameter. In the limited cohort studied here, it discriminated patients and healthy volunteers above the 80th percentile. Combinations with cAMP stimulation and/or receptor internalisation inhibition were more powerful than specific IgG levels alone. Compound values of all three properties together allowed discrimination of patients and healthy volunteers at the 97th percentile. It should be noted, that these sensitivities and specificities are most certainly overestimated in absolute terms due to the small cohort sizes. However, the predictive value of the parameters relative to each other should not be affected by cohort size.

4.4.2 Features associated with therapy response

The gain in LVEF during 3, 6 and 12 months after immunoadsorption was used to determine which properties of the removed β_1-AR-specific IgG were most clearly related to therapy response. Interestingly, improvement of left ventricular function following immunoadsorption was best correlated to the potency of the removed IgG to inhibit receptor internalisation and only to a lesser degree to its cAMP stimulatory potency and receptor specific level (Fig. 4.16).

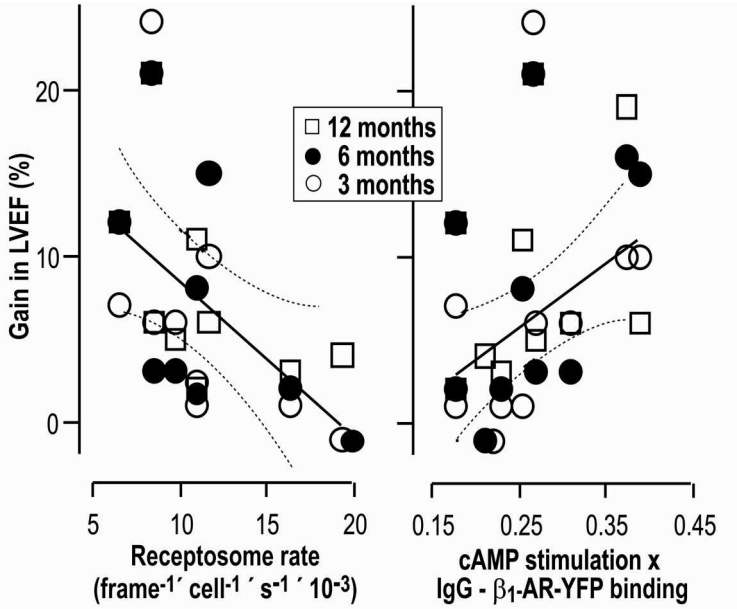

Figure 4.16: Statistic analysis of discriminative parameters and therapy response.
Gain in LVEF after 3, 6 and 12 months following immunoadsorption is correlated linearly (solid lines) to the potency of the removed IgG to inhibit receptor internalisation (left) or to the β_1-AR-specific IgG level (prior to immunoadsorption) multiplied with the cAMP-stimulatory potency of the removed IgG (right). Dashed lines show 99% confidential intervals of linear regression.

5. Discussion

Autoantibodies against the β_1-adrenregic receptor (β_1-AR), which is the most common receptor in myocytes, seem to play a major role in the development of dilated cardiomyopathy (DCM). There is compelling evidence that these autoantibodies actually cause this heart disease. However in this study the investigation of *bona fide* cardiopathogenic antibodies taken from DCM patients by immunoadsorption in terms of modulation and activation of the β_1-ARs was undertaken. In this chapter I want to discuss the results in relationship with the literature and give some future research prospects.

5.1 Conflicting views on the pathogenic mechanism

There is compelling evidence that humoral autoimmunity against extracellular epitopes of β_1-ARs plays a role in DCM (Dragun et al. 2009). However, there are conflicting views on how β_1-AR autoantibody interactions modify the β_1-AR signalling and how this is linked to the disease.

In one view autoantibodies are thought to act as allosteric receptor agonists (Hebert 2007) which are causing left ventricular failure through inappropriate ino- and chronotropism (Freedman et al. 2004; Dragun et al. 2009). This concept is based on immunisation experiments in rodents (Matsui et al. 1999; Matsui et al. 2000; Fukuda et al. 2004; Jahns et al. 2004; Buvall et al. 2006; Matsui et al. 2006; Jane-wit et al. 2007; Liu et al. 2008). In humans the correlation between the occurrence of cAMP-stimulatory β_1-AR autoantibodies and the prevalence, severity, mortality or complication rate of DCM contribute to this idea (Magnusson et al. 1996; Jahns et al. 1999; Chiale et al. 2001; Iwata et al. 2001; Wallukat et al. 2001; Nikolaev et al. 2006; Stork et al. 2006).

The other view is based on the properties of pathogenic autoantibodies removed from DCM patients in the course of immunoadsorption therapy. These studies show that hemodynamic improvements are not correlated to the removal of stimulatory β_1-AR autoantibodies alone. Actually, many studies suggest that removal of

autoantibodies that depress cardiac activity is more important (Felix et al. 2002; Wallukat et al. 2002; Dorffel et al. 2004; Kallwellis-Opara et al. 2007). This does not fit the concept of allosteric β_1-adrenergic receptor agonism of the autoantibodies being the pathogenic principle of the disease. Moreover, interactions of the cardiodepressant autoantibodies with myocardial Fcγ-receptors IIa seem also to play a role (Staudt et al. 2007; Staudt et al. 2010).

In this work I present data that may reconcile these controversial views. I found that modulation of β_1-adrenergic signal transduction by β_1-AR autoantibodies results from a very complex interplay of mechanisms and through their direct impact on receptor conformation autoantibodies can behave as partial agonists. It seems plausible that in the previous studies measuring cAMP-stimulation in cells these actions are mostly seen as stimulatory activities (Magnusson et al. 1996; Jahns et al. 1999; Chiale et al. 2001; Iwata et al. 2001; Nikolaev et al. 2006; Stork et al. 2006). However, this investigation shows clearly that such autoantibodies fall into two groups that increase or decrease receptor activity and thus potentiate or attenuate receptor-agonist responses (results Fig. 4.10). This suggests that some of these “cAMP-stimulatory” autoantibodies could in fact act attenuating (cardiodepressant), whereas others potentiate chatecholamine actions on the heart. In addition, some of the autoantibodies inhibit β_1-AR internalisation that also attenuates receptor-agonist responses and counteracts with conformational receptor activation (results Fig. 4.9). A random combination of these non-associated properties and modulatory effects is compatible with the results of experimental immunisation in rodents, the functional effects reported of cardiopathogenic autoantibodies from human patients and many other seemingly controversial autoantibody effects on β_1-AR function in the literature (Wallukat et al. 1995; Magnusson et al. 1996; Jahns et al. 1999; Jahns et al. 2000; Christ et al. 2001; Staudt et al. 2001; Jahns et al. 2004; Christ et al. 2006; Nikolaev et al. 2007).

5.2 Quantification and prevalence of autoantibodies

It has been known for some time that the autoantibodies against the first and second loop of the human β_1-AR playing a role, in DCM (Jahns et al. 1999) and Chagas disease, (Labovsky et al. 2007) recognising a conformational epitope that is not conserved upon denaturation and not adequately represented by peptides. The results of immunoprecipitation show moreover, that even ligand binding competent β_1-AR molecules in agent induced micelles are not an adequate antigen. Hence, IgG binding to native β_1-AR on the surface of living cells seems the only feasible approach to measure autoantibody titers to date. Using a biofluorescent receptor for this purpose, as done here, allows for a very controlled and standardised procedure. However, in order to translate this assay into clinical routine diagnostics, it will be necessary to find a fixation method that sufficiently conserves the native epitope.

In the limited study presented here (10 DCM patients and 10 controls) we found autoantibodies specific for β_1-AR in samples of both groups, patients and healthy volunteers. We even detected them in IgG pools from blood donors used to substitute pathogenic IgG following immunoadsorption. This suggests that low-level humoral autoimmunity against extracellular receptor epitopes is a harmless, ubiquitous, physiological condition. Given that both commercial donor IgG pools and a significant fraction of the IgG isolated from healthy individuals in our study induced inactive conformations of the receptor and did not inhibit receptor internalisation, one can assume that this is a physiological state of autoantibodies.

DCM patients have up to 10-fold higher levels of such autoantibodies, which is in agreement with other studies (Rose 2001; Jahns et al. 2006). Autoantibodies formed against a specific antigen like the second extracellular loop of the β_1-AR are believed to be overproduced by the humoral immune response. This could happen through repeated virus infection or other mechanisms triggering the immune system (Jahns et al. 2008). Thus, it is conceivable that the higher autoantibody levels in DCM patients are due to a boost of pre-existing autoimmunity by various infections thought to trigger the disease {Yoshikawa, 2009 #144; Silvina Lo Presti, 2008 #136; Kallwellis-

Opara, 2007 #117; Rose, 2001 #536; Bachmaier, 1999 #534; Luppi, 1998 #72; Cunha-Neto, 2006 #9}. It is plausible that the increase in concentration promotes or unmasks a pathogenic potential of the autoantibodies to induce active receptor conformations and/or inhibit agonist-triggered internalisation.

While immunoadsorption therapy has been clearly shown to significantly improve DCM (Dörffel et al. 1997; Felix et al. 2000; Felix et al. 2002; Dorffel et al. 2004), this therapy is expensive, involves hospitalisation and carries a certain risk. Therefore, it is to date only used when all other conservative therapy options were applied and progressive heart failure symptoms are still present. Therefore only critically ill DCM patients profit from immunoadsorption. However, at that stage of the disease improvement can be achieved, but stopping the disease fails. Using immunoadsorption at an earlier stage of DCM might stop the progression of the disease to the final stage. Such early treatment could provide the first step to a cure of DCM. However, given the high prevalence of autoantibodies in healthy persons, reliable diagnostic tests are needed to distinguish between pathogenic levels or types of autoantibodies that with a certain probability will trigger the disease in an as yet healthy person, and non-hazardous levels or types of autoantibodies. The test systems established and characterised within this work appear to be a suitable starting point for the development of a sensitive method to detect pathogenic autoantibody constellations.

5.3 IgG triggered β_1-AR conformational change via allosteric interactions

The hypothesis of DCM as an agonistic antibody disease (Cherezov et al. 2007) implies that β_1-AR autoantibodies are agonist-like and allosteric modifiers of receptor conformation. We provide here direct proof for this hypothesis by showing that autoantibodies indeed trigger conformational changes through interactions with the second extracellular loop (Fig. 5.1B) of the β_1-AR. This receptor domain reaches down into the ligand binding pocket and contacts the ligand (Fig. 5.1A). Two disulfide

bonds (yellow in Fig. 5.1) crucial for holding the entire loop out of the pocket (Cherezov et al. 2007) are located within the epitope to be involved in the triggering of the conformational change by the autoantibodies (see Fig. 5.1B).

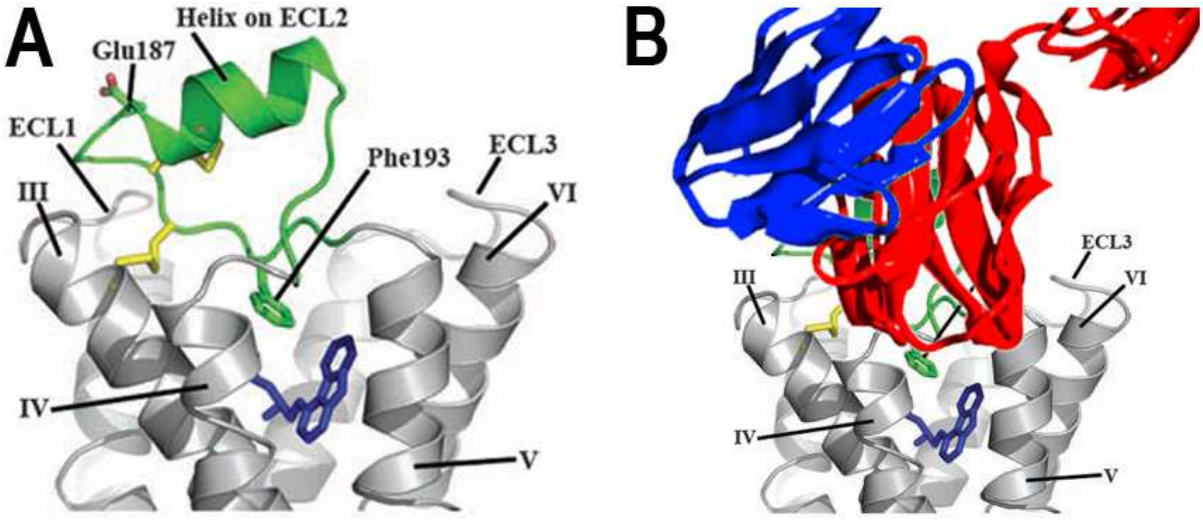

Figure 5.1: β-AR ligand binding.

(A) Ligand binding pocket of the β-adrenergic receptor, the 2nd extracellular loop (ECL2) (in green) and two disulfide bonds (yellow) holding the ECL2 out of the pocket are shown. The ligand carazol (dark blue) sits in the binding pocket. ECL2 interacts with ECL1 and the second disulfide bond links it to helix III. The ECL2 interacts with the ligand carazol at one interaction point at Phe193. N-terminus is not shown here. **(B)** Hypothetical structure model of the β-adrenergic receptor binding pocket with an IgG antibody (depicted in blue/red) bound to the extracellular receptor loop but not reaching in the binding pocket where carazol is still sitting. The IgG interacts with Ph193. Another binding site of the antibody could interact with the Glu187. Note: due to size restriction only a part of the Fab fragment of the antibody is shown. Receptor picture was adapted from (Cherezov et al. 2007) and modulated; IgG picture was adapted from http://biochemistryquestions.wordpress.com and was also modulated.

Thus, the antibodies interfere with the stability and/or proper conformation of the second extracellular loop, thereby triggering distortions of the ligand binding pocket that mimic the conformational switch induced by agonists (Cherezov et al. 2007). This investigation demonstrates a conserved capability of triggering conformational changes in all IgG antibodies that bind to the second extracellular loop of the native human β_1-AR irrespective of their association with DCM. However, DCM-associated β_1-AR autoantibodies act more like allosteric agonists, whereas putatively harmless autoantibodies (also present in IgG prepared from pooled donor plasma) act more

like partial agonists or antagonists. This supports allosteric agonism of the autoantibodies as a pathogenic principle.

5.4 Internalisation inhibition

The internalisation experiments showed that autoimmune antibodies have an inhibiting or even blocking effect on the β_1-AR recycling (results Fig 4.12 and 4.13). Even the agonist binding to the receptor was influenced by the autoantibodies meaning that the binding of the autoantibody influences the agonist binding site and therefore inhibits receptor internalisation, or the agonist-induced internalisation process itself is inhibited. Recycling of the isoproterenol-bound receptor was retarded after preincubation with autoantibodies. This work could show that 70% of the patient antibodies could be discriminated against volunteers by this method. One could imagine that this effect is due to a sterical block of the receptor binding pocket by the comparatively large autoantibody thus hindering agonist-induced receptor internalisation. Moreover, inhibition of β_1-AR internalisation could provide the mechanistic link between autoantibody interactions with Fcγ receptors and β_1-AR, both known to play a role in DCM (Staudt et al. 2007; Staudt et al. 2010). It is conceivable that in the patient this effect is enhanced by simultaneous interactions with Fcγ-receptors IIa. This receptor is specific for the IgG_3 subclass frequently associated with cardiodepressant autoantibodies removed form DCM patients (Staudt et al. 2007; Staudt et al. 2010). Unlike β_1-AR stimulation by agonists, stimulation by autoantibodies does not undergo desensitisation (Magnusson et al. 1996; Christ et al. 2006). So it can be proposed this is due to simultaneous inhibition of β_1-AR internalisation. This property is significantly more frequent and pronounced by autoantibodies from DCM patients and has a slightly higher power than receptor activation to discriminate patients from healthy volunteers. Moreover, in patients the extent of β_1-AR internalisation inhibition seems correlated to improvements of left ventricular function upon autoantibody removal. Thus, cAMP-dampening effects of autoantibodies via inhibition of receptor internalisation could be more crucial to left ventricular function than cAMP stimulating and catecholamine-sensitising effects via allosteric receptor agonism.

5.5 Conclusion

Findings are based on group sizes (10 patients and 10 volunteers) insufficient neither to draw valid epidemiological conclusions nor to determine sensitivity and specificity of disease markers in absolute terms. However, the predictive value of the parameters relative to each other should not be affected by cohort size.

Along these lines, proposing that the assessment of β_1-AR autoantibodies in the context of DCM and its therapy by immunoadsorption can be primarily based on the quantification of circulating IgG autoantibodies. These IgG capable of binding the native human β_1-ARs provide a sensitivity (80%) sufficient to discriminate increased levels in patients from normal levels in healthy individuals. A gain in allosteric receptor agonism and the ability to inhibit receptor internalisation are features that indicate an increase in the cardiopathogenic potential of an existing β_1-AR autoimmunity, and thus, may contribute to the decision on therapeutic intervention.

5.6 Outlook

In the future it will be necessary to investigate in detail the complex cellular system triggered by autoantibodies in order to understand DCM development. Therefore different appoaches are conceivable and a few of them are presented as following. Inhibition of receptor recycling in addition could be a tool to predict therapy response. This would require the design of a more sensitive cell model with a pH sensitive fluorophore coupled to the receptor. Such a pH-sensitive fluorophore is highly fluorescent when exposed at the cell surface to a medium of pH 7.4, but its fluorescence is rapidly and reversibly quenched in the acidic environment of the endocytic pathway (Yudowski et al. 2006). A pH-sensitive fluorophore integrated into the β_1-adrenergic receptor could yield more detailed insight into the recycling of the receptor. It would enable to discriminate between internalised receptors and recycled receptors being brought to the cell surface again as showed for the β_2AR (Yudowski et al. 2007).

Ligget and others found various gene polymorphisms in the β_1-AR which had an influence on the pharmacologic action (Swift et al. 2008) of β-AR blockers. This could be a reason for the complex results of interaction between DCM patient autoantibodies and the β_1-AR discovered in this work. Possibly the polymorphism, that means variability of certain amino acids in the ligand binding area of the receptor may change the binding affinities of the autoantibodies in terms of receptor binding strength, constancy, conformation, internalisation and therefore signal transduction. One could characterise patients in terms of the polymorphism of their β_1-ARs, and the resulting interactions with autoantibody binding could give further evidence about the importance of such β_1-AR polymorphisms in DCM. This also could reveal another basic principle important for diagnostics and therapy options in DCM.

There is ample evidence that more than one receptor is targeted by the humoral autoimmune reaction involved in DCM pathogenesis (Yoshikawa et al. 2009). Thus it seems unwise to focus large diagnostic studies solely on autoimmunity against human β_1-AR (Deubner et al. 2010). Instead it is heralded to get an overview of the binding characteristics of autoantibodies and to study possible modulations of other receptors and proteins for example the β_2-AR, the muscarinic receptors M2 and M3, troponin 1 or the Na-K-ATPase all possibly involved in DCM (Yoshikawa et al. 2009). Furthermore it is important to study the putative link between myocardial Fcγ-receptors IIa studies and β_1-adrenergic receptor in terms of DCM development.

Finally, it would be necessary to be able to discriminate between specific types of IgGs from patients in order to the improve immunoadsorption. Research in this field would enable to eliminate only the pathogenic IgGs without the necessity of substituting all IgG-antibodies from patients. Further this would improve the therapy options by developing specific pharmaceuticals against only one subset of autoanantibodies.

6. References

Azzi, M., P. G. Charest, S. Angers, G. Rousseau, T. Kohout, M. Bouvier and G. Pineyro (2003). "Beta-arrestin-mediated activation of MAPK by inverse agonists reveals distinct active conformations for G protein-coupled receptors." Proc Natl Acad Sci U S A **100**(20): 11406-11.

Biolo, A., A. S. Rosa, N. G. Mazzotti, S. Martins, A. Belló-Klein, R. E. and C. N. (2006). "The role of adrenergic receptor polymorphisms in heart failure." Brazilian Journal of Medical and Biological Research **39**: 1281-1290.

Biskup, C., T. Zimmer, L. Kelbauskas, B. Hoffmann, N. Klocker, W. Becker, A. Bergmann and K. Benndorf (2007). "Multi-dimensional fluorescence lifetime and FRET measurements." Microsc Res Tech **70**(5): 442-51.

Boege, F., M. Ward, R. Jurss, M. Hekman and E. J. Helmreich (1988). "Role of glycosylation for beta 2-adrenoceptor function in A431 cells." J Biol Chem **263**(18): 9040-9.

Bowles, N. E., P. J. Richardson, E. G. Olsen and L. C. Archard (1986). "Detection of Coxsackie-B-virus-specific RNA sequences in myocardial biopsy samples from patients with myocarditis and dilated cardiomyopathy." Lancet **1**(8490): 1120-3.

Bristow, M., R. Ginsburg, V. Umans, M. Fowler, W. Minobe and R. Rasmussen (1986). "Beta 1- and beta 2-adrenergic-receptor subpopulations in nonfailing and failing human ventricular myocardium: coupling of both receptor subtypes to muscle contraction and selective beta 1- receptor down-regulation in heart failure." Circ Res **59**: 297-309.

Burgi, S., K. Baltensperger and U. E. Honegger (2003). "Antidepressant-induced switch of beta 1-adrenoceptor trafficking as a mechanism for drug action." J Biol Chem **278**(2): 1044-52.

Buvall, L., E. Bollano, J. Chen, W. Shultze and M. Fu (2006). "Phenotype of early cardiomyopathic changes induced by active immunization of rats with a synthetic peptide corresponding to the second extracellular loop of the human beta(1)-adrenergic receptor." Clinical and Experimental Immunology **143**(2): 209-215.

Campbell, P., M. Hnatowich, B. O'Dowd, M. Caron, R. Lefkowitz and W. Hausdorff (1991). "Mutations of the human beta 2-adrenergic receptor that impair coupling to Gs interfere with receptor down-regulation but not sequestration." Mol Pharmacol **39**(2): 192-8.

Cherezov, V., D. M. Rosenbaum, M. A. Hanson, S. G. Rasmussen, F. S. Thian, T. S. Kobilka, H. J. Choi, P. Kuhn, W. I. Weis, B. K. Kobilka and R. C. Stevens (2007). "High-resolution crystal structure of an engineered human beta2-adrenergic G protein-coupled receptor." Science **318**(5854): 1258-65.

Chiale, P. A., I. Ferrari, E. Mahler, M. A. Vallazza, M. V. Elizari, M. B. Rosenbaum and M. J. Levin (2001). "Differential profile and biochemical effects of antiautonomic membrane receptor antibodies in ventricular arrhythmias and sinus node dysfunction." Circulation **103**(13): 1765-1771.

Chidiac, P., T. E. Hebert, M. Valiquette, M. Dennis and M. Bouvier (1994). "Inverse agonist activity of beta-adrenergic antagonists." Mol Pharmacol **45**(3): 490-9.

Christ, T., S. Schindelhauer, E. Wettwer, G. Wallukat and U. Ravens (2006). "Interaction between autoantibodies against the beta1-adrenoceptor and isoprenaline in enhancing L-type Ca2+ current in rat ventricular myocytes." J Mol Cell Cardiol **41**(4): 716-23.

Christ, T., E. Wettwer, D. Dobrev, E. Adolph, M. Knaut, G. Wallukat and U. Ravens (2001). "Autoantibodies against the beta(1)-adrenoceptor from patients with dilated cardiomyopathy prolong action potential duration and enhance contractility in isolated cardiomyocytes." Journal of Molecular and Cellular Cardiology **33**(8): 1515-1525.

Christensen, M. O., H. U. Barthelmes, S. Feineis, B. R. Knudsen, A. H. Andersen, F. Boege and C. Mielke (2002). "Changes in mobility account for camptothecin-induced subnuclear relocation of topoisomerase I." J Biol Chem **277**(18): 15661-5.

Collins, S. (2000). "ß-Adrenergic receptor signaling in adipocytes." Adipocyte Biology and Hormone Signaling: 51 - 62.

Cunha-Neto, E., A. M. Bilate, K. V. Hyland, S. G. Fonseca, J. Kalil and D. M. Engman (2006). "Induction of cardiac autoimmunity in Chagas heart disease: A case for molecular mimicry." Autoimmunity **39**(1): 41-54.

Deubner, N., D. Berliner, A. Schlipp, G. Gelbrich, A. L. Caforio, S. B. Felix, M. Fu, H. Katus, C. E. Angermann, M. J. Lohse, G. Ertl, S. Stork and R. Jahns (2010). "Cardiac beta1-adrenoceptor autoantibodies in human heart disease: rationale and design of the Etiology, Titre-Course, and Survival (ETiCS) Study." Eur J Heart Fail **12**(7): 753-62.

Dohlman, H. G., M. Bouvier, J. L. Benovic, M. G. Caron and R. J. Lefkowitz (1987). "The multiple membrane spanning topography of the beta 2-adrenergic receptor. Localization of the sites of binding, glycosylation, and regulatory phosphorylation by limited proteolysis." J Biol Chem **262**(29): 14282-8.

Dörffel, W., S. Felix and e. a. Wallukat G (1997). "Short-term hemodynamic effects of immunoadsorption in dilated cardiomyopathy." Circulation **95**: 1994-7.

Dorffel, W. V., G. Wallukat, Y. Dorffel, S. B. Felix and G. Baumann (2004). "Immunoadsorption in idiopathic dilated cardiomyopathy, a 3-year follow-up." Int J Cardiol **97**(3): 529-34.

Dragun, D., A. Philippe, R. Catar and B. Hegner (2009). "Autoimmune mediated G-protein receptor activation in cardiovascular and renal pathologies." Thromb Haemost **101**(4): 643-8.

Elliott, P. (2000). "CARDIOMYOPATHY Diagnosis and management of dilated cardiomyopathy." Heart Rhythm **84**: 106-112.

Engelhardt, S., Y. Grimmer, G. H. Fan and M. J. Lohse (2001). "Constitutive activity of the human beta(1)-adrenergic receptor in beta(1)-receptor transgenic mice." Molecular Pharmacology **60**(4): 712-717.

Fairweather, D., Rose N. R. . (2004). "Women and autoimmune diseases. " Emerging infectious diseases 10:, from http://www.cidpusa.org/AUTOIMMUNEDISEASES.

Felix, S., A. Staudt and W. e. a. Dörffel (2000). "Hemodynamic effects of immunoadsorption and subsequent immunoglobulin substitution in dilated cardiomyopathy: three-month results from a randomized study." J Am Coll Cardiol **35**: 1590-8.

Felix, S. B., A. Staudt, M. Landsberger, Y. Grosse, V. Stangl, T. Spielhagen, G. Wallukat, K. D. Wernecke, G. Baumann and K. Stangl (2002). "Removal of cardiodepressant antibodies in dilated cardiomyopathy by immunoadsorption." J Am Coll Cardiol **39**(4): 646-52.

Freedman, N. J. and R. J. Lefkowitz (2004). "Anti-beta(1)-adrenergic receptor antibodies and heart failure: causation, not just correlation." Journal of Clinical Investigation **113**(10): 1379-1382.

Frielle, T., M. Caron and R. J. Lefkowitz (1989). "Properties of the Beta1 and Beta2-Adrenergic Receptor Subtypes Revealed by Molecular Cloning." Clinical Chemistry **35**(5): 721-725.

Fukuda, Y., S. Miyoshi, K. Tanimoto, K. Oota, K. Fujikura, M. Iwata, A. Baba, Y. Hagiwara, T. Yoshikawa, H. Mitamura and S. Ogawa (2004). "Autoimmunity against the second extracellular loop of beta(1)-adrenergic receptors induces early afterdepolarization and decreases in K-channel density in rabbits." J Am Coll Cardiol **43**(6): 1090-100.

Gagnon, A. W., L. Kallal and J. L. Benovic (1998). "Role of clathrin-mediated endocytosis in agonist-induced down-regulation of the beta2-adrenergic receptor." J Biol Chem **273**(12): 6976-81.

Graham, F. L., J. Smiley, W. C. Russell and R. Nairn (1977). "Characteristics of a human cell line transformed by DNA from human adenovirus type 5." J Gen Virol **36**: 59-74.

Granier, S., S. Kim, A. M. Shafer, V. R. Ratnala, J. J. Fung, R. N. Zare and B. Kobilka (2007). "Structure and conformational changes in the C-terminal domain of the beta2-adrenoceptor: insights from fluorescence resonance energy transfer studies." J Biol Chem **282**(18): 13895-905.

Granneman, J. G. (2001). "The putative beta4-adrenergic receptor is a novel state of the beta1-adrenergic receptor." Am. J. Physiol. Endocrinol. Metab **280**: E199 - E202.

Hanahan, D. (1983). "Studies on transformation of Escherichia coli with plasmids." J Mol Biol **166**: 557-580.

Hebert, T. E. (2007). "Anti-beta1AR antibodies in dilated cardiomyopathy: are these a new class of receptor agonists?" Cardiovasc Res **76**(1): 5-7.

Hebert, T. E., S. Moffett, J. P. Morello, T. P. Loisel, D. G. Bichet, C. Barret and M. Bouvier (1996). "A peptide derived from a beta2-adrenergic receptor transmembrane domain inhibits both receptor dimerization and activation." J Biol Chem **271**(27): 16384-92.

Hoffmann, C., G. Gaietta, M. Bunemann, S. R. Adams, S. Oberdorff-Maass, B. Behr, J. P. Vilardaga, R. Y. Tsien, M. H. Ellisman and M. J. Lohse (2005). "A FlAsH-based FRET approach to determine G protein-coupled receptor activation in living cells." Nat Methods **2**(3): 171-6.

Hoonakker, M. E., N. Ruiterkamp and C. F. Hendriksen (2010). "The cAMP assay: a functional in vitro alternative to the in vivo Histamine Sensitization test." Vaccine **28**(5): 1347-52.

Hopkinson, H. E., M. L. Latif and S. J. Hill (2000). "Non-competitive antagonism of beta(2)-agonist-mediated cyclic AMP accumulation by ICI 118551 in BC3H1 cells endogenously expressing constitutively active beta(2)-adrenoceptors." Br J Pharmacol **131**(1): 124-30.

Horton, R. M., H. D. Hunt, S. N. Ho, J. K. Pullen and L. R. Pease (1989). "Engineering hybrid genes without the use of restriction enzymes: gene splicing by overlap extension." Gene **77**(1): 61-8.

Horton, R. M., H. D. Hunt, S. N. Ho, J. K. Pullen and L. R. Pease (1989). "Engineering hybrid genes without the use of restriction enzymes: gene splicing by overlap extension." Gene **77**: 61-68.

Iwata, M., T. Yoshikawa, A. Baba, T. Anzai, H. Mitamura and S. Ogawa (2001). "Autoantibodies against the second extracellular loop of beta(1)-adrenergic receptors predict ventricular tachycardia and sudden death in patients with idiopathic dilated cardiomyopathy." Journal of the American College of Cardiology **37**(2): 418-424.

Jahns, R., V. Boivin, L. Hein, S. Triebel, C. E. Angermann, G. Ertl and M. J. Lohse (2004). "Direct evidence for a beta(1)-adrenergic receptor-directed

autoimmune attack as a cause of idiopathic dilated cardiomyopathy." Journal of Clinical Investigation **113**(10): 1419-1429.

Jahns, R., V. Boivin, T. Krapf, G. Wallukat, F. Boege and M. J. Lohse (2000). "Modulation of beta(1)-adrenoceptor activity by domain-specific antibodies and-heart failure-associated autoantibodies." Journal of the American College of Cardiology **36**(4): 1280-1287.

Jahns, R., V. Boivin and M. J. Lohse (2006). "Beta 1-adrenergic receptor-directed autoimmunity as a cause of dilated cardiomyopathy in rats." International Journal of Cardiology **112**(1): 7-14.

Jahns, R., V. Boivin and M. J. Lohse (2006). "beta(1)-adrenergic receptor function, autoimmunity, and pathogenesis of dilated cardiomyopathy." Trends in Cardiovascular Medicine **16**(1): 20-24.

Jahns, R., V. Boivin, V. Schwarzbacher, G. Ertl and M. J. Lohse (2008). "Pathological autoantibodies in cardiomyopathy." Autoimmunity **41**(6): 454-461.

Jahns, R., V. Boivin, C. Siegmund, F. Boege, M. J. Lohse and G. Inselmann (1999). "Activating beta-1-adrenoceptor antibodies are not associated with cardiomyopathies secondary to valvular or hypertensive heart disease." Journal of the American College of Cardiology **34**(5): 1545-1551.

Jahns, R., V. Boivin, C. Siegmund, G. Inselmann, M. J. Lohse and F. Boege (1999). "Autoantibodies activating human beta1-adrenergic receptors are associated with reduced cardiac function in chronic heart failure." Circulation **99**(5): 649-54.

Jahns, R., C. Siegmund, V. Jahns, H. Reilander, A. Maidhof, W. Muller-Esterl, M. J. Lohse and F. Boege (1996). "Probing human beta 1- and beta 2-adrenoceptors with domain-specific fusion protein antibodies." Eur J Pharmacol **316**(1): 111-21.

Jane-wit, D., C. Z. Altuntas, J. M. Johnson, S. Yong, P. J. Wickley, P. Clark, Q. Wang, Z. B. Popovic, M. S. Penn, D. S. Damron, D. M. Perez and V. K. Tuohy (2007). "Beta 1-adrenergic receptor autoantibodies mediate dilated cardiomyopathy by agonistically inducing cardiomyocyte apoptosis." Circulation **116**(4): 399-410.

Kallwellis-Opara, A., A. Staudt, C. Trimpert, M. Noutsias, U. Kuhl, M. Pauschinger, H. P. Schultheiss, M. Grube, M. Bohm, G. Baumann, U. Volker, H. K. Kroemer and S. B. Felix (2007). "Immunoadsorption and subsequent immunoglobulin substitution decreases myocardial gene expression of desmin in dilated cardiomyopathy." J Mol Med **85**(12): 1429-35.

Kenakin, T. (2003). "Ligand-selective receptor conformations revisited: the promise and the problem." Trends Pharmacol Sci **24**(7): 346-54.

Kobilka, B. K. (2007). "G protein coupled receptor structure and activation." Biochim Biophys Acta **1768**(4): 794-807.

Kobilka, B. K. and X. Deupi (2007). "Conformational complexity of G-protein-coupled receptors." Trends Pharmacol Sci **28**(8): 397-406.

Kobilka, B. K. and U. Gether (1998). "Examination of ligand-induced conformational changes in the beta 2-adrenergic receptor by fluorescence spectroscopy." Adv Pharmacol **42**: 470-3.

Labovsky, V., C. R. Smulski, K. Gomez, G. Levy and M. J. Levin (2007). "Anti-beta1-adrenergic receptor autoantibodies in patients with chronic Chagas heart disease." Clin Exp Immunol **148**(3): 440-9.

Lavoie, C., J. F. Mercier, A. Salahpour, D. Umapathy, A. Breit, L. R. Villeneuve, W. Z. Zhu, R. P. Xiao, E. G. Lakatta, M. Bouvier and T. E. Hebert (2002). "Beta 1/beta 2-adrenergic receptor heterodimerization regulates beta 2-adrenergic receptor internalization and ERK signaling efficacy." J Biol Chem **277**(38): 35402-10.

Lefkowitz, R. J. and S. K. Shenoy (2005). "Transduction of receptor signals by beta-arrestins." Science **308**(5721): 512-7.

Lemoine, H., B. Ehle and A. J. Kaumann (1985). "Direct labelling of beta 2-adrenoceptors. Comparison of binding potency of 3H-ICI 118,551 and blocking potency of ICI 118,551." Naunyn Schmiedebergs Arch Pharmacol **331**(1): 40-51.

Lemoine, H. and A. J. Kaumann (1991). "Regional differences of beta 1- and beta 2-adrenoceptor-mediated functions in feline heart. A beta 2-adrenoceptor-mediated positive inotropic effect possibly unrelated to cyclic AMP." Naunyn Schmiedebergs Arch Pharmacol **344**(1): 56-69.

Lemoine, H. and C. Overlack (1992). "Highly potent beta-2 sympathomimetics convert to less potent partial agonists as relaxants of guinea pig tracheae maximally contracted by carbachol. Comparison of relaxation with receptor binding and adenylate cyclase stimulation." J Pharmacol Exp Ther **261**(1): 258-70.

Lemoine, H., C. Overlack, A. Kohl, H. Worth and D. Reinhardt (1992). "Formoterol, fenoterol, and salbutamol as partial agonists for relaxation of maximally contracted guinea pig tracheae: comparison of relaxation with receptor binding." Lung **170**(3): 163-80.

Levine, B., J. Kalman, L. Mayer, H. M. Fillit and M. Packer (1990). "Elevated circulating levels of tumor necrosis factor in severe chronic heart failure." N Engl J Med **323**(4): 236-41.

Limas, C. J., I. F. Goldenberg and C. Limas (1989). "Autoantibodies against beta-adrenoceptors in human idiopathic dilated cardiomyopathy." Circ Res **64**(1): 97-103.

Limas, C. J., I. F. Goldenberg and C. Limas (1990). "Influence of anti-beta-receptor antibodies on cardiac adenylate cyclase in patients with idiopathic dilated cardiomyopathy." Am Heart J **119**(6): 1322-8.

Linka, R. M., A. C. Porter, A. Volkov, C. Mielke, F. Boege and M. O. Christensen (2007). "C-terminal regions of topoisomerase IIalpha and IIbeta determine isoform-specific functioning of the enzymes in vivo." Nucleic Acids Res **35**(11): 3810-22.

Liu, J., W. Mao, C. Iwai, S. Fukuoka, R. Vulapalli, H. Huang, T. Wang, V. K. Sharma, S. S. Sheu, M. Fu and C. S. Liang (2008). "Adoptive passive transfer of rabbit beta1-adrenoceptor peptide immune cardiomyopathy into the Rag2-/- mouse: participation of the ER stress." J Mol Cell Cardiol **44**(2): 304-14.

Lohse, M. J. (1993). "Molecular mechanisms of membrane receptor desensitization." Biochim Biophys Acta **1179**(2): 171-188.

Lopez Bergami, P., K. A. Gomez, G. V. Levy, V. Grippo, A. Baldi and M. J. Levin (2005). "The beta1 adrenergic effects of antibodies against the C-terminal end of the ribosomal P2beta protein of Trypanosoma cruzi associate with a specific pattern of epitope recognition." Clin Exp Immunol **142**(1): 140-7.

Luttrell, L. M. and R. J. Lefkowitz (2002). "The role of beta-arrestins in the termination and transduction of G-protein-coupled receptor signals." J Cell Sci **115**(Pt 3): 455-65.

Magnusson, Y., A. Hjalmarson and J. Hoebeke (1996). "Beta 1-adrenoceptor autoimmunity in cardiomyopathy." Int J Cardiol **54**(2): 137-41.

Magnusson, Y., S. Marullo, S. Hoyer, F. Waagstein, B. Andersson, A. Vahlne, J. G. Guillet, A. D. Strosberg, A. Hjalmarson and J. Hoebeke (1990). "Mapping of a functional autoimmune epitope on the beta 1-adrenergic receptor in patients with idiopathic dilated cardiomyopathy." J Clin Invest **86**(5): 1658-63.

Magnusson, Y., G. Wallukat, F. Waagstein, A. Hjalmarson and J. Hoebeke (1994). "Autoimmunity in idiopathic dilated cardiomyopathy. Characterization of antibodies against the beta 1-adrenoceptor with positive chronotropic effect." Circulation **89**(6): 2760-7.

Mann, D. L. (2002). "Inflammatory Mediators and the Failing Heart: Past, Present, and the Foreseeable Future." Circ. Res **91**: 988-998.

Matsui, S., M. Fu, M. Hayase, S. Katsuda, N. Yamaguchi, K. Teraoka, T. Kurihara, H. Murano and N. Takekoshi (2006). "Transfer of immune components from rabbit autoimmune cardiomyopathy into severe combined immunodeficiency (SCID) mice induces cardiomyopathic changes." Autoimmunity **39**(2): 121-8.

Matsui, S., M. L. Fu, M. Hayase, S. Katsuda, N. Yamaguchi, K. Teraoka, T. Kurihara and N. Takekoshi (1999). "Active immunization of combined beta1-adrenoceptor and M2-muscarinic receptor peptides induces cardiac hypertrophy in rabbits." J Card Fail **5**(3): 246-54.

Matsui, S., L. Larsson, M. Hayase, S. Katsuda, K. Teraoka, T. Kurihara, H. Murano, K. Nishikawa and M. Fu (2006). "Specific removal of beta 1-adrenoceptor autoantibodies by immunoabsorption in rabbits with autoimmune cardiomyopathy improved cardiac structure and function." Journal of Molecular and Cellular Cardiology **41**(1): 78-85.

Matsui, S., M. Persson, H. M. Fu, M. Hayase, S. Katsuda, K. Teraoka, T. Kurihara and M. L. Fu (2000). "Protective effect of bisoprolol on beta-1 adrenoceptor peptide-induced autoimmune myocardial damage in rabbits." Herz **25**(3): 267-70.

McLean, A. J. and G. Milligan (2000). "Ligand regulation of green fluorescent protein-tagged forms of the human beta(1)- and beta(2)-adrenoceptors; comparisons with the unmodified receptors." Br J Pharmacol **130**(8): 1825-32.

Mercier, J. F., A. Salahpour, S. Angers, A. Breit and M. Bouvier (2002). "Quantitative assessment of beta 1- and beta 2-adrenergic receptor homo- and heterodimerization by bioluminescence resonance energy transfer." J Biol Chem **277**(47): 44925-31.

Mielke, C., M. Tummler, D. Schubeler, I. von Hoegen and H. Hauser (2000). "Stabilized, long-term expression of heterodimeric proteins from tricistronic mRNA." Gene **254**(1-2): 1-8.

Milligan, G. and R. A. Bond (1997). "Inverse agonism and the regulation of receptor number." Trends Pharmacol Sci **18**(12): 468-74.

Müller, J., G. Wallukat and M. e. a. Dandel (2000). "Immunoglobulin adsorption in patients with idiopathic dilated cardiomyopathy." Circulation **101**: 385-91.

Nikolaev, V. O., V. Boivin, S. Stork, C. E. Angermann, G. Ertl, M. J. Lohse and R. Jahns (2007). "A novel fluorescence method for the rapid detection of functional beta1-adrenergic receptor autoantibodies in heart failure." J Am Coll Cardiol **50**(5): 423-31.

Nikolaev, V. O., M. Bunemann, E. Schmitteckert, M. J. Lohse and S. Engelhardt (2006). "Cyclic AMP imaging in adult cardiac myocytes reveals far-reaching beta1-adrenergic but locally confined beta2-adrenergic receptor-mediated signaling." Circ Res **99**(10): 1084-91.

Olson, J. K., J. L. Croxford, M. A. Calenoff, M. C. Dal Canto and S. D. Miller. (2001). "A virus-induced molecular mimicry model of multiple sclerosis." The Journal of clinical investigation **108**: 311-318.

Orinius, E. (1968). "The late cardiac prognosis after Coxsackie-B infection." Acta Med Scand **183**(3): 235-7.

Richardson, P., W. McKenna, M. Bristow, B. Maisch, B. Mautner, J. O'Connell, E. Olsen, G. Thiene, J. Goodwin, I. Gyarfas, I. Martin and P. Nordet (1996). "Report of 1995 Wordl Health Ornaisation/International Society and Federation of Cardiology Task Force in the Definition and Classification of cardiomyopathies." Circulation(93): 841-842.

Rochais, F., J. P. Vilardaga, V. O. Nikolaev, M. Bunemann, M. J. Lohse and S. Engelhardt (2007). "Real-time optical recording of beta1-adrenergic receptor activation reveals supersensitivity of the Arg389 variant to carvedilol." J Clin Invest **117**(1): 229-35.

Ronspeck, W., R. Brinckmann, R. Egner, F. Gebauer, D. Winkler, P. Jekow, G. Wallukat, J. Muller and R. Kunze (2003). "Peptide based adsorbers for therapeutic immunoadsorption." Therapeutic Apheresis **7**(1): 91-97.

Rose, N. R. (2001). "Infection, mimics, and autoimmune disease." The Journal of clinical investigation **107**: 943-944.

Rose, N. R. and M. I. R. (2000). "Molecular mimicry: a critical look at exemplary instances in human diseases." Cell Mol Life Sci **57**: 542-551.

Rosenbaum, D. M., S. G. Rasmussen and B. Kobilka (2009). "The structure and function of G-protein coupled receptors." Nature **459**: 356-363.

Schenke-Layland, K., U. A. Stock, A. Nsair, J. Xie, E. Angelis, C. G. Fonseca, R. Larbig, A. Mahajan, K. Shivkumar, M. C. Fishbein and W. R. MacLellan (2009). "Cardiomyopathy is associated with structural remodelling of heart valve extracellular matrix." European Heart Journal **30**: 2254-2265.

Staudt, A., M. Bohm, F. Knebel, Y. Grosse, C. Bischoff, A. Hummel, J. B. Dahm, A. Borges, N. Jochmann, K. D. Wernecke, G. Wallukat, G. Baumann and S. B. Felix (2002). "Potential role of autoantibodies belonging to the immunoglobulin G-3 subclass in cardiac dysfunction among patients with dilated cardiomyopathy." Circulation **106**(19): 2448-53.

Staudt, A., P. Eichler, C. Trimpert, S. B. Felix and A. Greinacher (2007). "Fc(gamma) receptors IIa on cardiomyocytes and their potential functional relevance in dilated cardiomyopathy." J Am Coll Cardiol **49**(16): 1684-92.

Staudt, A., L. R. Herda, C. Trimpert, L. Lubenow, M. Landsberger, M. Dorr, A. Hummel, L. G. Eckerle, D. Beug, C. Muller, W. Hoffmann, K. Weitmann, K. Klingel, R. Kandolf, H. K. Kroemer, A. Greinacher and S. B. Felix (2010). "Fcgamma-receptor IIa polymorphism and the role of immunoadsorption in cardiac dysfunction in patients with dilated cardiomyopathy." Clin Pharmacol Ther **87**(4): 452-8.

Staudt, A., R. Mobini, M. Fu, Y. Grosse, V. Stangl, K. Stangl, A. Thiele, G. Baumann and S. B. Felix (2001). "beta(1)-adrenoceptor antibodies induce positive inotropic response in isolated cardiomyocytes." European Journal of Pharmacology **423**(2-3): 115-119.

Staudt, A., Y. Staudt, M. Dorr, M. Bohm, F. Knebel, A. Hummel, L. Wunderle, M. Tiburcy, K. D. Wernecke, G. Baumann and S. B. Felix (2004). "Potential role of humoral immunity in cardiac dysfunction of patients suffering from dilated cardiomyopathy." Journal of the American College of Cardiology **44**(4): 829-836.

Stork, S., V. Boivin, R. Horf, L. Hein, M. J. Lohse, C. E. Angermann and R. Jahns (2006). "Stimulating autoantibodies directed against the cardiac beta1-adrenergic receptor predict increased mortality in idiopathic cardiomyopathy." Am Heart J **152**(4): 697-704.

Stryer, L. (1978). "Fluorescence Energy Transfer as a Spectroscopic Ruler." Annual Review of Biochemistry **47**: 819-846.

Swift, S. M., B. R. Gaume, K. M. Small, B. J. Aronow and S. B. Liggett (2008). "Differential coupling of Arg- and Gly389 polymorphic forms of the β1-adrenergic receptor leads to pathogenic cardiac gene regulatory programs." Physiol Genomics **35**(1): 123-131.

Tutor, A. S., P. Penela and F. Mayor, Jr. (2007). "Anti-beta1-adrenergic receptor autoantibodies are potent stimulators of the ERK1/2 pathway in cardiac cells." Cardiovasc Res **76**(1): 51-60.

Wallukat, G., J. Muller and R. Hetzer (2002). "Specific removal of beta1-adrenergic autoantibodies from patients with idiopathic dilated cardiomyopathy." N Engl J Med **347**(22): 1806.

Wallukat, G. and E. Nisson (2001). "Anti beta(1)-adrenoceptor autoantibodies analyzed in spontaneously beating neonatal rat heart myocyte cultures - Comparison of methods." In Vitro Cellular & Developmental Biology-Animal **37**(3): 175-176.

Wallukat, G., A. Wollenberger, R. Morwinski and H. F. Pitschner (1995). "Anti-beta 1-adrenoceptor autoantibodies with chronotropic activity from the serum of patients with dilated cardiomyopathy: mapping of epitopes in the first and second extracellular loops." J Mol Cell Cardiol **27**(1): 397-406.

Witebsky, E., N. R. Rose, K. Terplan, J. R. Paine and R. W. Egan (1957). "Chronic thyroiditis and autoimmunization." J Am Med Assoc **164**(13): 1439-47.

Xiang, Y., E. Devic and B. Kobilka (2002). "The PDZ binding motif of the beta 1 adrenergic receptor modulates receptor trafficking and signaling in cardiac myocytes." J Biol Chem **277**(37): 33783-90.

Yoshikawa, T., A. Baba and Y. Nagatomo (2009). "Autoimmune mechanisms underlying dilated cardiomyopathy." Circ J **73**(4): 602-7.

Yudowski, G., M. Puthenveedu, D. Leonoudakis, S. Panicker, K. Thorn, E. Beattie and M. von Zastrow (2007). "Real-time imaging of discrete exocytic events mediating surface delivery of AMPA receptors." J Neurosci. **27**(41): 11112-21.

Yudowski, G. A., M. A. Puthenveedu, A. G. Henry and M. von Zastrow (2009). "Cargo-mediated regulation of a rapid Rab4-dependent recycling pathway." Mol Biol Cell **20**(11): 2774-84.

Yudowski, G. A., M. A. Puthenveedu and M. von Zastrow (2006). "Distinct modes of regulated receptor insertion to the somatodendritic plasma membrane." Nat Neurosci **9**(5): 622-7.

7. List of Abbreviations

ATP	Adenosine triphosphate
ACE-I	Angiotensin concerting enzyme inhibitor
ADP	Adenosine diphosphate
AMP	Adenosine monophoshate
AR	Adrenergic receptor
ARB	Angiotensinogen receptor blocker
β-blocker	β-adrenergic receptor blocking agents
bp	Base pair
B_{max}	Maximum specific binding
BSA	Bovin serum albumin
cAMP	Cyclic AMP
CFP	cyan fluorescence protein
DCM	Dilative Cardiomyopathy
DMSO	Dimethylsulfoxide
e.c.	et cetera
e.g.	Exempli gratia
ERK	Extracellular signal-regulated kinase
EtBr	Ethidium bromide
Fab	Fragment antigen binding
Fc	Fragment constant
FCS	Foetal bovine serum
Fig.	Figure
FLIM	Fluorescence Lifetime Imaging Microscopy
FRET	Förster Energy Resonance Transfer (Förster effect)
GDP	Guanosine diphosphat
GFP	Green fluorescent protein
GPCR	G-protein-coupled receptor
GRK	G-protein –coupled receptor kinase
GS	Goat serum

GTP	Guanosine-5'-triphosphate
h	hour
i.e.	id est
I	intensity
IgG	Immunoglobulin G
iso	(-)-isoproterenol = (-)-N-Isopropyl-L-noradrenaline hydrochloride
IRES	Internal ribosome entry site
kd	Kilo Dalton
K_D	Dissociation constant
K_i	Dissociation constant
LVEDD	Left ventricular enddiastolic diameter
LVEF	Left ventricular ejection fraction
MAP	Mitogen activated protein
min	minutes
NADH	Reduced nicotinamide adenine dinucleotide
NYHA	New York Heart Association
pac	Pyromycin-N-acetyltransferase
PBS	Phosphate buffered saline
PDE	Phosphodiesterase protein
PCR	Polymerase chain reaction
PKA	Protein kinase A
PKC	Protein kinase C
ROC	Receiver-operator-curve
s	seconds
SEM	Standard error of the mean
TIRF	Total internal reflection microscopy
τ_m	Mean lifetime
TMD	Transmembrane domain
YFP	Yellow fluorescent protein also EYFP - enhanced yellow fluorescent protein

8. Appendix

8.1 Scheme of bicistronic plamid contruction

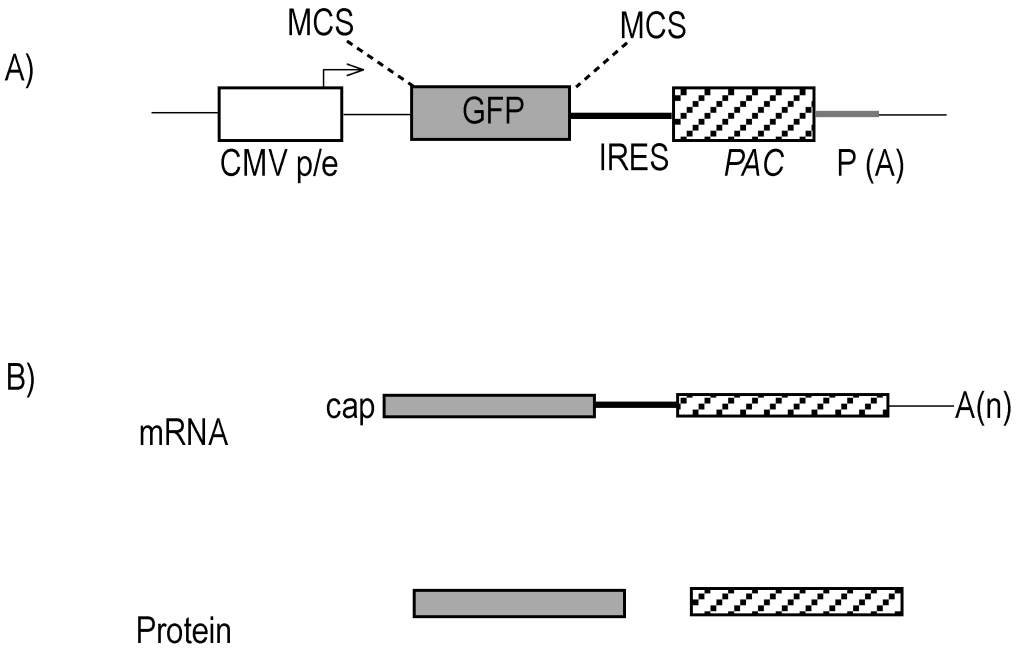

Figure 8.1: The construction scheme of a bicistronic plasmid.

(A) CMV promotor (open box), GFP an IRES element (black bar), pac (diagonally striped box), and SV40 P(A) site (grey bar). (B) Expression of bicistronic mRNA, in which the first cistron was translated by normal CAP dependent translation, and IRES element was responsible for translation of the second cistron.

8.2 Plasmid maps

8.2.A pMC-2PS-delta HindIII-P

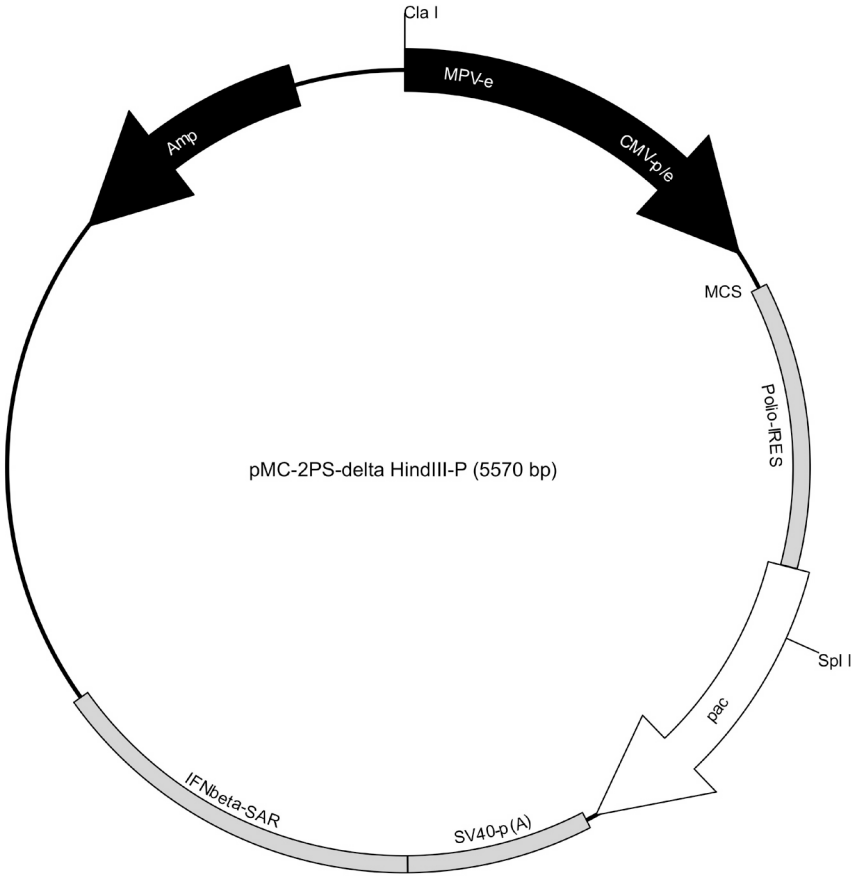

Figure 8.2: Basic bicistronic expression plasmid pMC-2PS-delta HindIII-P.
(Limas et al. 1990; Jahns et al. 1996; Mielke et al. 2000; Jahns et al. 2006). For details see

8.2.B pMC-EYFP-P-N

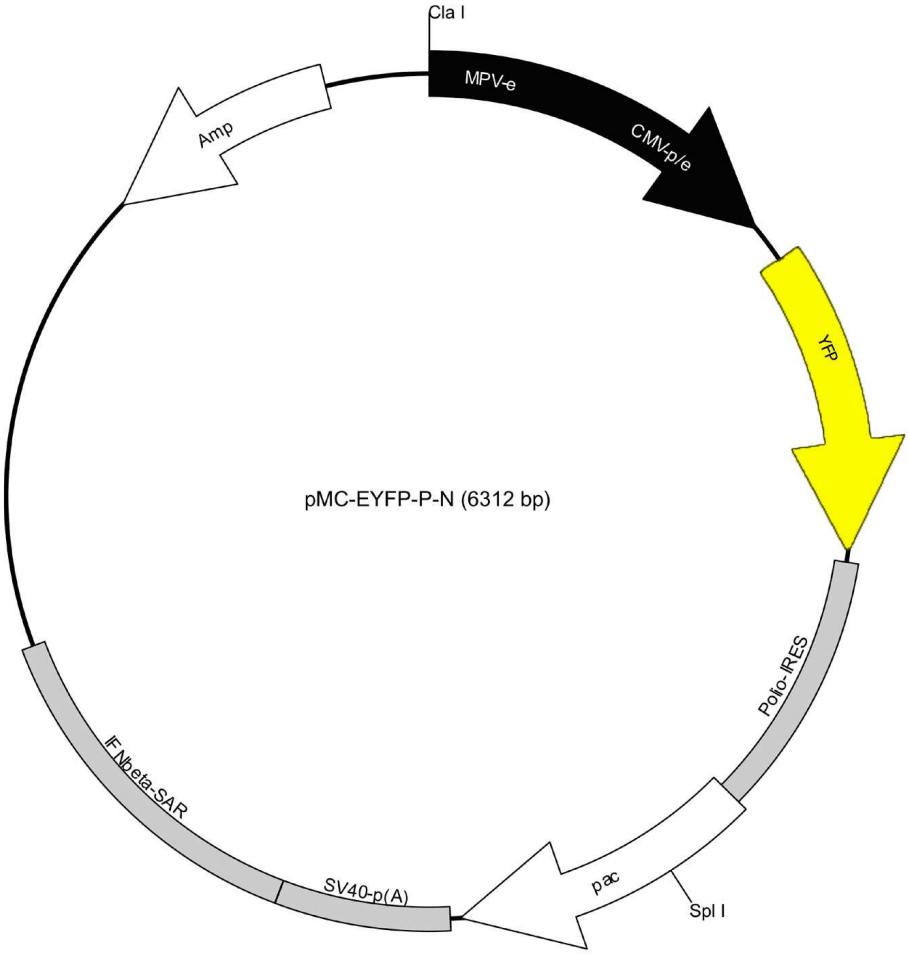

Figure 8.2: Bicistronic expression plasmid pMC-EYFP-P-N. For details see 2.1.1.

8.2.C pMC- EYFP-P

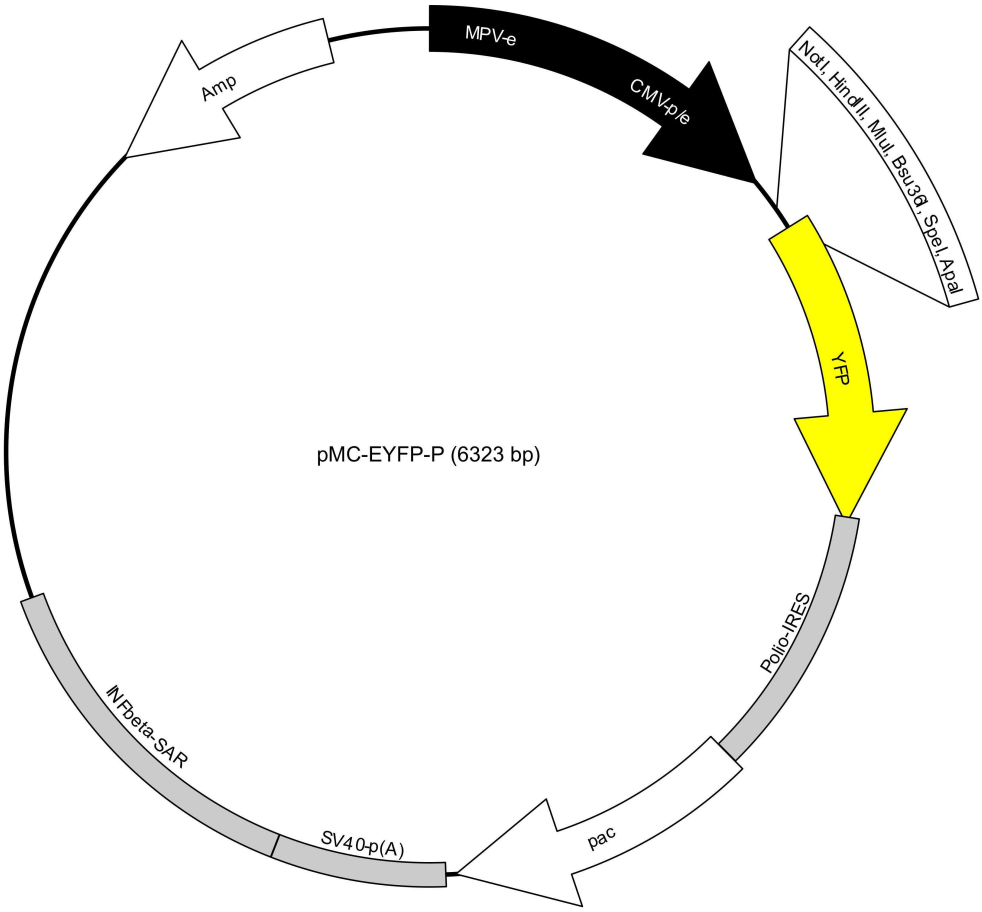

Fig. 8.3: Bicistronic expression plasmid pMC-EYFP-P.

8.3 Table of Figures

8.4 List of Tables

9. Acknowledgements

First of all, I would like to thank Prof. Fritz Boege for giving me the opportunity to work in his laboratory and for supervising my PhD project. The last years were very illuminating to me. Thank goes also to Dr. Christian Mielke and Dr. Morten Christensen for providing me with so much helpful advices during the time of working on my PhD thesis!

I am also grateful to all group members and former members that I had the pleasure to work with: Björn, Birgit, Christoph, Elke, Ellen, Faiza, Ilaria, Rene and Stefan (rigorously in alphabetical order). Thank you for your support and the good atmosphere. Thank goes also to Hans for his helpful reading of my thesis and the group around him with Britta, Isabella and Rebecca.

I would like to thank Stefanie Weidtkamp-Peters from the Institute of Molecular Physical Chemistry, Düsseldorf who assisted me with the FLIM and TIRF analysis and helped me so much. Thank goes to Prof. Felix and Dr. Herda for providing us with probes of patient IgG and patient data used in this work. I would like to thank Horst Lemoine who helped with the ligand binding experiment.
Furthermore I would like to thank Prof. Peter Westhoff for being my co-referee.

Many thanks to the Graduiertenkolleg 1089 “Proteininteraktionen und -modifikationen am Herzen“ for the financial support and great insights into the clinical side of life. Special thank goes to Ulrich Flögel, who always had time to solve problems and who was a great corrector of all my talks and writing during this time. Many thanks goes to my GK colleages especially Nadine Dyballa who shared all good and bad times during this PhD project.
I also want to thank Sieglinde Ott for being my mentor and for supporting me with a lot of encouragement as well as all the mentees I had a great time with during my time in the Selma Meyer Mentoring Program and Monika Demming-Pälmer.

I have to thank my family and friends without them this accomplishment would have been impossible. Thank goes to Sandra who read and read my thesis although the topic is hard for a non biologist. Thank goes to Tina, Katja and Anja who were with me and believed in my skills.

To my parents, and my grandmother thank you for providing endless encouragement. Thanks to Stefan who had the hardest time pushing me trough thesis writing and for helping me all the time.

10. Curriculum Vitae

PERSONAL INFORMATION

Name	Beatrice B o r n h o l z
Date and place of birth	25. August 1980, Potsdam - Babelsberg
Nationality	deutsch
Address	Hildebrandtstr 23, Düsseldorf 40215
E-mail	Beatrice.Bornholz@uni-duesseldorf.de

EDUCATION

since July 2008	PhD student in the institute of clinical chemistry and Laboratory Diagnostics, Heinrich Heine University, Medical School
12/ 2006 - 12/ 2007	Fellowship of the Selma-Meyer Mentoring-Program
09/ 2005 - 12/ 2006	Mastercourse in biochemistry
Juli 2005-juli 2008	Admittance in the GRK 1089
Nov. 2004-dec. 2004	Work experience as Research Assistant at the Mater Medical Research Institute, Brisbane (preparation and presentation of results for the HLDA8 workshop)
Sep. 2004-june 2005	Degree Course in biology at the University of Potsdam

Feb. 2004-aug. 2004	Diplomarbeit (Study finishing thesis) at the Robert-Koch-Institute, Berlin (Project: Biochemical characterisation of two functional described monoclonal antibodies; grade: very good)
Jan. 2003-aug. 2003	Practical work at the Mater Medical Research Institute, Brisbane (Project: Production of recombinant fusion proteins for members of the CMRF-35 like molecules)
June 2002-dec. 2002	Third year Course in Biomedical Science at Deakin University, Melbourne
Sep. 2000-aug. 2004	International Degree Course in Industrial and Environmental Biology (ISTAB-technical and applied biology) at Hochschule Bremen University of Applied Sciences
Aug. 1999-june 2000	Abitur (university entrance qualification) Secondary school with special subjects Biology and German at Kantgymnasium in Teltow; Finished with grade: good
Aug. 1997-july 1999	Secondary school in Kleinmachnow Weinberggymnasium
Aug. 1993-july 1997	10. Klasse-Abschluß (school leaving qualification) Secondary school at Espengrundgymnasium in Potsdam-Babelsberg

10. Erklärung

Hiermit erkläre ich, dass ich die vorliegende Dissertation eigenständig und ohne unerlaubte Hilfe angefertigt habe. Ich habe diese Dissertation in der vorgelegten oder in ähnlicher Form noch bei keiner anderen Institution eingereicht. Ich habe bisher keine erfolglosen Promotionsversuche unternommen.

Düsseldorf, den

Beatrice Bornholz